

ABSTRACT

Title of Document: VERIFICATION AND VALIDATION OF A CANDIDATE SOOT DEPOSITION MODEL IN FIRE DYNAMICS SIMULATOR VERSION 5.5.1

Brian David Cohan, M.S. 2010

Directed By: Assistant Professor, Peter B. Sunderland,
Department of Fire Protection Engineering

Deposition of soot generated from fires is important for tenability, smoke management, detector response, and fire forensics. Previous versions of Fire Dynamics Simulator (FDS) did not account for soot deposition, but FDS 5.3.1 includes an optional soot deposition model based on thermophoresis and turbulent deposition. This thesis analyzes the implementation of these deposition mechanisms independently. Predictions using FDS 5.5.1 are compared with measurements from three existing test series that involve small-scale hood tests, corridors, and large compartments, with heat release rates of 2 kW - 2 MW. Predictions of optical densities for well ventilated compartments generally agreed with experimental data. FDS over predicted optical density for small fires in large compartments and under predicted the mass deposition on surfaces in the small-scale hood test. Compartments without vents indicate that decreased smoke production rates or increased deposition rates would improve the agreement.

VERIFICATION AND VALIDATION OF THE SOOT DEPOSITION MODEL IN
FIRE DYNAMICS SIMULATOR

By

Brian David Cohan

Thesis submitted to the Faculty of the Graduate School of the
University of Maryland, College Park, in partial fulfillment
of the requirements for the degree of
Masters of Science
2010

Advisory Committee:

Assistant Professor Peter B. Sunderland, Ph.D., Chair

Professor James A. Milke, Ph.D., P.E.

Jason Floyd, Ph.D.

© Copyright by
Brian David Cohan
2010

Acknowledgements

First and foremost, I would like to thank Hughes Associate Inc. for providing me with this project and funding me while I worked. Even though this project was not funded by any grants, Hughes decided this project was a worthwhile project to be completed and allowed me to take on the task.

There are many people at Hughes who have helped me along the way. First, I would like to thank Dr. Beyler. Dr. Beyler was the one who suggested this project and oversaw my progress. Whenever I ran into a road block and got stressed out, Dr. Beyler would go over the situation and ease all stress. Next I would like to thank Dr. Floyd. Dr. Floyd developed the soot deposition algorithm and assisted me in getting familiar with the model. He has fielded countless questions and I would like to thank him for his answers and patience.

Next I would like to thank Terry Fay. I have been working alongside with Terry for over two years. Terry taught me skills in programing in VBA with excel. Knowing these skills allowed me to plot and interpret data more efficiently. Knowing VBA has helped saved me a lot of time and aggravation.

The last person from Hughes I would like to thank is Siamak Riahi. Siamak's project is one of the tests used in my thesis. He always kept a keen interest in how I was progressing and was always there to answer questions. Without Siamak's help, I would

still be wandering in the dark. I not only think of Siamak as a colleague, but a friend as well.

From the University of Maryland, I would like to thank my adviser, Dr. Sunderland. Dr. Sunderland was always excited to hear about progress in my thesis. If I was having an issue, Dr. Sunderland was always willing to sit down and discuss whatever questions I had for him. Most importantly, Dr. Sunderland has been a very supportive adviser. I had a few moments where I was unsure if I would finish my thesis in time, and Dr. Sunderland would always provide words of confidence and encouragement.

I would like to thank my thesis committee, Dr. Sunderland, Dr. Milke, and Dr. Floyd for their time. Having a committee knowledgeable about smoke movement and computer modeling has made me confident in the findings of this thesis.

Lastly, I would like to thank my family and my friends. This process has been a unique challenge and they have helped keep me sane throughout the process.

Table of Contents

Acknowledgements.....	ii
Table of Contents.....	iv
List of Tables.....	vi
List of Figures.....	vii
Nomenclature.....	ix
Abbreviations / Acronyms.....	x
Chapter 1: Introduction.....	1
1.1 Motivation.....	2
1.1.1 NIST/NRC Test Series.....	2
1.1.2 Corridor Test Series.....	4
1.1.3 Thermophoretic Deposition Chamber.....	6
1.2 FDS.....	8
1.2.1 Introduction to FDS.....	8
1.2.2 Limits.....	9
1.2.3 Using the Soot Deposition Model.....	10
1.3 Literature review.....	11
1.4 Objectives and Scope of Work.....	13
Chapter 2: Analytical Work / Methods.....	15
2.1 Thermophoresis.....	15
2.2 Turbulent Deposition.....	18
2.3 Sedimentation.....	19
Chapter 3: Verification of Soot Deposition Model.....	20
3.1 Thermophoretic Deposition Model.....	20
3.2 Turbulent Deposition Model.....	23
Chapter 4: Validation of Soot Deposition Model.....	25
4.1 Development of models.....	25
4.1.1 NIST/NRC Test Series.....	25
4.1.2 Corridor Test Series.....	30
4.1.3 Thermophoretic Deposition Chamber.....	34
4.2 Test matrix of models.....	36
4.2.1 NIST/NRC Test Series.....	36

4.2.2	Corridor Test Series	38
4.2.3	Thermophoretic Deposition Chamber.....	40
4.3	Evaluation of performance	41
4.3.1	NIST/NRC Test Series.....	41
4.3.2	Corridor Test Series	51
4.3.3	Thermophoretic Deposition Chamber.....	59
Chapter 5: Conclusions and Future Work.....		65
Appendix A – Sample FDS Files.....		67
A.1	Thermophoretic Deposition Validation Test.....	67
A.2	Turbulent Deposition Validation Test.....	68
A.3	Sample NIST/NRC FDS File	69
A.4	Sample Corridor FDS File.....	80
A.5	Sample Thermophoretic Deposition Chamber FDS File	84
Appendix B – FDS Soot Deposition Function		88
References.....		88

List of Tables

Table 1.1 – Comparison of Calculated Particle Deposition Modes ^[18]	13
Table 4.1 – Experimental Tests Performed for NIST/NRC Test Series ^[25]	37
Table 4.2 – Experimental Tests Performed for the ICFMP Test Series ^[2]	39
Table 4.3 – Select Experimental Tests Performed for Soot Deposition Study	40
Table 4.4 – Differences in FDS, with and without Soot Deposition Model, in Predicting Smoke Density vs. Test Data for NRC Tests.....	45
Table 4.5 – Comparison of Soot Yields for Small and Large Scale Heptane Fires ^[26] ...	51
Table 4.6 – Differences in FDS, with and without Soot Deposition Model, in Predicting Smoke Density vs. Test Data for Corridor Tests	58
Table 4.7 – Differences in FDS, with and without Soot Deposition Model, in Predicting Optical Density vs. Test Data for Hood Tets.....	63
Table 4.8 – Measured vs. predicted soot deposition on filters in hood tests	64

List of Figures

Figure 1.1 – Spot Detector Spacing for Smooth Ceilings (Left) and Waffle Construction with Beams 3 feet on Center (Right)	5
Figure 1.2 – Schematic of Hood Apparatus ^[7]	7
Figure 2.1 – K_{th} vs. Knudsen Number (Riahi S. , Beyler, Hartman, & Roddis, 2010).....	16
Figure 3.1 – Soot deposition mass for thermophoretic verification with adjusted values for viscosity and thermal conductivity.....	22
Figure 3.2 – Soot deposition mass for turbulent verification.....	24
Figure 4.1 – Experimental Setup for NIST/NRC Tests. (Top – Experimental Setup ^[25] , Bottom – FDS Setup).....	26
Figure 4.2 – Mesh Prescribed for NRC FDS Files. Plan View (Top) and Front View (Bottom).....	27
Figure 4.3 – Location of Heat Flux Gauges and Radiometers (Red) and the Optical Density Meter (Blue) ^[25]	29
Figure 4.4 – Fine and Coarse Mesh for Corridor Test Series	31
Figure 4.5 – Plan View of Device Locations in Corridor (Top – Experimental (Mealy, Floyd, & Gottuk, 2008), Bottom – FDS Model).....	33
Figure 4.6 – Front View of the Soot Deposition Hood.....	35
Figure 4.7 – FDS Model of the Soot Deposition Hood	35
Figure 4.8 – Smoke Density for Test 1 – 350 kW Fire Door Closed, Ventilation Off.....	42
Figure 4.9 – Smoke Density for Test 2 - 1MW Fire Door Closed, Ventilation Off.....	42
Figure 4.10 – Smoke Density for Test 3 - 1 MW Fire Door Open, Ventilation Off	43
Figure 4.11 – Smoke Density for Test 4 - 1 MW Fire Door Closed, Ventilation On.....	43
Figure 4.12 – Smoke Density for Test 5 - 1 MW Fire Door Open, Ventilation On	44
Figure 4.13 –Smoke Density for Test 13 – 2MW Fire Door Closed, Ventilation Off	44
Figure 4.14 –NRC Predicted vs. Measured Smoke Densities for FDS Model without Soot Deposition (Left) and with Soot Deposition (Right)	46

Figure 4.15 – Smoke Concentration (Left) and Heat Flux 6 and Radiometer 5 measurements (Right) for Test 1 – 350 kW Fire	49
Figure 4.16 – Smoke Concentration (Left) and Heat Flux 6 and Radiometer 5 measurements (Right) for Test 2 – 1 MW Fire.....	49
Figure 4.17 – Smoke Concentration (Left) and Heat Flux 6 and Radiometer 5 measurements (Right) for Test 13 – 2 MW Fire.....	50
Figure 4.18 – Optical Density vs. Time at Four Location along Corridor for Test 5 – Infinite Smooth Ceiling, 100 kW Fire	53
Figure 4.19 – Optical Density vs. Time at Four Locations along Corridor for Test 31 – 5 ft Wide Beamed Ceiling, 100 kW Fire	54
Figure 4.20 – Optical Density vs. Time at Four Locations along Corridor for Test 37 – 5 ft Wide Smooth Ceiling, 100 kW Fire	55
Figure 4.21 – Optical Density vs. Time at Four Locations along Corridor for Test 44 – 5 ft Wide Beamed Ceiling, 15 kW Fire	56
Figure 4.22 – Temperature Measured Above Fire Plume.....	57
Figure 4.23 – Corridor Predicted vs. Measured Smoke Densities for FDS Model without Soot Deposition (Left) and with Soot Deposition (Right).....	58
Figure 4.24 –Experimental and model heat release rate curves for hood tests.....	61
Figure 4.25 – Extinction coefficient for high and low filter locations in hood tests	61
Figure 4.26 – Optical density profile at four locations in the hood at 1000 s.....	62
Figure 4.27 – Temperature profile at four locations in the hood at 1000 s.....	62
Figure 4.28 – Hood Test Predicted vs. Measured Smoke Densities for FDS Model without Soot Deposition (Left) and with Soot Deposition (Right).....	63

Nomenclature

A	Area [m^2]
A_i	Empirical Constant
C	Cunningham slip correction
c_p	Specific Heat [$kJ/kg/K$]
d	Particle Diameter [m]
D^*	Characteristic Fire Diameter
D	Binary diffusion coefficient [m^2/s]
g	Gravitational Constant 9.81 [m/s^2]
h	Heat Transfer Coefficient [W/m^2K]
k	Thermal Conductivity [W/mK]
k_B	Boltzmann Constant 1.38×10^{-23} [J/K]
K_{th}	Thermophoretic Constant
Kn	Knudsen Number
L	Characteristic Length Scale [m]
m	Mass [kg]
n	Number of molecules
OD	Optical Density [$1/m$]
\dot{q}_{cond}''	Conductive Heat Flux [kW/m^2]
\dot{q}_{conv}''	Convective Heat Flux [kW/m^2]
\dot{q}_{rad}''	Radiative Heat Flux [kW/m^2]
\dot{q}_{tot}''	Total Heat Flux [kW/m^2]
\dot{Q}	Heat Released [kW]
t	Time [s]
T	Temperature [K]
u_f	Friction Velocity [m/s]
V	Volume [m^3]
\bar{v}_i	Mean Speed of Species i [m/s]
v_s	Settling Velocity [m/s]
v_T	Thermophoretic Velocity [m/s]
v_{Turb}	Turbulent Deposition Velocity [m/s]
Y	Mass Fraction
Z_i''	Wall Collision Frequency of Species i [Hz]
ε	Emissivity
λ	Mean Free Path [m]
μ	Dynamic Viscosity [kg/ms]
ρ	Density [kg/m^3]
σ	Stefan-Boltzmann Constant 5.67×10^{-8} [W/m^2K^4]
σ_i	Diameter of Molecule i [m]
$\sigma_{s,g}$	Gas Phase Mass Specific Extinction Coefficient [m^2/g]
τ_w	Shear Stress at the Wall [Pa]

Abbreviations / Acronyms

BE	Benchmark Exercise
CFD	Computational Fluid Dynamics
CFL	Courant–Friedrichs–Lewy
DNS	Direct Numerical Simulation
FDS	Fire Dynamics Simulator
HAI	Hughes Associates, Inc.
HVAC	Heating, Ventilation, and Air Conditioning
ICFMP	International Collaborative Fire Modeling Project
LES	Large Eddy Simulation
NIST	National Institute of Standards and Technology
NFPA	National Fire Protection Association
NRC	Nuclear Regulatory Commission
SFPE	Society of Fire Protection Engineers
V&V	Verification and Validation

Chapter 1: Introduction

Fire Dynamics Simulator (FDS) is one of the predominant computational fluid dynamics (CFD) models used in fire protection engineering. Engineers use FDS to simulate how occupancies or smoke detection devices will perform in the event of a fire. These simulations are used to demonstrate code compliance, or investigate fires as a forensics tool.

Soot generated from fire is a major factor in determining tenability and detector response. In forensics investigation, soot deposition can be used to determine information about the fire such as location and intensity. ^[6]

The standard FDS model does not account for soot deposition on surfaces. Without soot deposition in the FDS model, the optical density of the smoke layer is increased. Higher optical densities in the model lead to optimistic detector response times in the model as well as conservative tenability analysis. If performance based systems are designed based on erroneous FDS results, the designed systems could overcompensate for the amount of smoke in the upper layer.

User of FDS needs to be familiar with the limitations of the model and be able to apply their engineering judgment to the results. While engineers can adjust or interpret the model appropriately, it would be better if the model would inherently account for soot deposition on surfaces. Several studies have been conducted that demonstrate FDS over

predicting the amount of soot in the smoke layer^{[1][2]}. The severity of these errors demonstrates the need for a soot deposition algorithm to be used in the FDS model.

A soot deposition model was added to the FDS source code in version 5.3.1. The model includes two soot deposition mechanisms. The first mechanism is thermophoresis, which causes particles to move from a high temperature region to a lower temperature region. The second mechanism is turbulent deposition, which results from the shear stresses on the walls.

Before the soot deposition model can be implemented as a feature within FDS, it must undergo a verification and validation process. This thesis will analyze the equations in the model and test the equations in order to ensure they are working as they are designed. Next, experimental data from three separate test series will be used to analyze the current model's validity. The model's validity will be determined by comparison of optical density measurements taken from the various experiments. One study measured the total mass deposited on glass filters using optical and gravimetric methods. For this test, the quantity of soot deposited will be compared to the prediction from FDS to further validate the model.

1.1 Motivation

1.1.1 NIST/NRC Test Series

Historically, nuclear power plants were constructed according to codes and standards that were developed based on tests, engineering judgment, and experience. Recognizing that nuclear power plants provide unique hazards, a standard prescriptive code may not be the

best solution for all nuclear power plants. There is a movement to design nuclear power plants on a risk-informed, performance-based design.^[3]

The push for risk-informed, performance-based design requires engineers to employ analytical methods and the use of computer modeling. In 1999, the U.S. Nuclear Regulatory Commission (NRC) and the Society of Fire Protection Engineers (SFPE) met to discuss fire models and their application to a nuclear power plant. The NRC and SFPE started the International Collaborative Project to Evaluate Fire Models for Nuclear Power Plant Applications (ICFMP).

The ICFMP was established to evaluate the predictive capability of fire models for deterministic fire hazard analyses as well as probabilistic fire risk analyses. Five benchmark tests were used to determine the predictive capability of various fire models, as well as to see where the fire models needed improvement.

FDS was among the fire models evaluated under the ICFMP. Benchmark exercise 3 was used to evaluate FDS in the areas of hot gas layer temperature and height, ceiling jet temperature, plume temperature, flame height, oxygen and carbon dioxide concentration, smoke concentration, compartment pressure, heat fluxes and target temperatures, and wall and surface temperatures.

The FDS simulations of benchmark exercise 3 demonstrated that FDS was overall suitable for predicting the compartment conditions with temperatures, major gas species concentrations, and compartment pressures within 15% and heat fluxes and surface temperatures within 25%. The smoke concentration, however, was found to be 50%

higher than what was measured in the open door tests. In the closed door tests, the smoke concentration was found to be as high as six times the measured concentration. ^[4]

1.1.2 Corridor Test Series

The 2002 version of the National Fire Alarm Code (NFPA 72) states that the spacing for spot-type smoke detectors on a smooth, level ceiling is 9.1 m (30 ft). Factors such as ceiling height, slope, and beams can cause the spacing to be reduced. For example, Ceilings heights less than 3.66 m (12 ft) with beams greater than 0.3 m (1 ft) require a spot detector in every beam pocket.

A 27.4 m by 27.4 m (90 ft by 90 ft) square room with a ceiling height less than 3.66 m (12 ft) would require nine spot detectors for a smooth flat ceiling. If the same room had a ceiling of waffle type construction with beam depths of 0.3 m (1 ft) spaced 0.91 m (3 ft) on center, it would require a spot detector in each pocket for a total of 900 spot detectors^[5]. Figure 1.1 illustrates the difference in detector spacing for the flat ceiling and waffle construction ceilings. Without any engineering analysis, it is clear that 900 spot detectors for this room compared to the nine spot detectors needed for the flat ceiling is not only unnecessary, but not feasible from both cost and electrical standpoints.

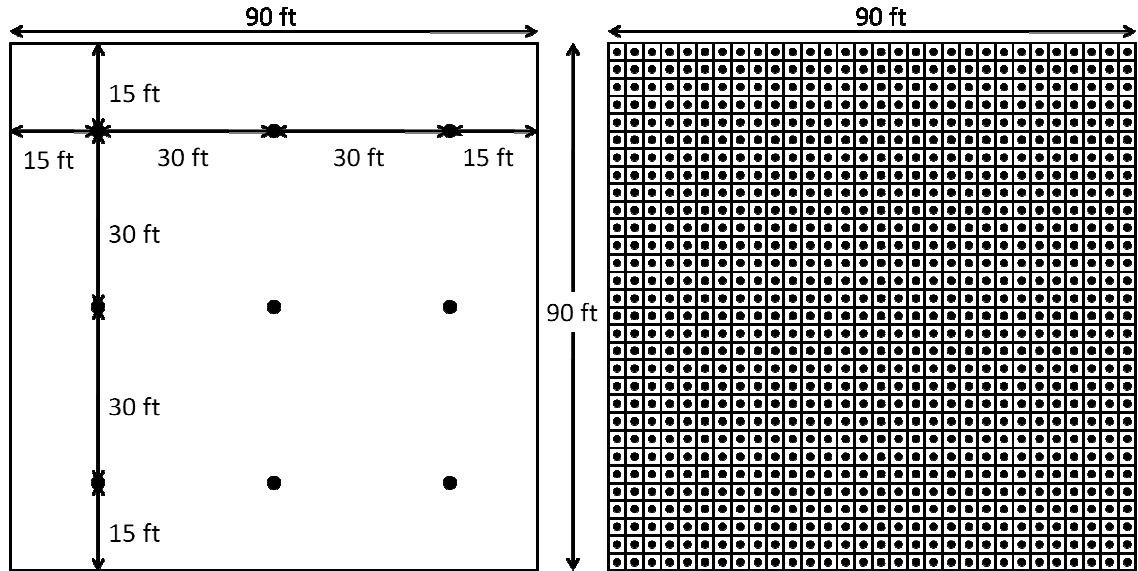


Figure 1.1 – Spot Detector Spacing for Smooth Ceilings (Left) and Waffle Construction with Beams 3 feet on Center (Right)

The Fire Protection Research Foundation sponsored a study to analyze appropriate smoke detector spacing for ceilings with deep beams and deep beam pocket configurations. The study was conducted in three projects. The first project modeled a number of scenarios for flat, beamed ceilings as well as a number of sloped, beamed ceilings. The second project was two parts. The first part used FDS to model smoke detector performance for hallways with perpendicular beams. The second part used FDS to model smoke detector performance for rooms with waffle type ceiling construction.

The final part of the project contained experimental and modeling parts to validate the previous FDS projects and to extend the modeling work to sloped ceilings with beams. Ethylene was used in the experiments to replicate the soot yield used in the previous modeling projects. The soot yield was based on hood tests. Several baseline tests were done on flat ceilings with no beams at various elevations. Ethylene was not able to

generate enough soot to activate the smoke detectors at higher ceiling heights. Upon investigation, it was noticed that a significant amount of soot, on the order of one half, was deposited on the ceiling. The fuel was changed to propylene in order to provide enough soot to activate the smoke detectors after soot was deposited on the ceiling.^[2]

At the time, FDS was not able to account for soot deposition. As found in the NIST/NRC study^[1], FDS was over predicting the amount of soot in the smoke layer. Conclusions from the first two projects were appropriate with slight modifications recommended as a result of the experimental work with respect to the soot concentrations.

1.1.3 Thermophoretic Deposition Hood

Riahi et al.^[6] developed a method to predict soot deposition on surfaces from a fire using a thermophoretic model. The test apparatus used for the experiments was a 0.6 m by 0.6 m by 0.9 m high (2 ft by 2 ft by 3 ft high) hood. On one side of the chamber is an exhaust plenum that leads to an exhaust duct. An orifice plate and blower in the exhaust duct was used to maintain the smoke layer at a constant height in the main hood. This aided in ensuring uniform properties at a given elevation throughout the chamber. In the experiments, samples of various fuels were burned and the soot generated was deposited on 9 cm (3.5 in) diameter glass filters. Two glass filters were used for each test at 54 and 76 cm (1.7 ft and 2.5 ft) above the fuel source. A schematic of the hood is shown in Figure 1.2.

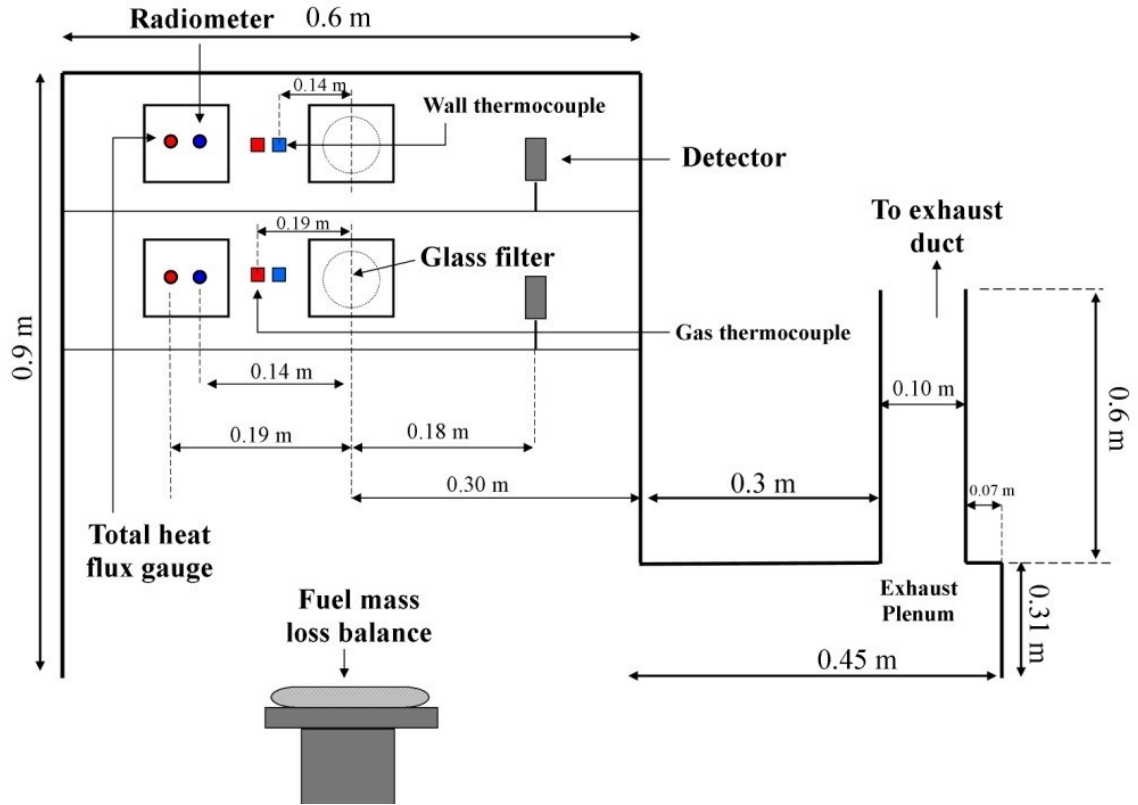


Figure 1.2 – Schematic of Hood Apparatus ^[7]

To protect the instrumentation, heat release rates were controlled to keep the temperature in the chamber below 400 °C. The small fuel sizes generated laminar flames within the hood. The position of the samples and the laminar flames helped ensure that thermophoresis was the dominant soot deposition mechanism. Instrumentation in the hood confirmed that thermophoresis accounted for 95% of the soot deposition on the filters.

In addition to the hood tests, a series of wall tests were performed. Soot deposition patterns were analyzed for a pan fire placed against a wall. Various pan sizes allowed for both laminar and turbulent fires. Instrumentation and filters were used to measure thermophoretic soot deposition on the wall and confirmed thermophoresis to be the

dominate soot deposition mechanism for vertical walls in both laminar and turbulent regimes.

1.2 FDS

1.2.1 Introduction to FDS

FDS is a CFD model of fire-driven fluid flow developed at the National Institute of Standards and Technology (NIST) ^[8]. The first version of FDS was publicly released in February of 2000. Since the first release, NIST has worked to continually improve and update the model to more accurately predict the effects of fire. FDS is applicable to fire modeling due to its hydrodynamic and combustion models.

The hydrodynamic model within FDS solves a low mach number form of the Navier-Stokes equations appropriate for thermally driven flows. Turbulence is treated by calculating the Smagorinsky form of Large Eddy Simulation (LES). If the underlying mesh is fine enough, a Direct Numerical Simulation (DNS) can be performed. The majority of simulations however, are performed with the LES model.

For most applications, FDS uses a single step mixture fraction model. By default, FDS tracks the mixture fraction of both burned and unburned fuel. If a more complex model is required to more accurately resolve the combustion process, a multi-step finite rate model is available.

1.2.2 Limits

In FDS, everything must conform to a rectilinear mesh. The mesh is one of the most important parameters of FDS. Grid cell resolution can greatly affect the results of the simulation. If the mesh is too coarse, FDS will not accurately resolve the flow within the domain. However, if the mesh is too fine, the simulation will take longer to run. Halving the size of the grid cells in each direction will result in doubling the run time for each dimension in space and time. Changing a mesh from a resolution of 2 cm to 1 cm will likely yield better results, however, there will be eight times the number of cells and the time step will be reduced by two in order to preserve the Courant–Friedrichs–Lewy (CFL) condition. Therefore, the reduction in cell size will take sixteen times longer to run.

One of the most sensitive parts of the model is the fuel source. If the cell size is too large, and there are not enough cells across the fuel source, the dynamics of the fuel will be changed. Too few cells will produce a jet-like flame. For buoyant plumes, a non-dimensional expression of $D^*/\delta x$ can be used to measure how well the flow field is resolved^[8]. D^* is the characteristic fire diameter and δx is the size of a mesh cell.

$$D^* = \left(\frac{\dot{Q}}{\rho_{\infty} c_p T_{\infty} \sqrt{g}} \right)^{2/5} \quad (1.1)$$

A validation study sponsored by the U.S. Nuclear Regulatory Commission revealed adequate ranges of $D^*/\delta x$ ranging from 4 to 16. These values worked for that set of simulations, but may not apply to all situations.

1.2.3 Using the Soot Deposition Model

The soot deposition model is found in the wall.f90 file of the FDS source code. The subroutine can be found in Appendix B. The model currently contains two modes of soot deposition: thermophoretic deposition and turbulent deposition. By default, the soot deposition model is not enabled in FDS. This model has been included since FDS version 5.3.1. Since then, the thermophoretic model has changed to use a heat transfer balance to determine the temperature gradient at the wall for thermophoretic soot deposition. Custom executables were compiled to test the thermophoretic and turbulent deposition models independently. Subversion revision 6263 includes options to enable and disable the models without specially compiling multiple versions of FDS. These options were made available with the release of FDS version 5.5.1. Subversion revision 6263 was used to model all the simulations in the validation discussed in Chapter 4.

One of the largest challenges for the turbulent deposition mechanism is accurately resolving the shear stresses on the wall. With FDS 5.5, the Werner-Wengle wall model. The Werner-Wengle model is a simplified formula for the streamwise velocity which holds instantaneously within the LES ^[9].

The properties that enable the soot deposition model are within the MISC namelist group. The relevant properties are `SOOT_DEPOSITION`, `TURBULENT_DEPOSITION`, and `THERMOPHORETIC_DEPOSITION`. The default value of `SOOT_DEPOSITION` is `.FALSE..` `TURBULENT_DEPOSITION` and `THERMOPHORETIC_DEPOSITION` default to `.TRUE..`, but have no context unless `SOOT_DEPOSITION` is enabled. To enable the soot deposition model, the MISC line should read

```
&MISC SOOT_DEPOSITION=.TRUE. /
```

To run the thermophoretic model without the turbulent model, the MISC line should be modified as follows

```
&MISC SOOT_DEPOSITION=.TRUE. TURBULENT_DEPOSITION=.FALSE. /
```

The thermophoretic deposition property can be disabled if the user wishes to run the simulation using the turbulent deposition model only. When using the turbulent deposition model, it is recommended to enable the dynamic Smagorinsky model by adding `DYSMAG=.TRUE.` to the MISC line.

1.3 Literature review

Smoke is considered the biggest threat in a fire due to the ability for smoke to travel to remote parts of buildings threatening both life and property^[10]. A large amount of work has been done in studying soot generation and transport from fires. Most of the work is used to determine visibility and toxic analysis and its effect on egress.

Tewarson^[11] studied ignition criteria for a large range of fuels. Along with analyzing ignition points of fuels, Tewarson generated tables of combustion product yields for well ventilated fires. Smoke transport has been well analyzed for compartments. Correlations have been found to determine transport via fire plumes and ceiling jets^{[12][13]}.

Few studies have examined soot deposition on surfaces resulting from fires. Ciro et. al.^[14] determined soot deposition characteristics for a cylinder immersed in a jet fuel pool fire. Experiments were performed to determine how much soot was deposited on a cold cylinder and what the thermal insulating effects were of the soot deposited on the surface.

Soot deposited on the cylinders measured up to 1.2 mm thick. Comparison of the experimental results to analytical models determined that thermophoresis was the primary mechanism for soot deposition.

Sippola ^[15] examined particle deposition in ventilation ducts. The primary focus of the study was to determine how particle deposition in heating, ventilation, and air conditioning (HVAC) systems would influence exposure to occupants and to determine the effect on HVAC performance.

Smoke damage to electronic equipment is a major concern to industries such as nuclear energy and data centers. Two concerns are interruption in the electrical systems and the long term corrosion of components. Tanaka ^[16] and Tewarson ^[17] studied the effects of smoke on exposed circuits. It was found that the smoke had an effect on the resistance of the circuit boards. Performance of the equipment returned to normal after smoke was vented from the compartment. Tewarson further concluded that water applied from sprinklers washed smoke from the surfaces without increasing the corrosion rate.

Butler et. al ^[18] reviewed multiple mechanisms for soot deposition. The focus of the study was to review potential for smoke aerosols to transport toxic vapors into the lungs. The study considered thermophoresis, sedimentation, and diffusion to determine hazard levels in an enclosure. For small particles, less than 1 μm , thermophoresis was found to be the dominant mechanism of transportation as seen in Table 1.1.

Table 1.1 – Comparison of Calculated Particle Deposition Modes ^[18]

Particle Diameter, μm	Thermophoresis	Sedimentation
0.01	2.8×10^6	6.7×10^2
0.1	2.0×10^6	8.6×10^3
1.0	1.3×10^6	3.5×10^5
10.0	7.8×10^5	3.1×10^7

Particles sticking to a 1 cm^2 surface during a 100 s period for a suspended particle density of 10^6 particles/ cm^3 .

Butler also concluded that the rate of deposition is much greater for turbulent buoyant flow compared to laminar flow. The difficulty in applying the turbulent analysis was found to be determining the boundary layer and the shear stress on the wall for deposition.

Riahi et. al. ^{[6][7][19]} studied soot deposition in a small hood. The purpose of the study was to develop a method of determining the amount of soot deposited on a surface by using an optical density method. Using optical and gravimetric measurements, an analytical model was developed to determine a correlation between a surface optical density and mass deposited on a surface.

The thermophoretic model was developed using the small hood, and was found to be appropriate for measuring soot deposition for turbulent fires against a wall. Thermophoresis was found to account for over 95% of the soot deposited on the filters.

1.4 Objectives and Scope of Work

Any new addition to FDS requires a verification and validation of the new algorithms. First, verification of the algorithms for thermophoresis and turbulent deposition will be

evaluated using a FDS model with a simple geometry. The parameters of the simulations will allow boundary conditions to be easily controlled in order to test the algorithms. The data collected for soot deposition will be compared against hand calculations. Data for the hand calculations will be obtained from the FDS output file. This will allow for the deposition algorithms to be tested independently of the other algorithms in FDS.

Once the algorithms are verified to be working as designed, simulations will be conducted to test the performance of the algorithm. Experimental data for the experiments mentioned in Section 1.1 has been collected. Simple models of the experiments will be generated and run. Finally, a comparison of the data from FDS will be compared against the data from the experiments to determine the validity of the soot deposition algorithms.

Chapter 2: Analytical Work / Methods

Soot and aerosols can deposit on surfaces due to many phenomena. Effects such as Brownian diffusion and electrophoresis were not included in the model due to their relatively small effects for fire induced flows. Below is a discussion of mechanisms relevant to this paper.

2.1 Thermophoresis

Thermophoresis is the deposition of particles on a surface due to a thermal gradient. Particles in a hot gas layer are pushed towards a colder region by the movement of the hot gasses. The thermophoretic deposition velocity for soot particles is calculated by ^[18]

$$v_T = \frac{K_{th}\mu_{air}}{\rho_{air}T} \nabla T \quad (2.1)$$

where μ and ρ are properties of air at a film temperature. The film temperature is the average of the gas and wall temperatures. T is the temperature of the gas. K_{th} is a constant, 0.55, derived from the following equation.

$$K_{th} = \frac{2C_s \left(\frac{k_g}{k_s} + C_t Kn \right) \left(1 + Kn \left(A_1 + A_2 \exp \left(\frac{-2A_3}{Kn} \right) \right) \right)}{(1 + 3C_m Kn) \left(1 + 2 \frac{k_g}{k_s} + 2C_t Kn \right)} \quad (2.2)$$

C_s , C_t , and C_m are dimensionless coefficients calculated from kinetic theory and A_1 , A_2 , and A_3 are dimensionless constants as well. The other values, k_g and k_s , are the conductivity of the gas and solid particles. Kn is the Knudsen number defined as

$$Kn \equiv \frac{\lambda}{L} \quad (2.3)$$

The Knudsen number is the ratio of the molecular mean free path to a representative length scale. The mean free path are defined as ^[20]

$$\lambda \equiv \frac{1}{2^{0.5} \pi \left(\frac{n_{tot}}{V} \right) \sigma_i^2} \quad (2.4)$$

The diameter of soot falls in the range of 0.1.-10. μm ^[18]. The small diameter yields a large mean free path. The boundary layer is used for the length scale for the Knudsen number. The mean free path, divided by a length less than 1 meter yields a high Knudsen number on the order of 10^{10} . Figure 2.1 shows K_{th} vs. Kn for various k_g/k_s ratios. Knudsen numbers greater than 10^2 yields $K_{th} \approx 0.55$.

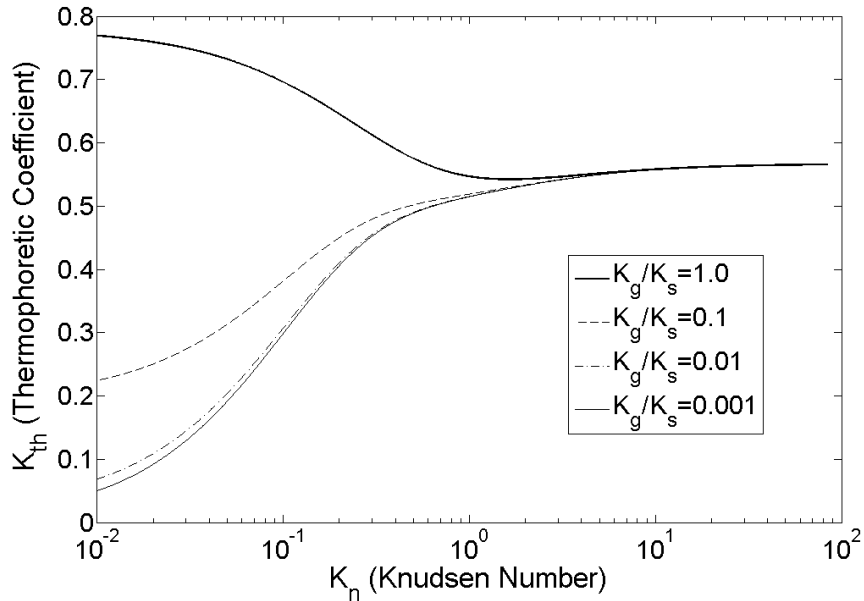


Figure 2.1 – K_{th} vs. Knudsen Number ^[6]

The temperature gradient is what drives the thermophoretic process. A heat transfer balance of convection and conduction is used to determine the temperature equation.

$$\dot{q}_{cond}'' = k_{air} \frac{dT}{dx} \quad (2.5)$$

$$\dot{q}_{conv}'' = h(T_{gas} - T_{wall}) \quad (2.6)$$

$$k_{air} \frac{dT}{dx} = h(T_{gas} - T_{wall}) \quad (2.7)$$

$$\frac{\Delta T}{\Delta x} \approx \frac{dT}{dx} = \frac{h(T_{gas} - T_{wall})}{k_{air}} \quad (2.8)$$

The final equation used to measure thermophoretic velocity is

$$v_T = \frac{(0.55)\mu_{air}}{\rho_{air}T} \frac{h(T_{gas} - T_{wall})}{k_{air}} \quad (2.9)$$

For experimental setups where it may be difficult to estimate the heat transfer coefficient h , it is possible to obtain a value for h using a radiometer and heat flux gauge to estimate the convective heat flux.

$$h = \frac{\dot{q}_{tot}'' - \dot{q}_{rad}''}{(T_{gas} - T_{water})} \quad (2.10)$$

$$\frac{\Delta T}{\Delta x} = \frac{(\dot{q}_{tot}'' - \dot{q}_{rad}'')(T_{gas} - T_{wall})}{k_{air}(T_{gas} - T_{water})} \quad (2.11)$$

Where T_{water} is the temperature of the water used to cool the heat flux gauge and radiometer. The equation for thermophoretic velocity for an experimental setup is

$$v_T = \frac{(0.55)\mu_{air}(\dot{q}_{tot}'' - \dot{q}_{rad}'')(T_{gas} - T_{wall})}{\rho_{air}T k_{air}(T_{gas} - T_{water})} \quad (2.12)$$

To find the mass deposited on a surface, the soot density must be found near the wall. Optical density is used to measure soot density. The thermophoretic velocity, optical density must be integrated over an area with respect to time. The value used for the gas phase mass specific extinction coefficient, $\sigma_{s,g}$, is 8.7 m²/g. The 95% confidence interval for $\sigma_{s,g}$ is 1.1 m²/g. [21]

$$m = A \int v_T \left(\frac{OD}{\sigma_{s,g}} \right) dt \quad (2.13)$$

2.2 Turbulent Deposition

Turbulence is a common occurrence in fire induced flows. When a turbulent eddy interacts with a surface, it imposes a shear stress on that surface. Given a no slip boundary condition, the larger the velocity of the eddy, the greater the shear stress.

An important scaling quantity in the region near the wall is friction velocity. Friction velocity is defined as [9]

$$u_f \equiv (\tau_w/\rho)^{0.5} \quad (2.14)$$

To keep computational cost low, a simple model for turbulent deposition was selected. The model selected to compute the turbulent deposition velocity is as follows.

$$v_{turb} = 0.037u_f \quad (2.15)$$

The key factor that drives turbulent deposition is the shear stress generated on a surface. Therefore, as velocity near the wall increases, so does turbulent deposition.

2.3 Sedimentation

Sedimentation is the settling velocity of a particle which is derived from the force balance between gravitational force which pulls particles down and the drag force which resists the falling motion. The velocity is calculated by

$$v_s = \frac{\rho_p d^2 g C}{18\mu} \quad (2.16)$$

Where d is the particle diameter, ρ_p is the density of the particle and g is the acceleration due to gravity. The Cunningham slip correction, C is found by

$$C(d) = 1 + K_n [A_1 + A_2 \exp(-A_3/K_n)] \quad (2.17)$$

Where $A_1 = 1.142$, $A_2 = 0.558$, and $A_3 = 0.999$.^[18]

Another factor that plays into sedimentation is coagulation of smoke particles. Smoke particles undergoing Brownian motion stick together to form larger agglomerates^[22]. The agglomerates will have a higher gravitational force which will increase their settling velocity.

Due to the current limitations within FDS, sedimentation is not currently a part of the soot deposition model.

Chapter 3: Verification of Soot Deposition Model

ASTM E 1355 ^[23] defines verification as

The process of determining that the implementation of a calculation method accurately represents the developer's conceptual description of the calculation method and the solution to the calculation method. The fundamental strategy of verification of computational models is the identification and quantification of error in the computational model and its solution.

To verify the soot deposition model is working correctly, the thermophoretic and turbulent deposition model were tested independently of each other. Simple tests were conducted to determine that the models were predicting correct deposition amounts as well as determining the proper response to altered boundary conditions.

3.1 Thermophoretic Deposition Model

To test the thermophoretic deposition model, simulations were run in a simple 1 m cube room with a burner and a vertical vent. The same geometry was run under two different boundary conditions. The first boundary condition held all walls at a constant temperature of 20 °C. The second test held all walls at 400 °C. These values were chosen to control thermophoretic soot deposition. With the two conditions, the thermophoretic velocity could be controlled. A large quantity of soot was expected to be deposited on the 20 °C walls whereas the 400 °C walls were expected to have a deposition quantity near zero.

Deposition was modeled on a 0.64 m^2 surface centered on the wall opposite of the vent 0.74 m above the floor. The open vent measured 0.6 m (2 ft) wide by 0.6 m (2 ft) high. The burner was a 20 kW fire on a 0.2 m (0.66 ft) square vent flowing propane. Instrumentation included heat flux to the wall, temperature, convective heat transfer, thermal conductivity, density, viscosity, and optical density. All properties other than heat flux were evaluated at the wall and at 2 cm away from the wall.

Equations 2.9 and 2.13 were used to calculate the mass of soot deposited on the surface using the conductivity, viscosity, density, and temperatures from FDS. Deposition mass was calculated for each time step and compared to the FDS deposition mass.

The comparison of mass calculated by hand to the mass deposited by FDS initially had a significant error of 30%. Upon investigation, it was noted that viscosity and thermal conductivity in the model were not the same as the output viscosity and thermal conductivity from FDS. FDS will provide the values evaluated at the gas temperature whereas the soot deposition model will evaluate the viscosity and conductivity at the film temperature as proposed by Riahi ^[6].

Incropera et. al. ^[24] tabulated data for thermal properties of air at various temperatures. These values were used to derive an equation to evaluate the viscosity and thermal conductivity at air at any temperature between 100 and 3000 K. The tables showed that viscosity evaluated at the film temperature was on average, 53% of the viscosity evaluated at the gas temperature. Thermal conductivity at the film temperature was found to be on average, 69% of the value evaluated at gas temperature.

The values for viscosity and thermal conductivity were reduced to the percentages found above to compensate for the difference in values between the two temperatures. Figure 3.1 shows that after the values were adjusted, the hand calculations and FDS predictions demonstrate a good agreement.

In addition to the values showing good agreement, the difference between the two cases shows the anticipated behavior. There is a reasonable amount of deposition for the 20 °C wall case while the 400 °C wall case had a very small amount of deposition. Deposition in the 400 °C wall case is attributed to noise in the gas temperature. The noise is likely a result of the poorly resolved mesh used for the model.

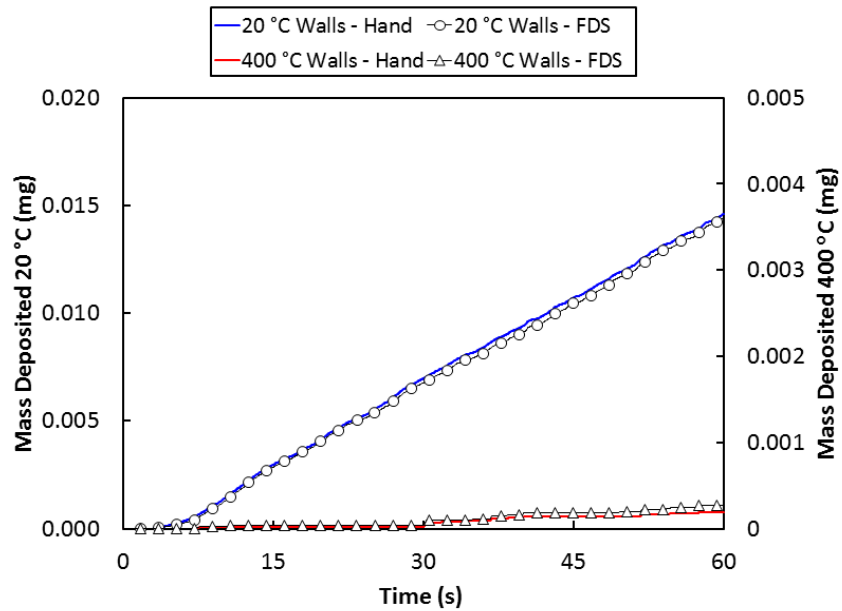


Figure 3.1 – Soot deposition mass for thermophoretic verification with adjusted values for viscosity and thermal conductivity.

3.2 Turbulent Deposition Model

A simple FDS simulation was created to determine if the turbulent deposition model was working correctly. The model consisted of a 0.6 m (2 ft) square burner centered below a chimney. The chimney started 0.3 m (1 ft) above the base of the fire and extended up 0.6 m (2 ft). The cross section of the chimney was equal to the area of the burner. As the fire burned, soot was deposited and measured on the inside of the chimney.

FDS does not currently have the appropriate outputs required to check the equations as was done for the thermophoretic validation. Even though the equations could not be checked directly, a demonstration of the principle was performed.

The test set up was run under two configurations. First, a 90 kW fire was modeled on the burner and the chimney was left open at the top. Next, a fan was placed on top of the chimney to pull smoke through the chimney at a higher velocity. This increased the shear stresses on the walls without increasing the soot yield by increasing the fire.

Figure 3.2 shows that the addition of the fan increased soot deposition on the walls of the chimney. While a more rigorous verification would be useful, this test demonstrates that the turbulent deposition model provides the proper trend of increasing deposition rates with higher velocities.

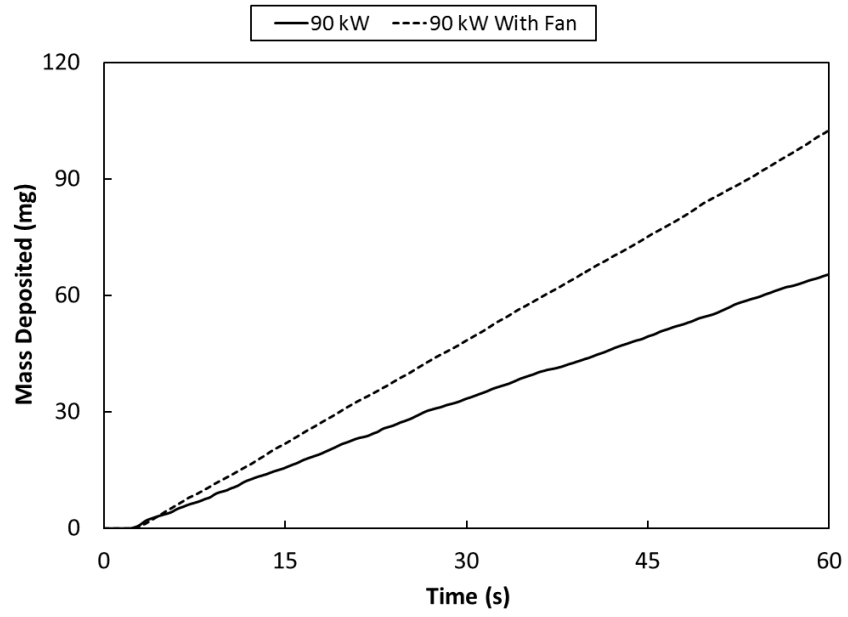


Figure 3.2 – Soot deposition mass for turbulent verification

Chapter 4: Validation of Soot Deposition Model

ASTM E 1355 ^[23] defines validation as:

The process of determining the degree to which a calculation method is an accurate representation of the real world from the perspective of the intended uses of the calculation method. The fundamental strategy of validation is the identification and quantification of error and uncertainty in the conceptual and computational models with respect to intended uses.

In testing the soot deposition model of FDS, a wide range of configurations were tested. Fire sizes ranged from 2 kW to 2 MW, three fuels with varying soot yields were examined, and compartments ranging from 0.34 m³ to 582 m³ (12 ft³ to 20,559 ft³). This range provides the ability to determine the validity for small and large fire and room sizes as well as determine fuel independence. A few simulations were also performed at various grid cell resolutions to determine grid dependence.

4.1 Development of models

4.1.1 NIST/NRC Test Series

The test setup used a 7.04 m x 21.66 m x 3.82 m (23.1 ft x 71.2 ft x 12.5 ft) room ^[25]. Figure 4.1 shows a photograph of the test compartment before testing and a view of the compartment rendered in smokeview. The grid used for the NRC tests is shown in Figure 4.2. Mesh stretching was used to reduce computational time while allowing a high grid resolution around the fire.

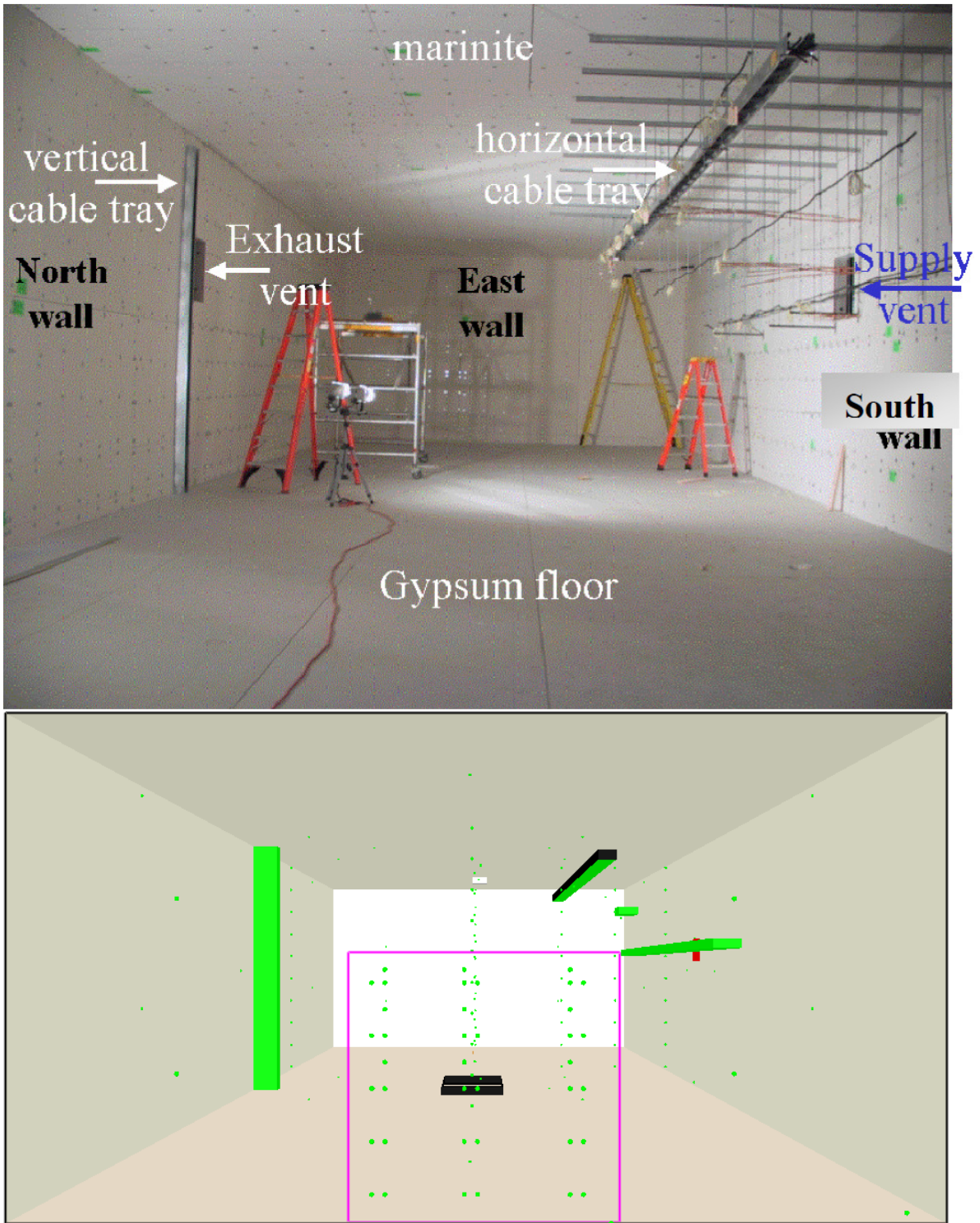


Figure 4.1 – Experimental Setup for NIST/NRC Tests.
 (Top – Experimental Setup^[25], Bottom – FDS Setup)

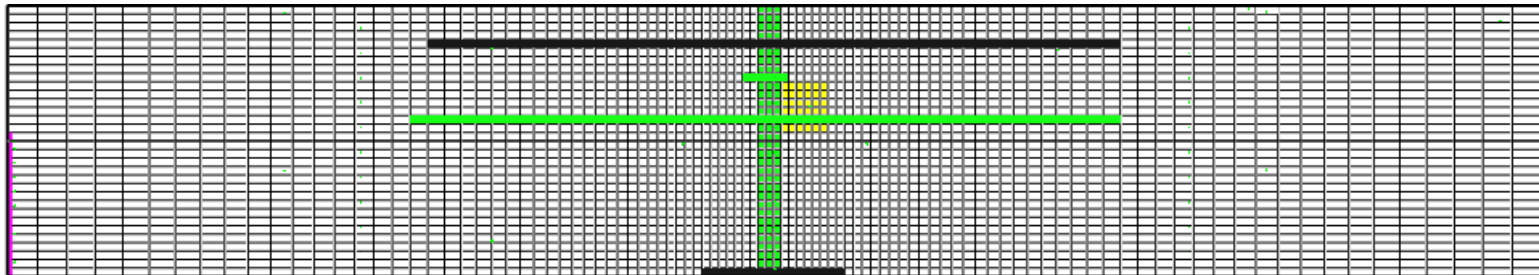
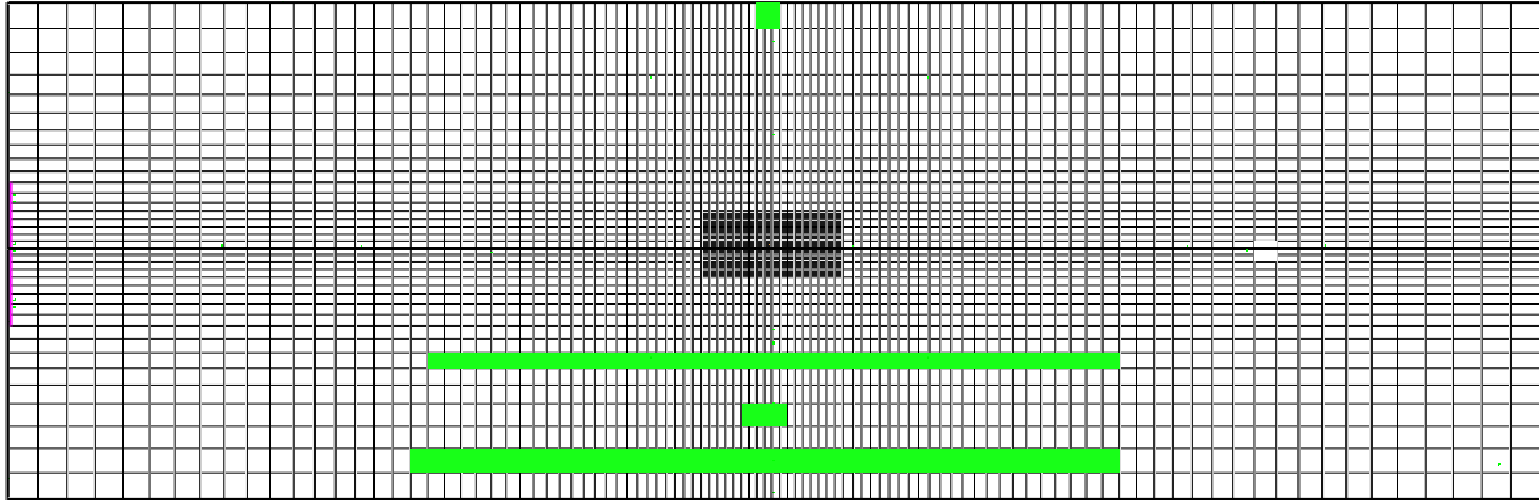


Figure 4.2 – Mesh Prescribed for NRC FDS Files. Plan View (Top) and Front View (Bottom)

The test series uses a heptane spray burner located in the center of the room. A nozzle was aimed downward towards a 1 m by 2 m (3.33 ft by 6.66 ft) stainless steel pan. Flow rates through the nozzle were used to control fire size. For open door tests, calorimetry was used to confirm the burning rate.

Multiple cable trays were located in the room. Heat flux gauges and thermocouples were positioned throughout the room to monitor conditions in the room and heat transfer to the various targets in the room. Supply and exhaust forced ventilation was used for various tests providing 5 air changes per hour. A 2.00 m by 2.00 m (6.56 ft by 6.56 ft) door was located in the west wall which was either open or closed as the test required.

Heat flux gauges, radiometers, and the optical density meter were the primary devices of interest. All heat flux gauges and radiometers were placed along the midline running north to south. The optical density meter was located in the southeast corner near the ceiling. The location of these devices can be found in Figure 4.3.

The NIST/NRC test series was modeled by NIST in FDS. The FDS input files were downloaded from the FDS subversion repository and run as they were downloaded. No changes were made to the files in order to compare the results of the soot deposition model simulations to the results found without the soot deposition model with the exception of the MISC line. The MISC line was edited to enable soot deposition as explained in Section 1.2.3.

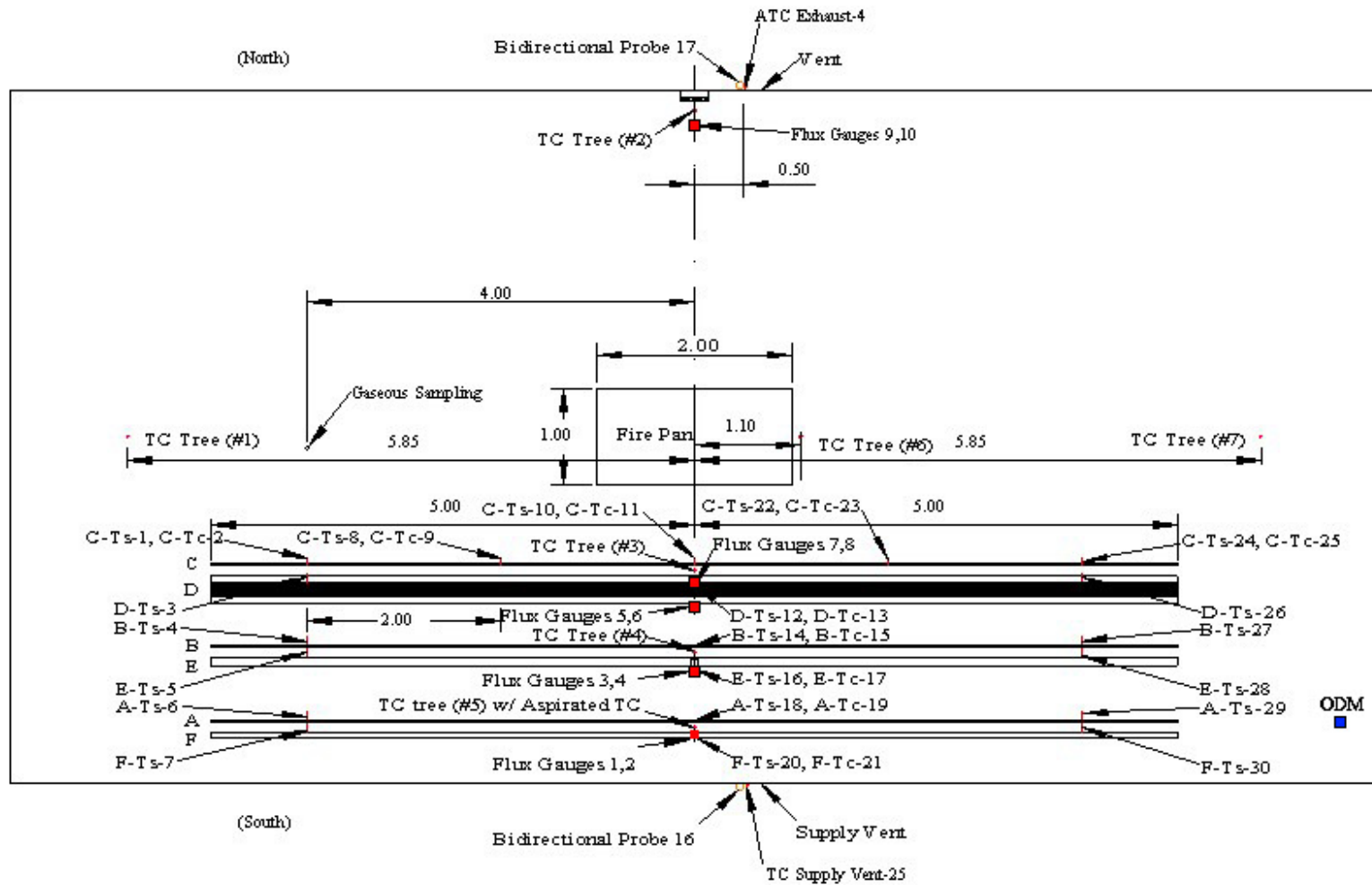


Figure 4.3 – Location of Heat Flux Gauges and Radiometers (Red) and the Optical Density Meter (Blue) ^[25]

4.1.2 Corridor Test Series

The test corridor is a 14.6 m (48 ft) long corridor with a width of either 1.52 m (5 ft) or 3.66 m (12 ft). Walls were movable to simulate the two corridor widths as well as an infinite ceiling by removing the walls. The walls were constructed by hanging sheets of gypsum board for the top 1.2m (4 ft) of the corridor. Below the gypsum, plastic sheeting was hung to reduce weight and allow for the corridor to be tested at elevations of 2.7, 3.7, and 5.5m (9, 12, and 18 ft).

Beams were constructed to be modular and allow the corridor to be tested with beams that were 0.3m or 0.6m (1 ft or 2 ft) deep. The beams could also be removed to simulate a smooth ceiling corridor.

The fire used for most tests was a 100 kW propylene fire from a sand burner. Seven tests used a 15 kW fire. Surrounding the sand burner was a baffle consisting of 1.2 m wide by 0.6m tall (4 ft by 2 ft) gypsum boards.

A cell size of 5 cm (2 in) was determined to optimize resolving the flame and jet flow against computational cost. Areas which required the fine mesh were around the fire and along the ceiling. The fine mesh extended 0.91 m (3 ft) from the center of the fire in each direction along the corridor as well as 1.2 m (4 ft) below the ceiling. A small mesh was placed on either end of the corridor extending 1.2 m (4 ft) and 0.3 m (1 ft) above the ceiling to account for the eddies that would form beyond the corridor. The rest of the domain was modeled with a 10 cm (4 in) cell size. Figure 4.4 shows the locations of fine and coarse meshes.

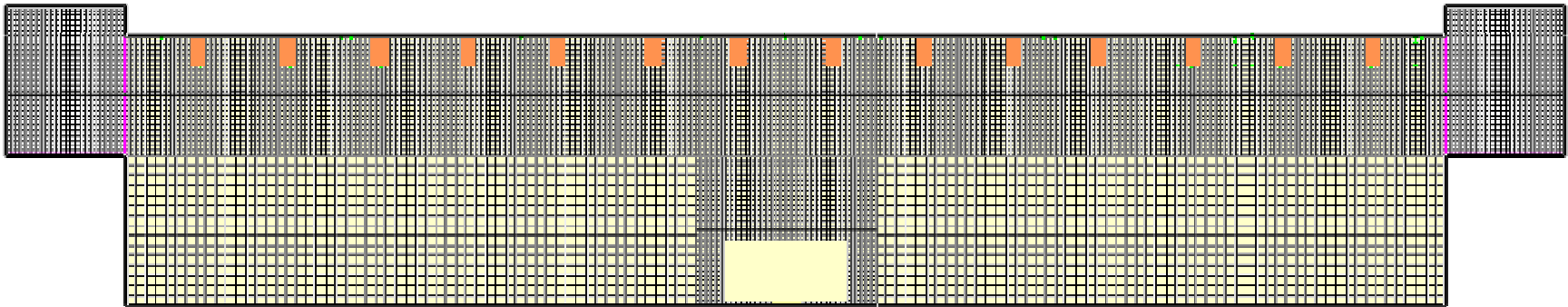


Figure 4.4 – Fine and Coarse Mesh for Corridor Test Series

All simulations were 2.7 m (9 ft) tall and 1.5 m (5 ft) wide. The length of the corridor spanned 6.7 m (22 ft) in each direction from the fire for a total of 13.4 m (44 ft). For tests that required beams, 0.3 m (1 ft) beams were spaced 0.9 m (3 ft) apart on center, and centered so that the fire was centered between two beams as done in the experimental tests. All surfaces except the floor were modeled as gypsum board.

Thermocouples, optical density meters, and velocity meters were placed throughout the model as they were placed in the test series. The various smoke detectors were omitted from the model. Figure 4.5 shows the location of all the devices in the experimental setup and the models.

The burner was modeled as a propylene burner with a soot yield of $0.047 \text{ g}_{\text{soot}}/\text{g}_{\text{fuel}}$. The burner was a 0.3 m by 0.3 m (1 ft by 1 ft) square elevated 5 cm (2 in) above the ground. Surrounding the burner a baffle was modeled to replicate the baffle used in the experiments. The baffle consisted of 4 walls 1.2 m (4 ft) long by 0.6 m (2 ft) high. A 5 cm (2 in) gap was left under the baffle to allow for air flow to the burner.

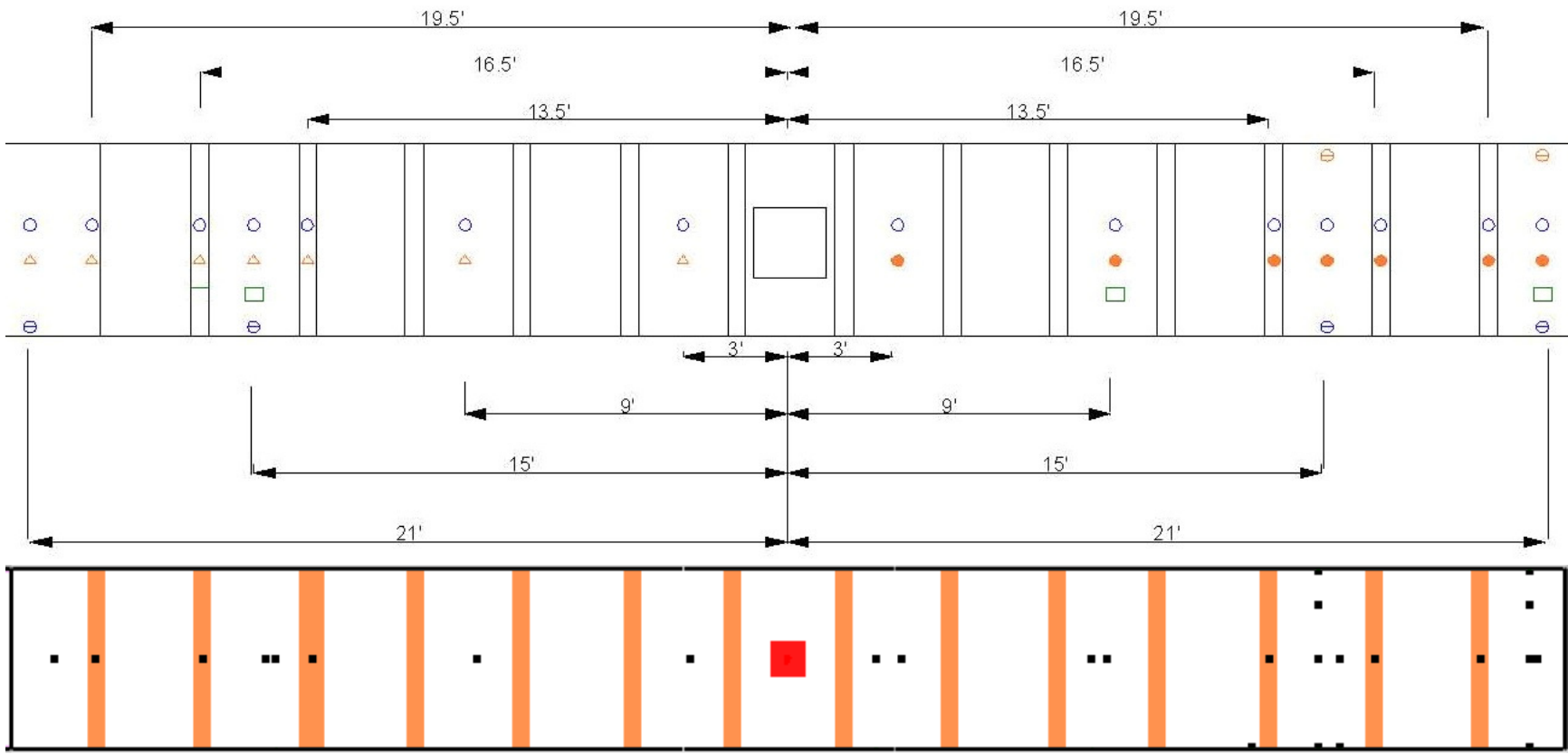


Figure 4.5 – Plan View of Device Locations in Corridor (Top – Experimental^[2], Bottom – FDS Model)

4.1.3 Thermophoretic Deposition Hood

The hood used by Riahi ^[1] was a 0.6 m by 0.6 m by 0.9 m high (2 ft by 2 ft by 3 ft high) chamber with a burner centered in the bottom. On one side, there was a 0.46 m by 0.3 m by 0.3 m high (1.5 ft by 1 ft by 1 ft high) exhaust plenum. All walls of the hood were made of Fiberfrax Duraboard® held together by a steel frame. The bottom of the hood was left open. Instrumentation was located on the front of the hood at elevations of 0.54 m (1.7 ft) and 0.76 m (2.5 ft). Instrumentation included a heat flux gauge, radiometer, optical density meter, gas and wall thermocouples, and 9 cm (3.5 in) diameter glass fiber filter at each location. Figure 4.6 shows the hood and instrumentation used for the experiments.

A sensitivity study was performed to determine the optimal mesh size for the simulation. A 1 cm mesh did not provide a sufficient benefit over a 2 cm mesh. In order to reduce computational cost, the entire domain was modeled with a 2 cm mesh. The mesh was extended 0.3 m (1 ft) below the hood to properly resolve the flow field for air entering the hood.

Another study was performed to determine the length of the exhaust duct required in the model to replicate the conditions in the hood. Running models with various lengths of duct extending from the exhaust plenum showed no difference in the main part of the hood. Therefore, the exhaust duct was modeled as a vent at the top of the exhaust plenum.

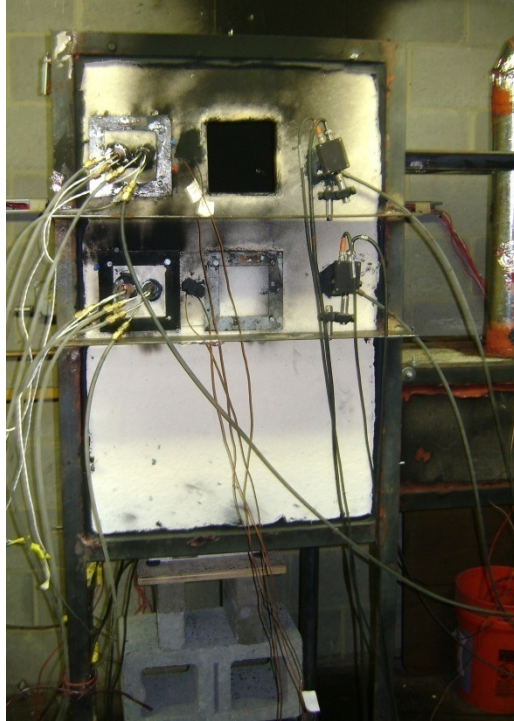


Figure 4.6 – Front View of the Soot Deposition Hood

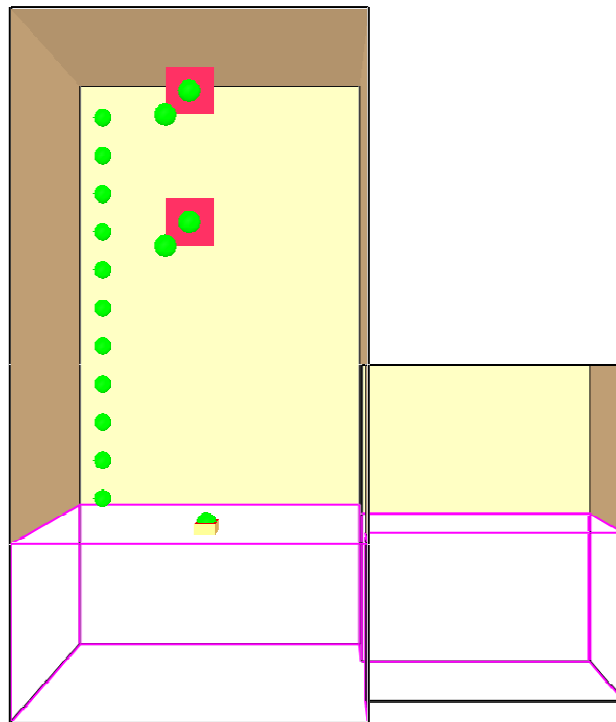


Figure 4.7 – FDS Model of the Soot Deposition Hood

The primary difference between the hood and the model is the location of the instrumentation. One assumption made by Riahi ^[1] was that at any given elevation, the smoke layer was uniform in temperature and optical density. Therefore, all the instrumentation was centered on the front wall.

Filters were placed within the model to compare the mass deposited in the experiments to the mass deposited in the model. Due to the constraints of FDS, the filters were modeled as 8 cm by 8 cm squares. The error in the filter size was less than 1%. Figure 4.7 shows the location of the filters within the hood.

4.2 Test matrix of models

4.2.1 NIST/NRC Test Series

The original experiments consisted of 18 experiments where experiments 7 through 12 were replicates of tests 1 through 6. Tests 6, 11, and 12 were not conducted. Of the 11 unique tests, 6 tests were run for validation purposes.

Tests 2-5 provide a variety of ventilation configurations ranging from a closed room with no air movement to a room with an open door and a ventilation system. The four configurations provided in tests 2 through 5 allow for examination of ventilation effects on the soot deposition algorithm. Forced air will affect the turbulent model, while the open door will lead to lower upper gas layer temperatures.

Tests 1 and 13 have the same setup as test 2 except for the nominal heat release rate. Test 1 used a 350 kW fire where Test 13 used a 2 MW fire. The inclusion of Tests 1 and 13

allowed the validation to be extended to a wider range of fire sizes. Table 4.1 shows all experiments tested for this series.

A total of 12 simulations were run. Each test setup was run with no soot deposition to compare values to those obtained from the FDS simulations run for the study. All 6 configurations were then run with the soot deposition model turned on, allowing for both thermophoretic and turbulent deposition.

Table 4.1 – Experimental Tests Performed for NIST/NRC Test Series ^[25]

Test	Nominal Peak \dot{Q} (kW)	Fuel	Burner Location	Door	Ventilation
1*	350	Heptane	Center	Closed	Off
2*	1000	Heptane	Center	Closed	Off
3*	1000	Heptane	Center	Open	Off
4*	1000	Heptane	Center	Closed	On
5*	1000	Heptane	Center	Open	On
7	350	Heptane	Center	Closed	Off
8	1000	Heptane	Center	Closed	Off
9	1000	Heptane	Center	Open	Off
10	1000	Heptane	Center	Closed	On
13*	2000	Heptane	Center	Closed	Off
14	1000	Heptane	1.8 m from N wall on E-W centerline	Open	Off
15	1000	Heptane	1.25 m from S wall on E-W centerline	Open	Off
16	2000	Heptane	Center	Closed	On
17	1000	Toluene	Center	Closed	Off
18	1000	Heptane	1.55 m from S wall, 1.50 m E of centerline	Open	Off

* Test series was simulated and tested for soot deposition

4.2.2 Corridor Test Series

The corridor tests involved a series of 49 tests.. The tests were conducted using a movable ceiling which allowed experiments to be run at elevations of 2.7, 3.7, and 5.5 m (9, 12, and 18 ft). The walls on either side of the corridor were movable to allow tests to be conducted for corridor widths of 1.5 m (5 ft) and 3.6 m (12 ft). The walls could also be removed in order to simulate a large open room where walls would not trap the smoke in the area above a fire. Beams were removable to allow smooth, flat ceilings as well as beamed ceilings with beams spaced every 0.9 m (3 ft) on center and 0.3 and 0.6 m (1 ft and 2 ft) deep. The configuration of the modular corridor allowed for 21 unique geometries to be arranged. Each arrangement was tested twice with 100 kW fires. Additionally, a series of 7 experiments were conducted testing various arrangements with a 15 kW fire. Table 4.2 shows the various configurations tested.

Four test series were modeled in FDS for soot deposition validation. Test 5 simulates a large, open room while tests 31 and 37 model a corridor with and without beams respectively. Test 44 was included in order to test two fire sizes with the same geometry. All four experiments which were modeled had 2.7 m (9 ft) ceiling heights, and the three corridors were 1.5 m (5 ft) wide. The reason for this selection was to reduce the size of the computational domain and allow the models to run in less time without sacrificing grid resolution.

Table 4.2 – Experimental Tests Performed for the ICFMP Test Series ^[2]

Test	Corridor		Beam		Fire Size
	Height (ft)	Width (ft)	Spacing (ft)	Depth (ft)	kW
1 & 2	18	Open		No Beams	100
3 & 4	12	Open		No Beams	100
5 & 6*	9	Open		No Beams	100
7 & 8	9	12		No Beams	100
9 & 10	12	12		No Beams	100
11 & 12	18	12		No Beams	100
13 & 14	18	12	3	1	100
15 & 16	12	12	3	1	100
17 & 18	9	12	3	1	100
19 & 20	18	12	3	2	100
21 & 22	12	12	3	2	100
23 & 24	9	12	3	2	100
25 & 26	18	5	3	2	100
27 & 28	12	5	3	2	100
29 & 30	9	5	3	2	100
31 & 32*	9	5	3	1	100
33 & 34	12	5	3	1	100
35 & 36	18	5	3	1	100
37 & 38*	9	5		No Beams	100
39 & 40	12	5		No Beams	100
41 & 42	18	5		No Beams	100
43	9	5	3	2	15
44*	9	5	3	1	15
45	12	5	3	1	15
46	18	5	3	1	15
47	9	5		No Beams	15
48	12	5		No Beams	15
49	18	5		No Beams	15

* Test series was simulated and tested for soot deposition

4.2.3 Thermophoretic Deposition Hood

Over 50 tests were performed to test five different fuels: PMMA, PP, gasoline, ABS, and fiberboard. For each fuel, sample size was constant for all tests. The primary difference between two tests for the same fuel was duration. For solid fuels such as PMMA, several 3 in by 3 in samples were stacked on top of each other. For liquid fuels such as gasoline, the liquid volume changed with the surface area remaining constant.

Table 4.3 – Select Experimental Tests Performed for Soot Deposition Study

Fuel	Sample Size	Peak HRR[†]	Exhaust Rate[†]	Soot Yield[†]	CO Yield[†]
PMMA	3" x 3" Square	6.55 kW	12.5 g/s	0.015 g/g	0.008 g/g
PP	4" Diameter Pan	6.77 kW	16.7 g/s	0.045 g/g	0.023 g/g
Gasoline*	2.5" Diameter Pan	1.97 kW	16.4 g/s	0.080 g/g	0.011 g/g

[†] Calculated by experiments

* Test series was simulated and tested for soot deposition.

For this test series, gasoline was the only arrangement modeled. Gasoline was chosen for the model due to its quasi-steady heat release rate and high soot yield. Due to the computational cost of modeling the hood tests, the other fuels in Table 4.3 were not simulated.

4.3 Evaluation of performance

4.3.1 NIST/NRC Test Series

The inclusion of the soot deposition model in FDS improved the NIST/NRC simulations. Figure 4.8 through Figure 4.13 show the smoke density as measured from the experiments compared to the prediction from FDS, with and without the soot deposition model. In all cases, the soot deposition model reduces the prediction of soot density.

Due to noise in the models, the data was averaged over 7 data points (± 3) which equated to 60 s (± 30 s). Shifting the data in time allowed for better agreement in smoke density for most tests. However, the shifting in time resulted in an increase in error in layer height and heat flux measurements. It was determined that leaving the time as originally reported provided the best and most accurate results across all data considered.

Figure 4.8 shows that Test 1 does not have much of a difference between the two models, however, the soot deposition model is predicting slightly lower smoke concentrations compared to the model without soot deposition. The peak temperature for Test 1 near the optical density meter was 155 °C. Low gas temperatures result in a low thermophoretic deposition velocity. Riahi ^[6] discovered that thermophoresis accounts for 95% of soot deposition in open compartments.

While Test 1 was not an open compartment, Riahi's findings show the relative effect of the two soot deposition mechanisms included in the model. Since thermophoresis is highly dependent on the temperature gradient, and thermophoretic deposition is the dominant mechanism, we see that the models yield similar results for Test 1.

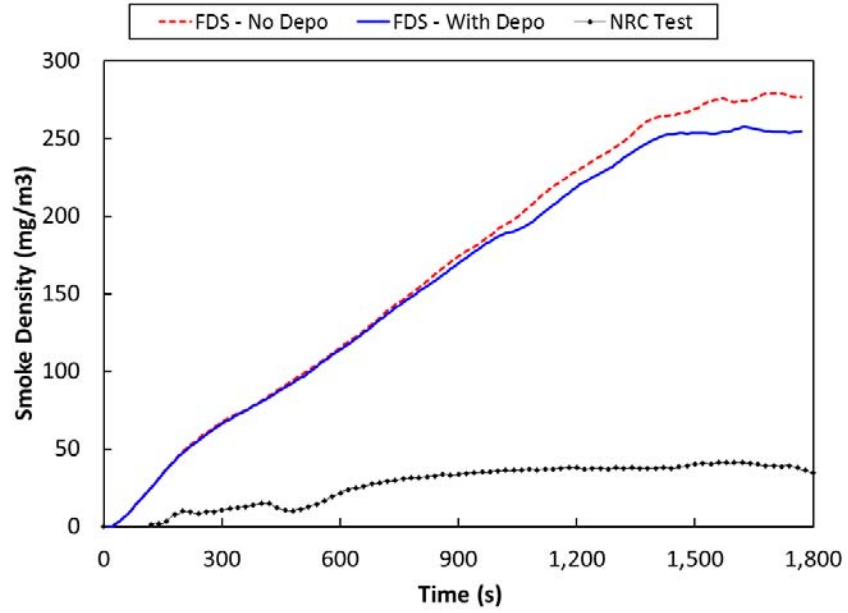


Figure 4.8 – Smoke Density for Test 1 – 350 kW Fire
Door Closed, Ventilation Off

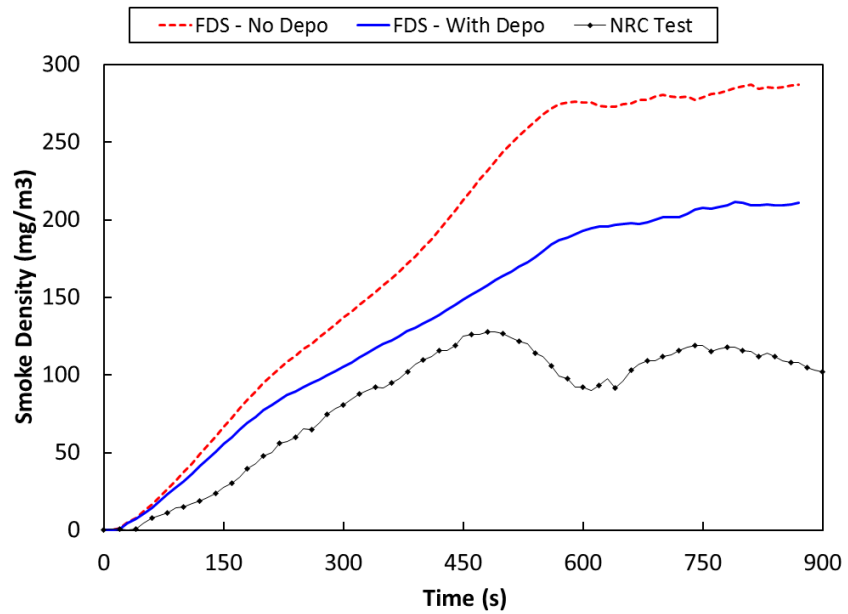


Figure 4.9 – Smoke Density for Test 2 - 1MW Fire
Door Closed, Ventilation Off

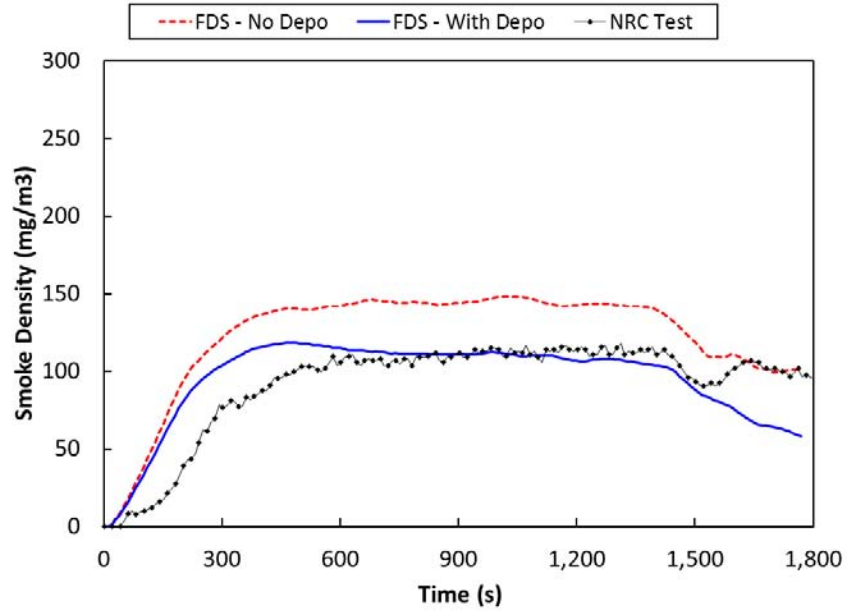


Figure 4.10 – Smoke Density for Test 3 - 1 MW Fire
Door Open, Ventilation Off

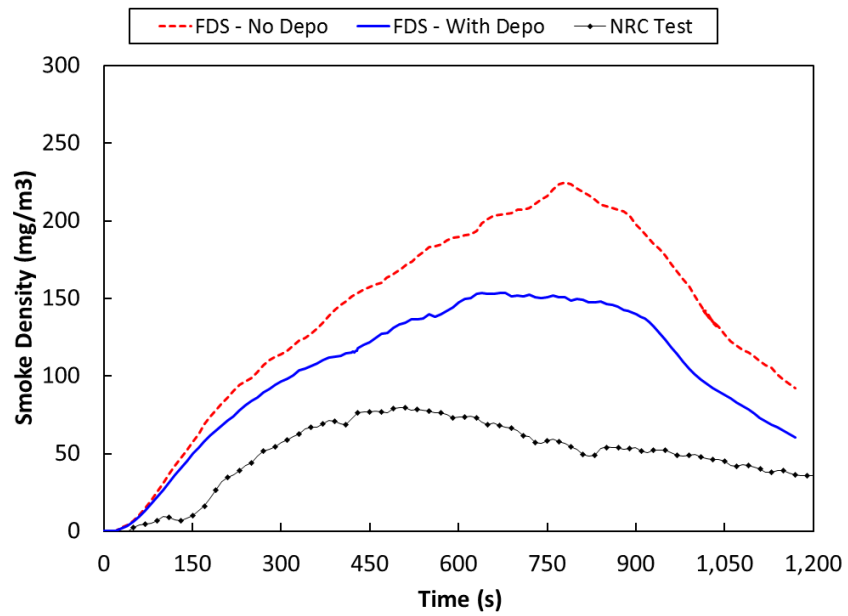


Figure 4.11 – Smoke Density for Test 4 - 1 MW Fire
Door Closed, Ventilation On

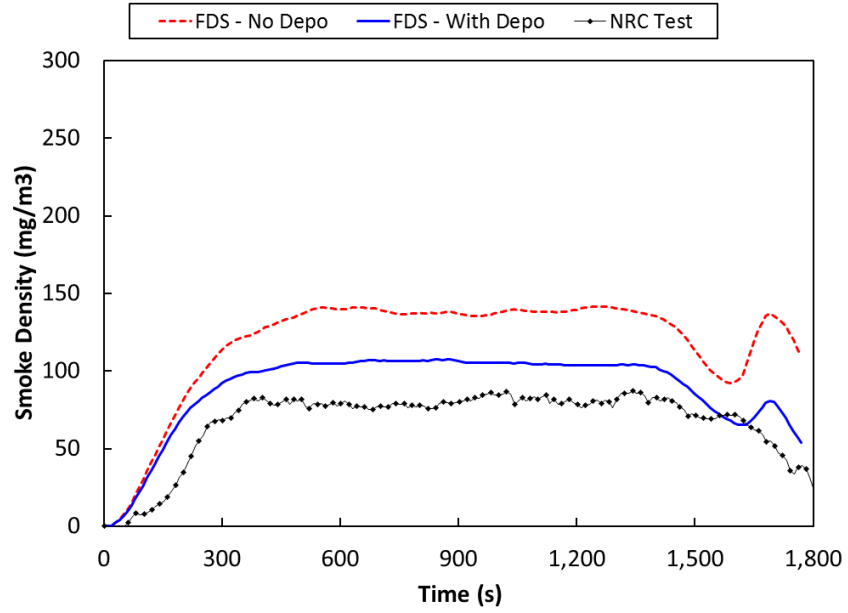


Figure 4.12 – Smoke Density for Test 5 - 1 MW Fire
Door Open, Ventilation On

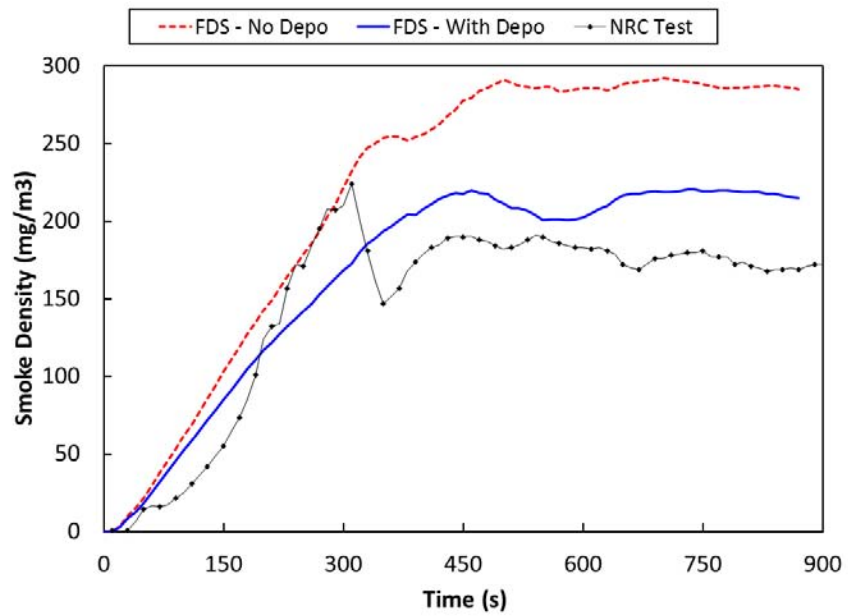


Figure 4.13 – Smoke Density for Test 13 – 2MW Fire
Door Closed, Ventilation Off

Tests 2, 3, 4, 5 and 13 all yielded more accurate results. Smoke densities were improved on average by 45%. Table 4.4 shows the difference in the two FDS models compared to the test data. Eight points were averaged from each test to determine the accuracy of the model. The eight points were evenly spaced throughout the test and covered ramp up, quasi-steady state, and ramp down periods. Error is defined as the difference between the model results and experimental results normalized by the experimental results.

$$\%Error = abs\left(\frac{Numerical - Experimental}{Experimental}\right) \quad (4.1)$$

Table 4.4 – Differences in FDS, with and without Soot Deposition Model, in Predicting Smoke Density vs. Test Data for NRC Tests

Test Number	No Deposition Model %	With Deposition Model %	Difference
1	480 %	464 %	16 %
2	113 %	60 %	53 %
3	55 %	29 %	26 %
4	217 %	144 %	73 %
5	79 %	40 %	38 %
13	59 %	25 %	34 %
Average ¹	105 %	60 %	45 %
Open Door Average ²	67 %	35 %	32 %
Closed Door Average ^{1,3}	130 %	76 %	54 %

¹ Test 1 was omitted from the calculation

² Tests 3, and 5

³ Tests 2, 4, and 13

Figure 4.14 shows the data points comparing predicted smoke density to the measured smoke density. From the graphs, it is clear that FDS is over predicting the smoke density. When FDS incorporates soot deposition into the model, data tends to lie closer to the measured values.

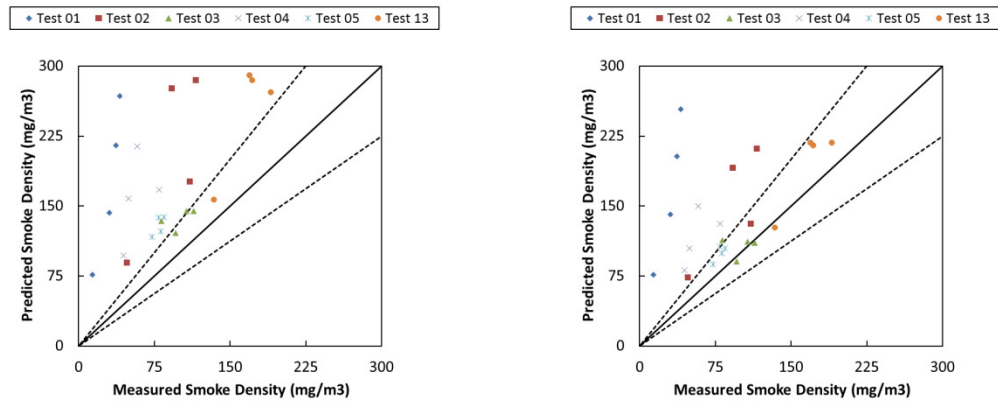


Figure 4.14 –NRC Predicted vs. Measured Smoke Densities for FDS Model without Soot Deposition (Left) and with Soot Deposition (Right)

On average, FDS was over predicting the soot density by 105%. With the soot deposition model, the average simulation over predicted by 60%. From looking at the graphs, a trend is noticed that the two open door tests perform better than the four closed door simulations.

The model without soot deposition over predicted the smoke density by 67% for the open door cases. For closed door tests the rate increased to 130%. With soot deposition incorporated into the model, the over prediction of soot fell to 35% and 76% for open and closed door tests respectfully.

The overall drop in smoke density predicted by the soot deposition model implies that the current model has an impact on the optical density in the room. Figure 4.10 shows that the soot deposition model agrees very well with the test data for Test 3. On average, the soot deposition model is over predicting the smoke density by 26%. However, the majority of the error lies within the ramp up and down of the fire. Neglecting the error in the beginning and end of the test, on average, the error in the model is less than 5%.

Test 5 proved to have good agreement between the soot deposition model and the test data as well. The incorporation of the soot deposition reduced the predicted smoke density levels in FDS from 79% to 40%. If the error in the growth phase of the fire is ignored, the error drops from 40% to below 30%.

For the closed door tests, the soot deposition model has a greater effect. Closed door tests improved by 54% whereas open door tests only improved by 32%. This difference can easily be explained by the higher soot density in the room. Thermophoretic and turbulent deposition are both dependent on the smoke concentration near the wall. In the closed door tests, smoke remains in the compartment, increasing the smoke concentration. The higher concentration yields a higher deposition rate which in turn has a larger effect in removing smoke from the hot layer.

Despite the larger effect from thermophoretic and turbulent deposition, there is still a larger error with the model in closed door tests compared to the open door tests. As seen in Table 4.4, FDS over predicts the smoke density by 76% with the soot deposition model in a closed compartment. The larger error implies that other effects are not being accounted for.

Including sedimentation in the soot deposition model will reduce the error in both open and closed compartments. Soot particles will sediment on their own due to the fact that they are solid and denser than air. The rates at which soot particles will settle is a balance between gravitational and drag forces ^[18]. Additionally, with higher soot concentrations, the collision rate of particles will increase. As soot particles collide, they tend to agglomerate. These larger particles tend to have a higher settling rate than smaller particles as seen in Table 1.1.

In addition to the effects of ventilation in the compartments, effects from the fire size make a difference in the accuracy of the model. Figure 4.15 through Figure 4.17 relate to a progression in fire size. All three tests were closed door tests with ventilation off. The only difference between the tests is the fire size. As fire size increases, the error in the model decreases.

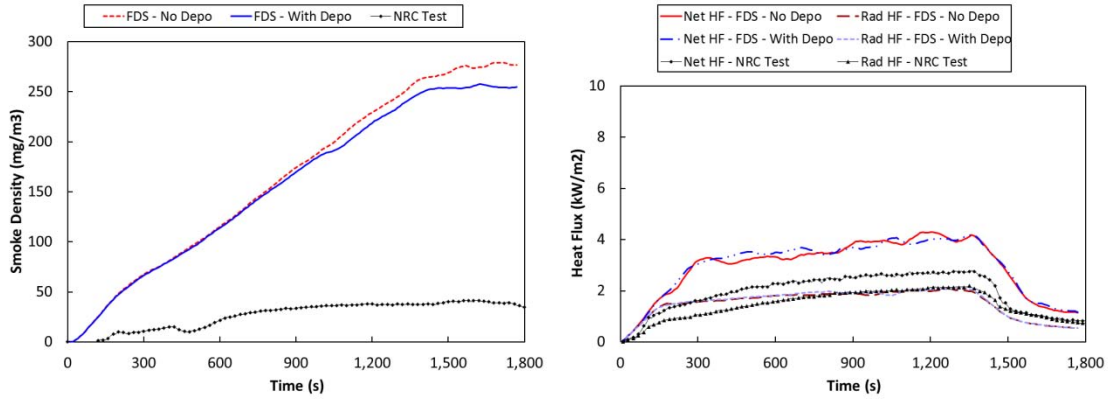


Figure 4.15 – Smoke Concentration (Left) and Heat Flux 6 and Radiometer 5 measurements (Right) for Test 1 – 350 kW Fire

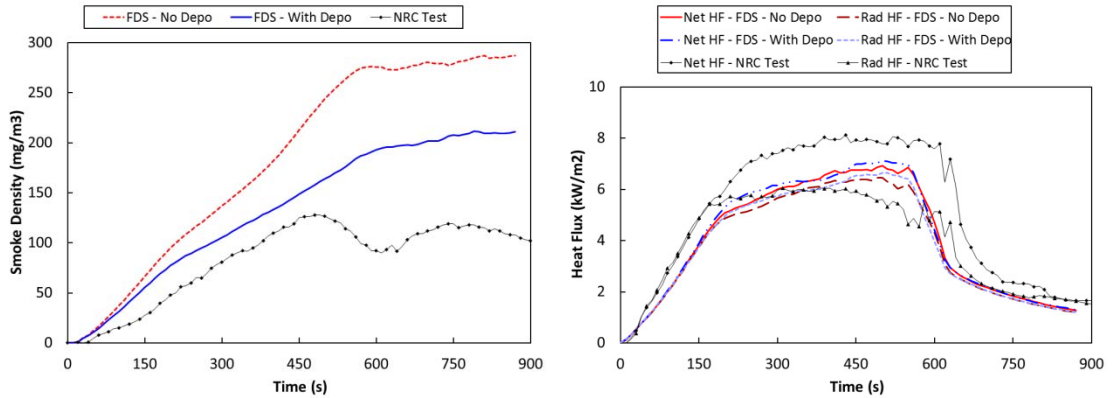


Figure 4.16 – Smoke Concentration (Left) and Heat Flux 6 and Radiometer 5 measurements (Right) for Test 2 – 1 MW Fire

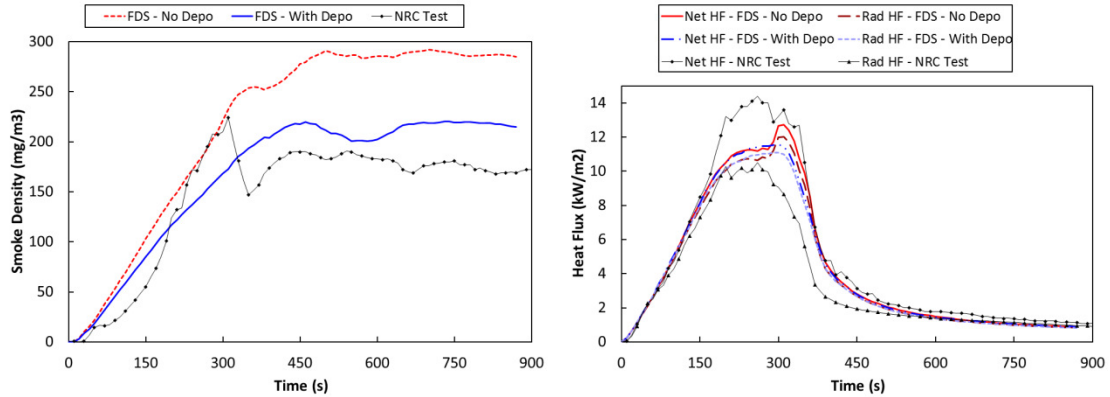


Figure 4.17 – Smoke Concentration (Left) and Heat Flux 6 and Radiometer 5 measurements (Right) for Test 13 – 2 MW Fire

Quintiere ^[13] states that fuel behavior changes within enclosures due to thermal effects and ventilation effects. These effects drive the heat release rate. A comparison could be performed to check that burning rates are matched between the models and test data. However, the heat release rates for the open door tests were calculated by calorimetry. Since the compartment doors need to be open to use the calorimetry, data is not available for the heat release rate for the closed door tests.

Mulholland ^[26] studied the effect of scale on smoke emission. He found that by applying an external radiant flux to the smaller samples, he was able to match the mass loss rates for small and large scale fires. However, Mulholland was not able to reproduce other phenomena across scales. Table 5.5 shows data from the experiments performed with heptane pool fires ranging from 60 mm (2.4 in) to 500 mm (19.7 in) in diameter

Table 4.5 – Comparison of Soot Yields for Small and Large Scale Heptane Fires ^[26]

Conditions	Heat Flux (kW/m ²)	\dot{Q} (kW)	Y_s
Large Scale 500 mm Pool		240	0.012
Large Scale 310 mm Pool		70	0.009
	0	3	0.010
Small Scale 85 mm Pool	10	7	0.013
	20	10	0.010
	30	15	0.006
	0	1	0.015
Small Scale 60 mm Pool	10	3	0.016
	20	5	0.013
	30	7	0.013

It is evident that soot yield varies with scale. All the FDS input files used the same soot yield. Without knowing the exact soot yield of each test, it is difficult to know how much error is due to the soot yield versus other aspects of the model.

4.3.2 Corridor Test Series

Overall, the models for the corridor tests performed well. There was not a significant difference observed between FDS with and without the soot deposition model. The observation where FDS was over predicting the optical density by a factor of two found by Mealy et. al. ^[2] was not replicated. For the 100 kW fires, the optical densities tended to agree within 20%.

All model data for the corridor was smoothed with a 41 point (± 20 points) average which equated to averaging 3.6 s (± 1.8 s) for each time step. Times were shifted so optical density data measured 0.6 m (2 ft) from the fire lined up.

To determine the average error in the tests, eight data points were taken from each model in each test and compared to the test data. All data points were based off the optical density meter located 2.4 m (8 ft) from the fire source in the direction of the corridor. The optical density meter at 0.6 m (2 ft) from the fire was not used for this analysis due to the large amount of noise in test 5 which represented an infinite ceiling configuration.

All data points were chosen from the second half of the tests. This was done because there is a large error in temperatures and optical densities for the beginning of the tests. This error is believed to be the difference between the sand burner used for the tests and the design fire prescribed in the models. When a sand burner is first ignited, a mixture of fuel and air that was in the plenum flow through the sand burner. It was believed that the error in the beginning of the tests was due to the differences in fuel flow from the model and the burner. Once the sand burner was purged of air, the fire reached a quasi-steady state. The design fire modeled was a 100 kW steady state fire. Once steady state was reached, the data had good agreement for the remainder of the tests as seen in Figure 4.18 through Figure 4.20.

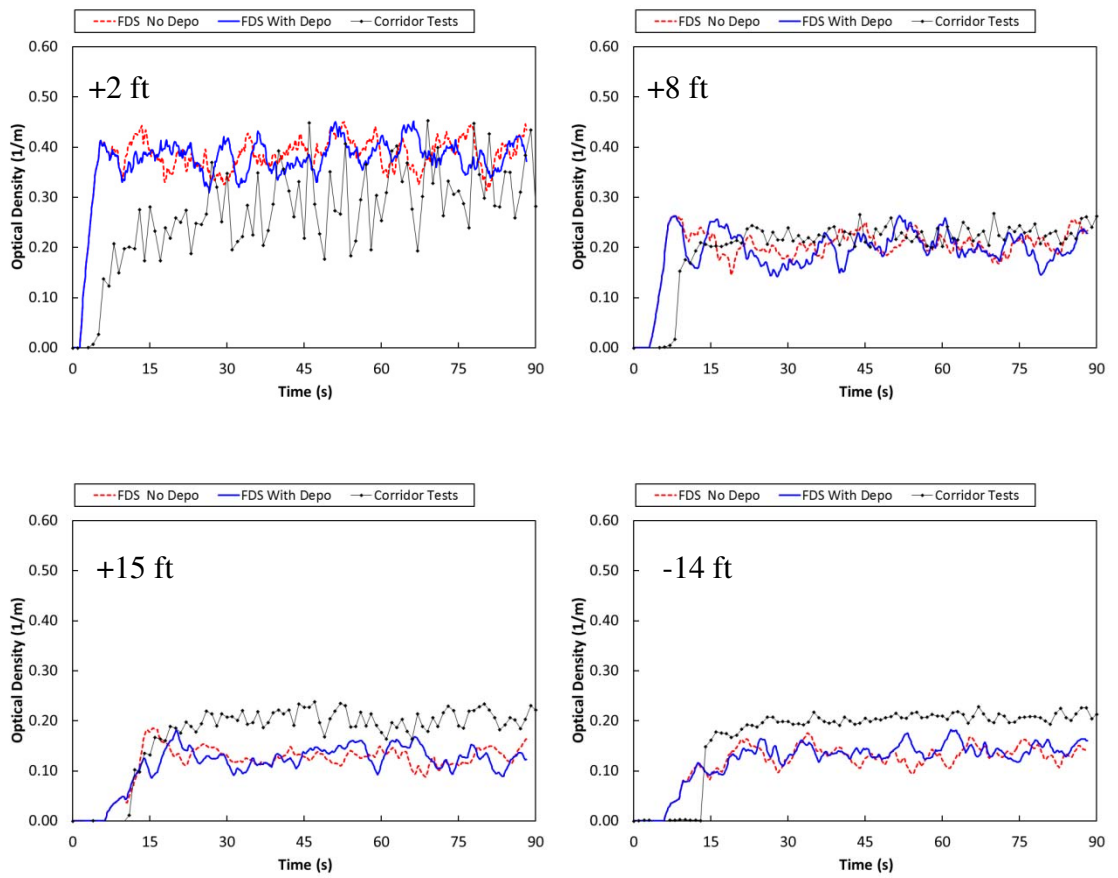


Figure 4.18 – Optical Density vs. Time at Four Location along Corridor for Test 5 – Infinite Smooth Ceiling, 100 kW Fire

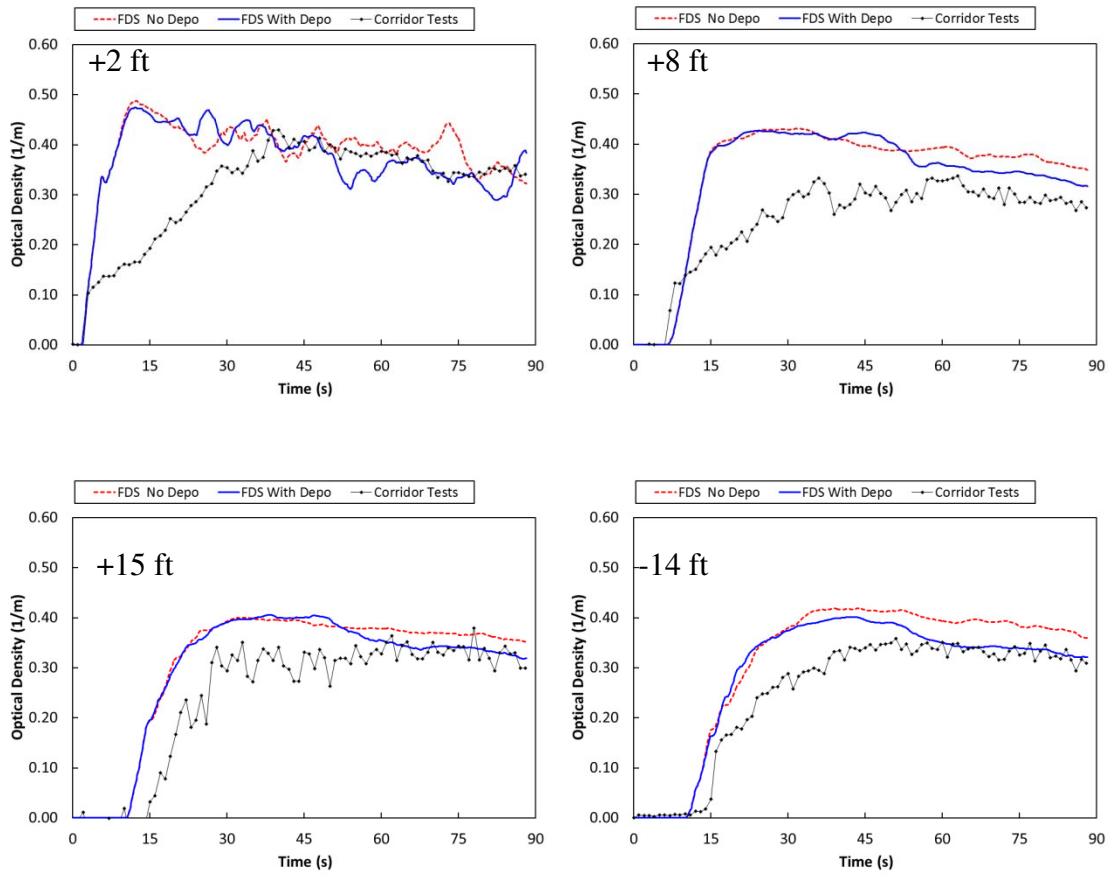


Figure 4.19 – Optical Density vs. Time at Four Locations along Corridor for Test 31 – 5 ft Wide Beamed Ceiling, 100 kW Fire

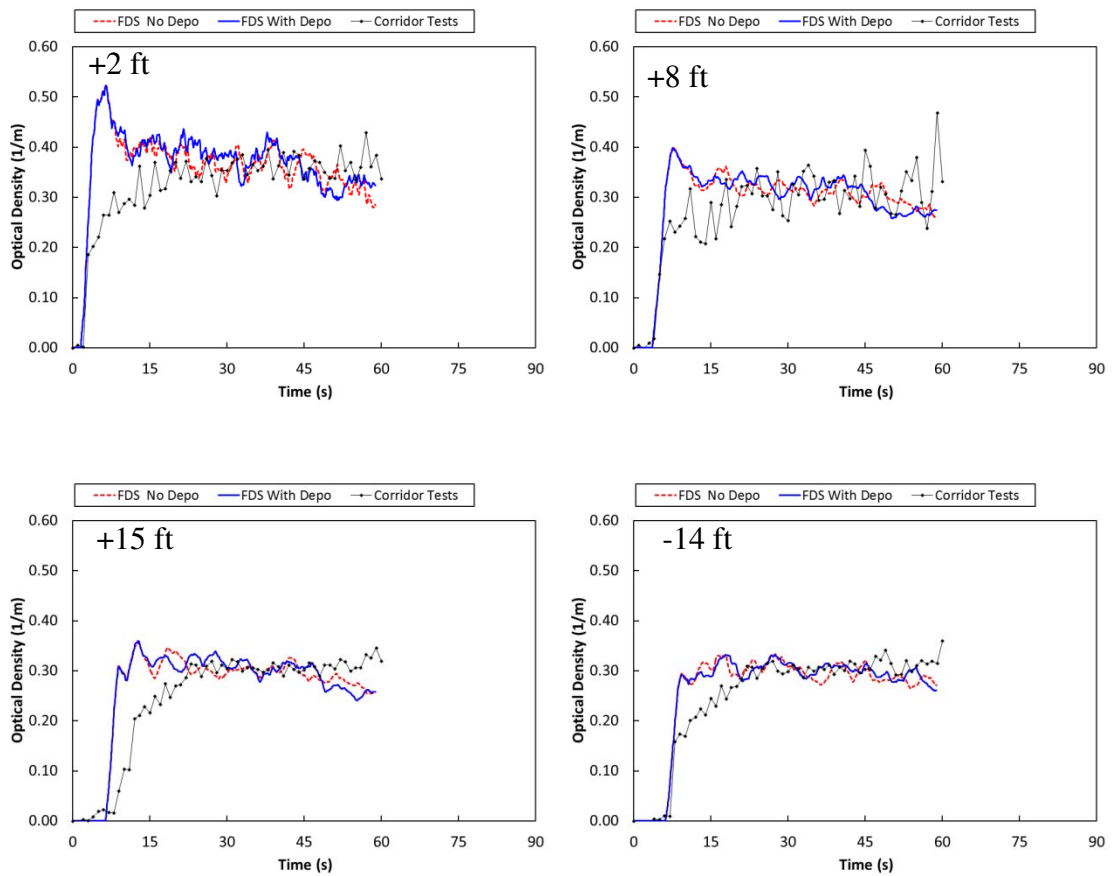


Figure 4.20 – Optical Density vs. Time at Four Locations along Corridor for Test 37 – 5 ft Wide Smooth Ceiling, 100 kW Fire

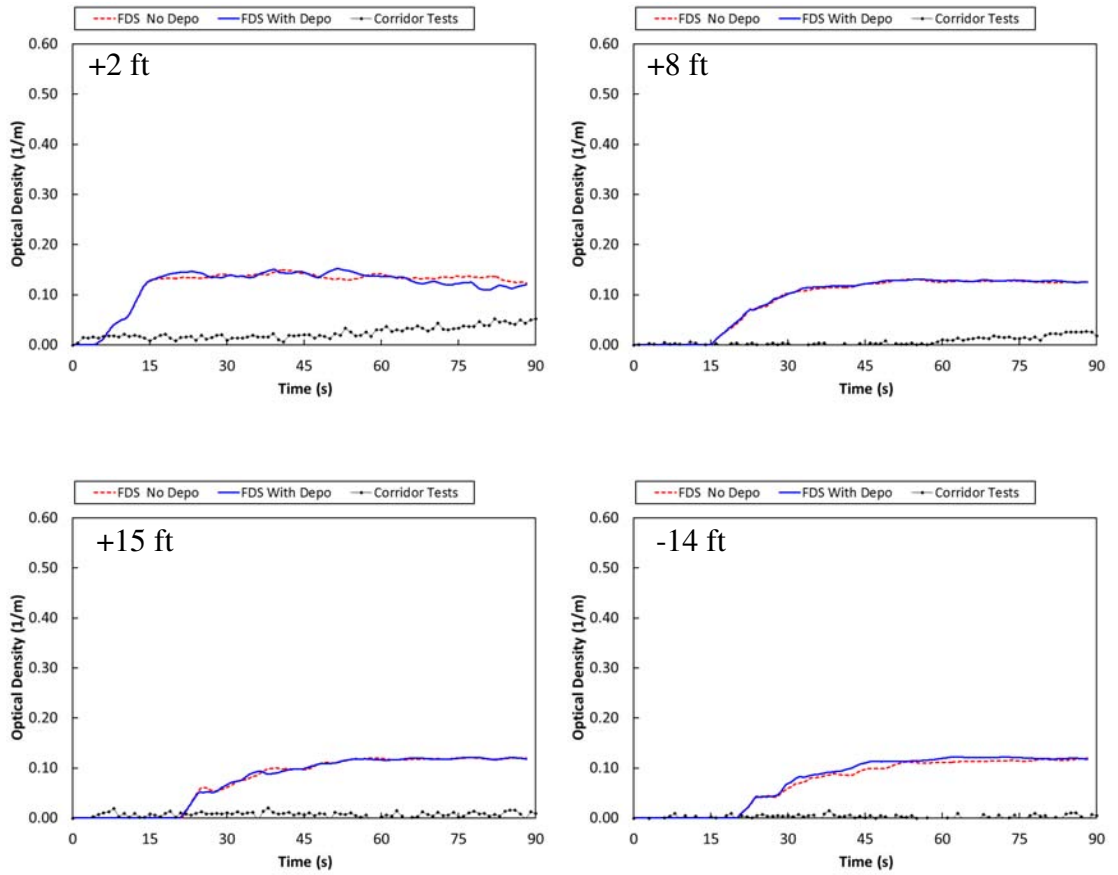


Figure 4.21 – Optical Density vs. Time at Four Locations along Corridor for Test 44 – 5 ft Wide Beamed Ceiling, 15 kW Fire

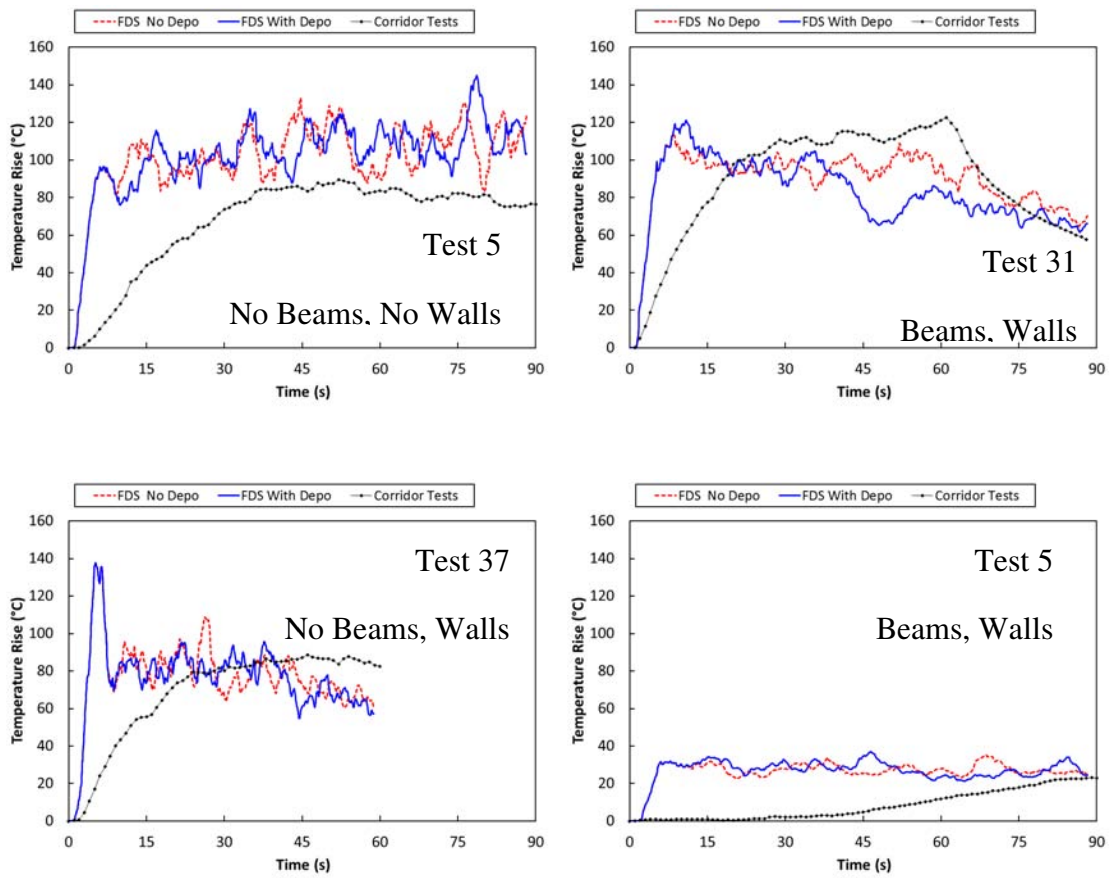


Figure 4.22 – Temperature Measured Above Fire Plume

Table 4.6 shows the calculated errors for all four corridor tests simulated. Figure 4.23 shows that most data is bounded within a 25% error.

Table 4.6 – Differences in FDS, with and without Soot Deposition Model, in Predicting Smoke Density vs. Test Data for Corridor Tests

Test Number	No Deposition Model %	With Deposition Model %	Difference
5	13 %	14 %	2 %
31	27 %	21 %	6 %
37	11 %	14 %	3 %
44	2496 %	2504 %	7 %
Average ¹	17 %	16 %	1 %

¹ Test 44 was omitted from average

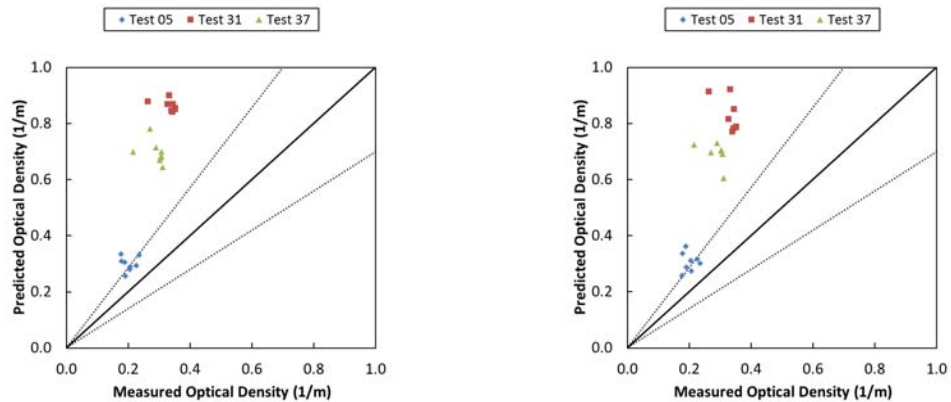


Figure 4.23 – Corridor Predicted vs. Measured Smoke Densities for FDS Model without Soot Deposition (Left) and with Soot Deposition (Right)

FDS better predicted the optical densities for a smooth ceiling. Tests 5 and 37 have roughly half the error compared to test 31 which had beams. Test 31 however, had a larger difference between the two models that were tested. Introducing beams into the corridors would increase the amount of turbulence in the ceiling jet. The ceiling jet would therefore deposit more soot due to turbulent deposition.

Test 44 demonstrated the same issue as seen in the NRC tests regarding fire size. Figure 4.21 shows FDS over predicting the optical density. Smoke yields for the corridor series were evaluated for a 100 kW fire. As discussed in the previous section, the smoke yields for the 100 kW fire may not scale down to a 15 kW fire.

In addition to the soot yield for Test 44, the delay in the sand burner was a large source of error. Due to the smaller flow rate, the sand burner would have taken longer to purge the air in the plenum. Figure 4.22 shows that the plume temperatures matched at the end of the test. However, the plume temperature steadily increased throughout the duration of the test. For the other tests, this was not the case.

4.3.3 Thermophoretic Deposition Hood

The hood tests yielded some unique results in analyzing the soot deposition model. The test setup was a much smaller scale in compartment and fire sizes compared to the NRC and corridor test series. The fire defined in the model was prescribed using mass loss data from the experiments. While the heat release rate curves were similar in shape and magnitude, the small fluctuations in the experimental heat release rate curve seen in

Figure 4.24 were reflected in the rest of the data. The difference in the two heat release rate curves is a significant source of error for the hood tests.

Figure 4.25 shows the extinction coefficient measurements for both FDS models compared to the experimental data for the hood tests. The predicted extinction coefficient is linear for the majority of the test. The linearity of the extinction coefficient is due to the prescribed heat release rate curve for the models. Even though the predicted extinction coefficient does not steadily ramp up as seen in the experiments, the values are in reasonable agreement.

It is important to note that in Figure 4.25, the data for the high filter location and low filter location lie on top of each other for a given model. The two distinguishable lines are the model without soot deposition and the model with soot deposition and not the difference in filter locations.

To determine why the two lines for a given model overlapped, the uniformity of the upper layer in FDS was examined. Figure 4.26 and Figure 4.27 show the optical density and temperature profiles at four locations within the hood. The four locations were all 0.24 m away from the fire in each direction along the x and y axis.

The locations of the filters are indicated by vertical lines. The optical density and temperature are relatively uniform in the top half of the hood. This provides insight as to why the optical densities for both locations were similar for each test. This uniformity in the hood was not found in Riahi's experimental data^[6].

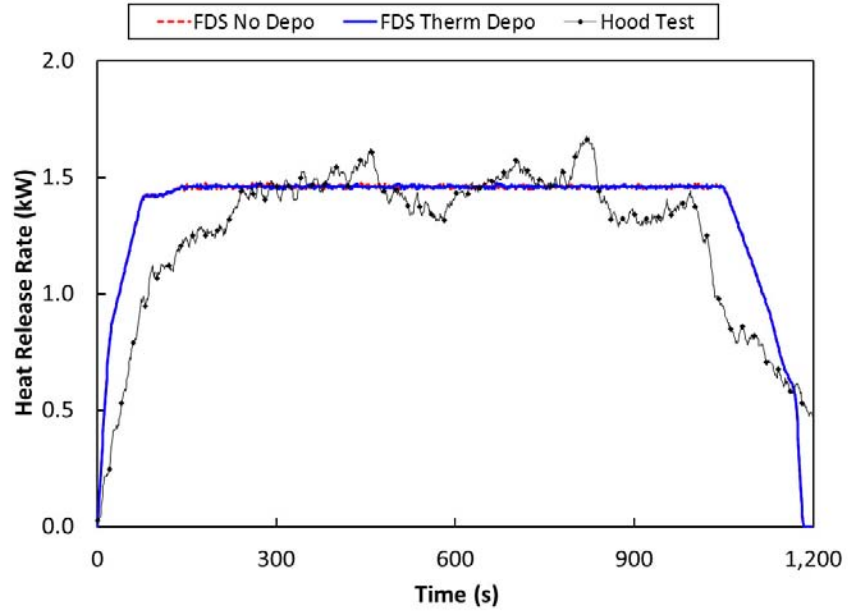


Figure 4.24 –Experimental and model heat release rate curves for hood tests.

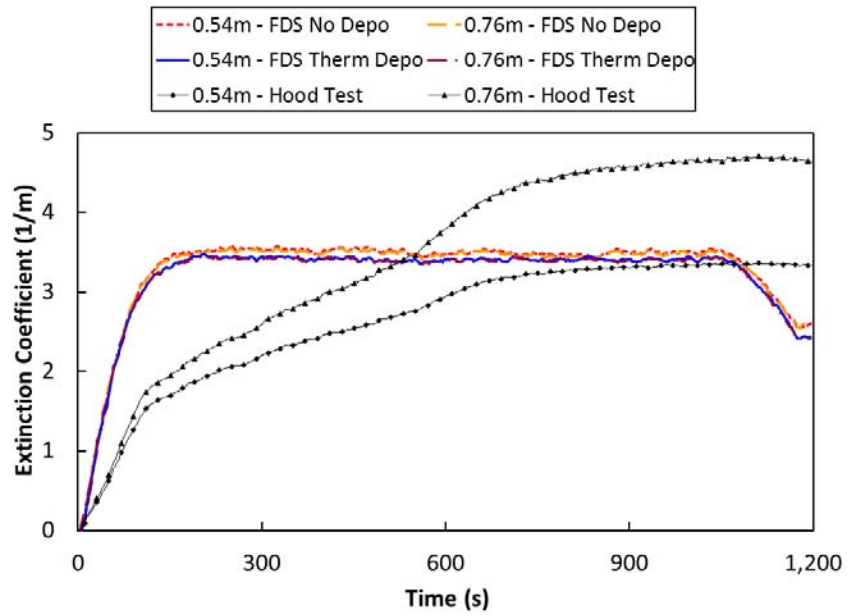


Figure 4.25 – Extinction coefficient for high and low filter locations in hood tests

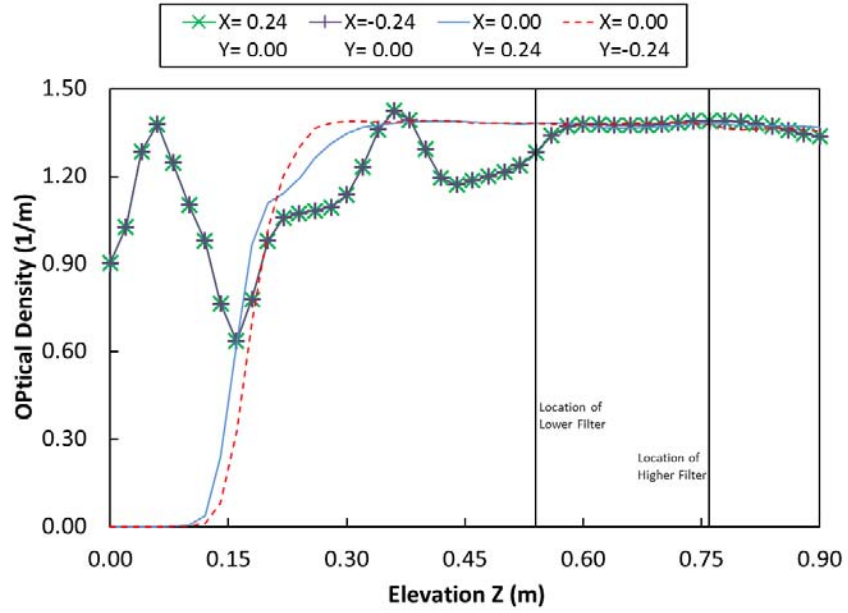


Figure 4.26 – Optical density profile at four locations in the hood at 1000 s

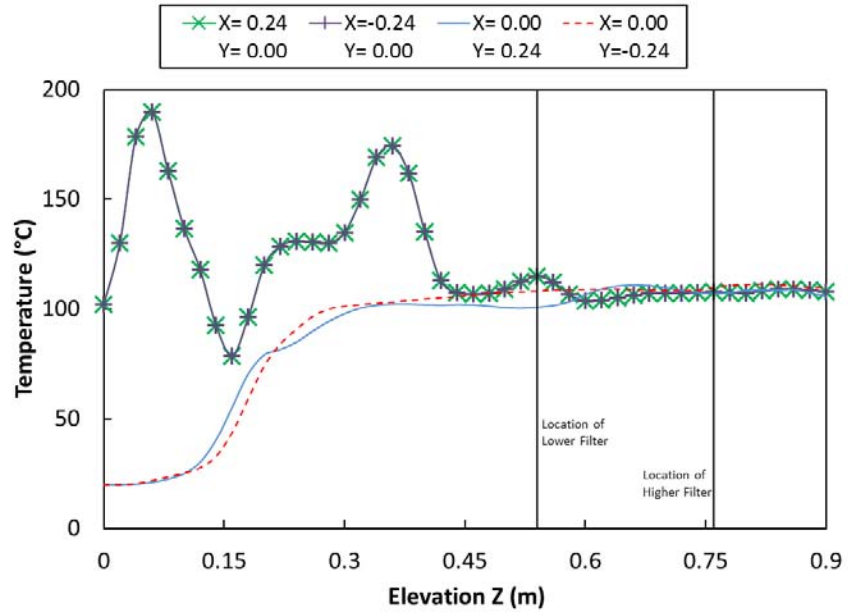


Figure 4.27 – Temperature profile at four locations in the hood at 1000 s

Table 4.7 – Differences in FDS, with and without Soot Deposition Model, in Predicting Optical Density vs. Test Data for Hood Tets

Filter Location	No Deposition Model %	With Deposition Model %	Difference
0.76 m Above Fire	23.83 %	23.40 %	2.37 %
0.54 m Above Fire	32.43 %	29.07 %	3.36 %
Average	28.13 %	26.24 %	1.89 %

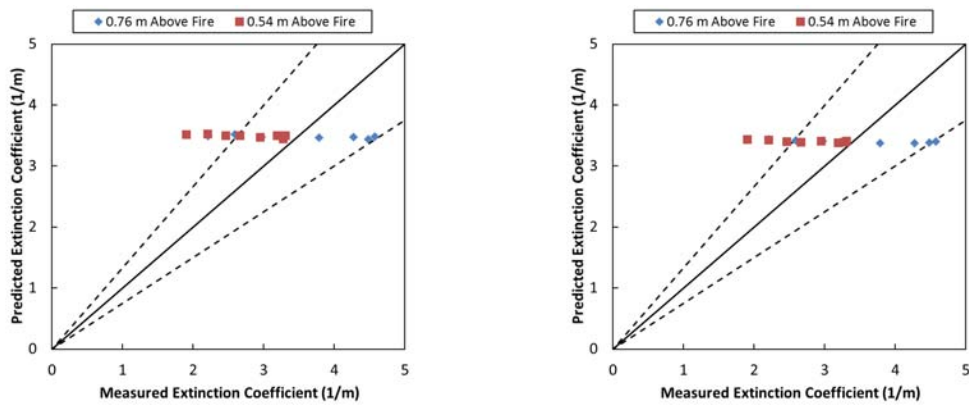


Figure 4.28 – Hood Test Predicted vs. Measured Smoke Densities for FDS Model without Soot Deposition (Left) and with Soot Deposition (Right)

Even though the soot deposition model did not have a large impact on the results, FDS was able to reasonably predict the properties found in the hood. As noted in Table 4.7, the average error for the two models is less than 30%. Figure 4.28 shows that most of the

data lies within 25% of the predicted values. This error would be greatly reduced if the heat release rate curve was edited to more closely match the curve from the experiments

While FDS was able to reasonably predict the optical density in the hood, there was a larger discrepancy between the mass deposited on the filters between the model and experiment. Table 4.8 shows an error in predicted mass of 70% for the high filter location and 62% error for the low filter location.

In order for FDS to be reasonably predicting optical densities and have a significant error in the prediction of mass deposited on a surface is for the soot to be removed from the system by ventilation. The exhaust duct was modeled using a total mass flux boundary condition. The value for the mass flux was based on the volumetric flow rate and density of the exhaust measured by Riahi.

Table 4.8 – Measured vs. predicted soot deposition on filters in hood tests

Filter Location	Soot Measured	Soot Predicted	Error
High (0.76 m)	0.0183 mg/cm ²	0.0055 mg/cm ²	69.8 %
Low (0.54 m)	0.0118 mg/cm ²	0.0045 mg/cm ²	62.2 %

Chapter 5: Conclusions and Future Work

The candidate soot deposition model allowed FDS to more accurately predict the optical densities for most enclosure fires. Although FDS without deposition yielded reasonable optical densities for medium-scale fires (such as the corridor test), the inclusion of soot deposition improved the results.

The predicted optical densities for well ventilated compartments generally agreed with the experimental data. In particular, the open door NRC tests and the 100 kW corridor tests showed good agreement in the optical density predictions from the soot deposition model.

FDS over predicted the optical density for small fires in large compartments. There was significant error in the 350 kW fire for the NRC tests as well as the 15 kW fire in the corridor test. One possible source of error for the small fires is that the assumed soot yield is invariant with fire size. Mulholland [26] showed that soot yields vary for different fire sizes. Another possible source of error is that the mesh size may not have been adequate for the small fires.

The predictions of mass deposited on surfaces were less than half of those measured in the small-scale hood tests.

Closed compartments involved large over predictions of optical density. The large error seen in the closed door tests compared to the open door tests in the NRC study imply that lower smoke production rates or higher deposition rates should be incorporated.

This study included a large range of compartment geometries and configurations. However, there are more areas to research to further validate the soot deposition model. For example, all the present fuels were gas or liquid. A study should be done to examine how well FDS predicts optical densities resulting from solid fuels.

The corridor, small-scale hood, and open door NRC tests were well ventilated. The closed door NRC tests were stopped when the oxygen concentration fell below 15% for safety reasons. Validation needs to be performed for under ventilated fires.

Finally, a study should be performed to generate a more comprehensive list of soot yields for fuels. This study should also include the effects of scale of both fire and compartment size.

Appendix A – Sample FDS Files

A.1 Thermophoretic Deposition Validation Test

```
&HEAD CHID='Therm_20C_Valdiation', TITLE='Validation_For_Therm_Depo'/
&TIME T_END=60/
&MISC FDS6=.TRUE.,H_CHILTON_COLBURN=.TRUE.,SOOT_DEPOSITION=.TRUE./
&MESH XB= 0.0, 1.0, 0.0, 1.0, 0.0, 1.0, IJK= 50, 50, 50/
&SURF ID          = 'BURNER',
      HRRPUA       = 500,
      COLOR        = 'RED'/ 20 kW Burner

&VENT XB= 0.4, 0.6, 0.4, 0.6, 0.0, 0.0, SURF_ID='BURNER'/
&VENT XB= 1.0, 1.0, 0.2, 0.8, 0.0, 0.6, SURF_ID='OPEN'/

&DEVC XYZ= 0.00, 0.50, 0.74, IOR=1, ID='Net Heat Flux',
      QUANTITY='NET HEAT FLUX'/
&DEVC XYZ= 0.00, 0.50, 0.74, IOR=1, ID='Radiative Heat Flux',
      QUANTITY='RADIATIVE HEAT FLUX'/
&DEVC XYZ= 0.00, 0.50, 0.74, IOR=1, ID='Convective Heat Flux',
      QUANTITY='CONVECTIVE HEAT FLUX'/
&DEVC XYZ= 0.00, 0.50, 0.74, IOR=1, ID='Wall Temperature',
      QUANTITY='WALL TEMPERATURE'/
&DEVC XYZ= 0.00, 0.50, 0.74, ID='Gas Temperature',
      QUANTITY='TEMPERATURE'/
&DEVC XYZ= 0.00, 0.50, 0.74, ID='Extinction Coefficient at Wall',
      QUANTITY='EXTINCTION COEFFICIENT'/
&DEVC XYZ= 0.00, 0.50, 0.74, ID='Optical Density at Wall',
      QUANTITY='OPTICAL DENSITY'/
&DEVC XYZ= 0.02, 0.50, 0.74, ID='Extinction Coefficient',
      QUANTITY='EXTINCTION COEFFICIENT'/
&DEVC XYZ= 0.02, 0.50, 0.74, ID='Optical Density',
      QUANTITY='OPTICAL DENSITY'/
&DEVC XB= 0.00, 0.00, 0.46, 0.54, 0.70, 0.78, ID='Soot Deposition',
      QUANTITY='SOOT SURFACE DENSITY', STATISTICS='SURFACE INTEGRAL'/

&BNDF QUANTITY='RADIATIVE HEAT FLUX'/
&BNDF QUANTITY='CONVECTIVE HEAT FLUX'/
&BNDF QUANTITY='NET HEAT FLUX'/
&BNDF QUANTITY='WALL TEMPERATURE'/

&SLCF PBX=0.5, QUANTITY='TEMPERATURE', VECTOR=.TRUE./
&SLCF PBY=0.5, QUANTITY='TEMPERATURE', VECTOR=.TRUE./
&SLCF PBX=0.5, QUANTITY='VELOCITY', VECTOR=.TRUE./
&SLCF PBY=0.5, QUANTITY='VELOCITY', VECTOR=.TRUE./
&SLCF PBX=0.5, QUANTITY='U-VELOCITY', VECTOR=.TRUE./
&SLCF PBY=0.5, QUANTITY='U-VELOCITY', VECTOR=.TRUE./
&SLCF PBX=0.5, QUANTITY='V-VELOCITY', VECTOR=.TRUE./
&SLCF PBY=0.5, QUANTITY='V-VELOCITY', VECTOR=.TRUE./
&SLCF PBX=0.5, QUANTITY='W-VELOCITY', VECTOR=.TRUE./
&SLCF PBY=0.5, QUANTITY='W-VELOCITY', VECTOR=.TRUE./
&TAIL/
```

A.2 Turbulent Deposition Validation Test

```
&HEAD CHID='TurbVerification-90kWf', TITLE='Verification_for_turb' /

&MISC FDS6=.TRUE., SOOT_DEPOSITION=.TRUE.
      THERMOPHORETIC_DEPOSITION=.FALSE., H_LOGLAW=.TRUE./

&MESH XB = -0.3, 0.3,-0.3, 0.3, 0.0, 3.0, IJK= 15, 15, 75 /

&TIME T_END=60 /

&REAC ID              = 'PROPYLENE'
      C                = 8
      H                = 14
      O                = 1
      SOOT_YIELD       = 0.0477
      CO_YIELD        = 0.017
      HEAT_OF_COMBUSTION = 45800/

&SURF ID              = 'BURNER'
      HRRPUA           = 250
      COLOR            = 'RED'/90 kW

&SURF ID              = 'FAN'
      MASS_FLUX_TOTAL = 1/

&VENT XB = -0.3,-0.3,-0.3, 0.3, 0.0, 1.0, SURF_ID='OPEN' /
&VENT XB =  0.3, 0.3,-0.3, 0.3, 0.0, 1.0, SURF_ID='OPEN' /
&VENT XB = -0.3, 0.3,-0.3,-0.3, 0.0, 1.0, SURF_ID='OPEN' /
&VENT XB = -0.3, 0.3, 0.3, 0.3, 0.0, 1.0, SURF_ID='OPEN' /

&VENT XB = -0.3, 0.3,-0.3, 0.3, 3.0, 3.0, SURF_ID='FAN' /
&VENT XB = -0.3, 0.3,-0.3, 0.3, 0.0, 0.0, SURF_ID='BURNER' /

&DEVC XB= 0.30, 0.30,-0.30, 0.30, 1.00, 3.00, ID='Soot Deposition +X',
      QUANTITY='SOOT SURFACE DENSITY', STATISTICS='SURFACE INTEGRAL'/
&DEVC XB=-0.30,-0.30,-0.30, 0.30, 1.00, 3.00, ID='Soot Deposition -X',
      QUANTITY='SOOT SURFACE DENSITY', STATISTICS='SURFACE INTEGRAL'/
&DEVC XB=-0.30, 0.30, 0.30, 0.30, 1.00, 3.00, ID='Soot Deposition +Y',
      QUANTITY='SOOT SURFACE DENSITY', STATISTICS='SURFACE INTEGRAL'/
&DEVC XB=-0.30, 0.30,-0.30,-0.30, 1.00, 3.00, ID='Soot Deposition -Y',
      QUANTITY='SOOT SURFACE DENSITY', STATISTICS='SURFACE INTEGRAL'/

&TAIL/
```

A.3 Sample NIST/NRC FDS File

```
&HEAD CHID='NIST_NRC_05_v5_no', TITLE='NIST/NRC Test 5' /

&MESH IJK=100,36,32, XB=0.0,21.7,0.0,7.04,0.0,3.82 /
&TRNX IDERIV=0,CC= 10.80, PC=10.8 /
&TRNX IDERIV=1,CC= 10.80, PC=0.5 /
&TRNY IDERIV=0,CC= 3.58, PC=3.58 /
&TRNY IDERIV=1,CC= 3.58, PC=0.5 /

&TIME TWFIN=1800. /

&MISC TMPA=31.,SURF_DEFAULT='MARINITE', POROUS_FLOOR=.FALSE.,
      FDS6=.TRUE., H_CHILTON_COLBURN=.TRUE., SOOT_DEPOSITION=.TRUE. /
&DUMP NFRAMES=1800,DT_DEVC=10.,DT_HRR=10. /

&RADI RADIATIVE_FRACTION=0.44 /
&REAC ID          = 'HEPTANE'
      FUEL='N-HEPTANE'
      FYI          = 'Heptane, C_7 H_16'
      C            = 7.
      H            = 16.
      CO_YIELD     = 0.006
      SOOT_YIELD   = 0.015 /

&OBST XB= 9.8,11.8, 3.1, 4.1, 0.0, 0.0, SURF_ID='STEEL SHEET' /Fire Pan
&OBST XB= 9.8,11.8, 3.1, 3.1, 0.0, 0.1, SURF_ID='STEEL SHEET' /
&OBST XB= 9.8,11.8, 4.1, 4.1, 0.0, 0.1, SURF_ID='STEEL SHEET' /
&OBST XB= 9.8, 9.8, 3.1, 4.1, 0.0, 0.1, SURF_ID='STEEL SHEET' /
&OBST XB=11.8,11.8, 3.1, 4.1, 0.0, 0.1, SURF_ID='STEEL SHEET' /

&PART ID='heptane droplets',FUEL=.TRUE.,DENSITY=688.,
      QUANTITIES(1:2)='DROPLET_DIAMETER','DROPLET_TEMPERATURE',
      DIAMETER=500.,HEAT_OF_COMBUSTION=45000.,
      SAMPLING_FACTOR=1 /

&PROP ID='nozzle', PART_ID='heptane droplets', FLOW_RATE=2.307,
      FLOW_RAMP='FIRE_RAMP',DROPLET_VELOCITY=25., SPRAY_ANGLE=0.,45. /

&RAMP ID='FIRE_RAMP',T= 0, `F=0.0 /
&RAMP ID='FIRE_RAMP',T=180, F=1.0 /
&RAMP ID='FIRE_RAMP',T=1380, F=1.0 /
&RAMP ID='FIRE_RAMP',T=1560, F=0.0 /

&SURF ID='INFLOW' , VOLUME_FLUX=-0.9, COLOR='RED', VEL_T=0.0,4.0 /
&SURF ID='OUTFLOW', VOLUME_FLUX= 1.7, COLOR='YELLOW', RAMP_V='exhaust' /

&RAMP ID='exhaust',T= 0, F=0.0 /
&RAMP ID='exhaust',T= 1, F=0.6 /
&RAMP ID='exhaust',T=180, F=1.0 /
&RAMP ID='exhaust',T=400, F=0.9 /

&OBST XB= 5.85,15.85,1.90,2.10,3.20,3.30,SURF_IDS='XLP TRAY
      CONTROL','STEEL SHEET','XLP TRAY CONTROL' / Cable Tray D
```

```

cOBST XB=10.70,11.00,1.10,1.30,2.70,2.90, SURF_ID='PVC SINGLE CONTROL'
/ Slab Target E
&OBST XB=10.40,11.00,1.10,1.30,2.70,2.90, SURF_ID='XLP SINGLE CONTROL'
/ Control Cable B
&OBST XB= 5.80,15.80,0.40,0.60,2.20,2.30, SURF_ID='XLP SINGLE POWER'
/ Power Cable F
&OBST XB=10.58,10.88,6.80,7.04,0.00,3.82, SURF_ID='XLP TRAY CONTROL'
/ Vertical Ladder Tray G
&OBST XB=17.55,17.85,3.37,3.67,3.72,3.82, SURF_ID='FERALOY'
/ Junction Box

&VENT MB='ZMIN',SURF_ID='GYPSUM BOARD' /

&VENT XB= 0.00,0.00,2.51,4.51,0.00,2.00, SURF_ID='OPEN' /

&VENT XB=10.88,11.58,0.00,0.00,2.05,2.40, SURF_ID='INFLOW' /
&VENT XB=10.88,11.58,7.04,7.04,2.05,2.76, SURF_ID='OUTFLOW' /

&SLCF PBX= 3.5, QUANTITY='TEMPERATURE',VECTOR=.TRUE. /
&SLCF PBX= 3.5, QUANTITY='HRRPUV' /
&SLCF PBX= 3.5, QUANTITY='MIXTURE_FRACTION' /
&SLCF PBX=11.2, QUANTITY='TEMPERATURE',VECTOR=.TRUE. /
&SLCF PBX=11.2, QUANTITY='HRRPUV' /
&SLCF PBX=11.2, QUANTITY='MIXTURE_FRACTION' /

&BNDF QUANTITY='WALL_TEMPERATURE' /
&BNDF QUANTITY='GAUGE_HEAT_FLUX' /

&MATL ID = 'PVC'
FYI = 'NISTIR 1013-1'
CONDUCTIVITY_RAMP = 'k_pvc'
SPECIFIC_HEAT_RAMP = 'c_pvc'
DENSITY = 1380.
EMISSIVITY = 0.95 /
&RAMP ID='k_pvc',T= 23.,F=0.192 /
&RAMP ID='k_pvc',T= 50.,F=0.175 /
&RAMP ID='k_pvc',T= 75.,F=0.172 /
&RAMP ID='k_pvc',T=100.,F=0.147 /
&RAMP ID='k_pvc',T=125.,F=0.141 /
&RAMP ID='k_pvc',T=150.,F=0.134 /
&RAMP ID='c_pvc',T= 23.,F=1.289 /
&RAMP ID='c_pvc',T= 50.,F=1.353 /
&RAMP ID='c_pvc',T= 75.,F=1.407 /
&RAMP ID='c_pvc',T=100.,F=1.469 /
&RAMP ID='c_pvc',T=125.,F=1.530 /
&RAMP ID='c_pvc',T=150.,F=1.586 /

&MATL ID = 'XLP'
FYI = 'NISTIR 1013-1'
CONDUCTIVITY_RAMP = 'k_xlp'
SPECIFIC_HEAT_RAMP = 'c_xlp'
DENSITY = 1374.
EMISSIVITY = 0.95 /

```

```

&RAMP ID='k_xlp',T= 23.,F=0.235 /
&RAMP ID='k_xlp',T= 50.,F=0.232 /
&RAMP ID='k_xlp',T= 75.,F=0.223 /
&RAMP ID='k_xlp',T=100.,F=0.210 /
&RAMP ID='k_xlp',T=125.,F=0.190 /
&RAMP ID='k_xlp',T=150.,F=0.192 /
&RAMP ID='c_xlp',T= 23.,F=1.390 /
&RAMP ID='c_xlp',T= 50.,F=1.476 /
&RAMP ID='c_xlp',T= 75.,F=1.526 /
&RAMP ID='c_xlp',T=100.,F=1.560 /
&RAMP ID='c_xlp',T=125.,F=1.585 /
&RAMP ID='c_xlp',T=150.,F=1.607 /

&MATL ID                = 'MARINITE'
FYI                     = 'BNZ Materials Marinite I'
EMISSIVITY              = 0.8
DENSITY                 = 737.
SPECIFIC_HEAT_RAMP     = 'c_mar'
CONDUCTIVITY_RAMP      = 'k_mar' /

&RAMP ID='k_mar',T= 24.,F=0.13 /
&RAMP ID='k_mar',T=149.,F=0.12 /
&RAMP ID='k_mar',T=538.,F=0.12 /
&RAMP ID='c_mar',T= 93.,F=1.172 /
&RAMP ID='c_mar',T=205.,F=1.255 /
&RAMP ID='c_mar',T=316.,F=1.339 /
&RAMP ID='c_mar',T=425.,F=1.423 /

&MATL ID                = 'STEEL'
FYI                     = 'Quintiere, Fire Behavior'
SPECIFIC_HEAT           = 0.46
CONDUCTIVITY            = 45.8
DENSITY                 = 7850. /

&MATL ID                = 'FERALOY'
FYI                     = 'NISTIR 1013-1'
SPECIFIC_HEAT           = 0.456
CONDUCTIVITY            = 78.2
DENSITY                 = 787. /

&MATL ID                = 'GYPSUM PLASTER'
FYI                     = 'Quintiere, Fire Behavior'
CONDUCTIVITY            = 0.48
SPECIFIC_HEAT           = 0.84
DENSITY                 = 1440. /

&MATL ID                = 'YELLOW PINE'
FYI                     = 'Quintiere, Fire Behavior'
CONDUCTIVITY            = 0.14
SPECIFIC_HEAT           = 2.85
DENSITY                 = 640. /

&SURF ID='PVC TRAY CONTROL', MATL_ID='PVC', COLOR='RED',
THICKNESS=0.01 /

```

```

&SURF ID='PVC SINGLE CONTROL',MATL_ID='PVC', COLOR='RED',
  THICKNESS=0.005, GEOMETRY='CYLINDRICAL' /
&SURF ID='PVC SINGLE POWER', MATL_ID='PVC', COLOR='RED',
  THICKNESS=0.008, GEOMETRY='CYLINDRICAL' /

&SURF ID='XLP TRAY CONTROL', MATL_ID='XLP', COLOR='GREEN',
  THICKNESS=0.01 /
&SURF ID='XLP SINGLE CONTROL',MATL_ID='XLP', COLOR='GREEN',
  THICKNESS=0.005, GEOMETRY='CYLINDRICAL' /
&SURF ID='XLP SINGLE POWER', MATL_ID='XLP', COLOR='GREEN',
  THICKNESS=0.0095, GEOMETRY='CYLINDRICAL' /

&SURF ID          = 'STEEL SHEET'
  MATL_ID          = 'STEEL'
  COLOR            = 'BLACK'
  BACKING          = 'EXPOSED'
  THICKNESS        = 0.00635 /

&SURF ID          = 'FERALOY'
  MATL_ID          = 'FERALOY'
  COLOR            = 'SILVER'
  BACKING          = 'EXPOSED'
  THICKNESS        = 0.007 /

&SURF ID          = 'MARINITE'
  MATL_ID          = 'MARINITE'
  COLOR            = 'BEIGE'
  BACKING          = 'EXPOSED'
  LEAK_PATH        = 1,0
  THICKNESS        = 0.0254 /

&SURF ID          = 'GYPSUM BOARD'
  FYI              = 'Compartment floor'
  MATL_ID(1:2,1)  = 'GYPSUM PLASTER','YELLOW PINE'
  COLOR            = 'ANTIQUUE WHITE'
  THICKNESS(1:2)  = 0.0127,0.0127 /

```

TC Trees

```

&DEVC XYZ= 5.00, 3.58, 0.35,QUANTITY='THERMOCOUPLE',ID='Tr 1-1' /
&DEVC XYZ= 5.00, 3.58, 0.70,QUANTITY='THERMOCOUPLE',ID='Tr 1-2' /
&DEVC XYZ= 5.00, 3.58, 1.05,QUANTITY='THERMOCOUPLE',ID='Tr 1-3' /
&DEVC XYZ= 5.00, 3.58, 1.40,QUANTITY='THERMOCOUPLE',ID='Tr 1-4' /
&DEVC XYZ= 5.00, 3.58, 1.75,QUANTITY='THERMOCOUPLE',ID='Tr 1-5' /
&DEVC XYZ= 5.00, 3.58, 2.10,QUANTITY='THERMOCOUPLE',ID='Tr 1-6' /
&DEVC XYZ= 5.00, 3.58, 2.45,QUANTITY='THERMOCOUPLE',ID='Tr 1-7' /
&DEVC XYZ= 5.00, 3.58, 2.80,QUANTITY='THERMOCOUPLE',ID='Tr 1-8' /
&DEVC XYZ= 5.00, 3.58, 3.15,QUANTITY='THERMOCOUPLE',ID='Tr 1-9' /
&DEVC XYZ= 5.00, 3.58, 3.50,QUANTITY='THERMOCOUPLE',ID='Tr 1-10' /

&DEVC XYZ=10.85, 6.48, 0.35,QUANTITY='THERMOCOUPLE',ID='Tr 2-1' /
&DEVC XYZ=10.85, 6.48, 0.70,QUANTITY='THERMOCOUPLE',ID='Tr 2-2' /
&DEVC XYZ=10.85, 6.48, 1.05,QUANTITY='THERMOCOUPLE',ID='Tr 2-3' /
&DEVC XYZ=10.85, 6.48, 1.40,QUANTITY='THERMOCOUPLE',ID='Tr 2-4' /
&DEVC XYZ=10.85, 6.48, 1.75,QUANTITY='THERMOCOUPLE',ID='Tr 2-5' /

```



```

&DEVC XYZ=16.70, 3.58, 2.10, QUANTITY='THERMOCOUPLE', ID='Tr 7-6' /
&DEVC XYZ=16.70, 3.58, 2.45, QUANTITY='THERMOCOUPLE', ID='Tr 7-7' /
&DEVC XYZ=16.70, 3.58, 2.80, QUANTITY='THERMOCOUPLE', ID='Tr 7-8' /
&DEVC XYZ=16.70, 3.58, 3.15, QUANTITY='THERMOCOUPLE', ID='Tr 7-9' /
&DEVC XYZ=16.70, 3.58, 3.50, QUANTITY='THERMOCOUPLE', ID='Tr 7-10' /

```

Wall TCs

```

&DEVC XYZ= 3.91, 7.04, 1.49, QUANTITY='WALL_TEMPERATURE', IOR=-2, ID='TC N
U-1' /
&DEVC XYZ= 3.91, 7.04, 3.72, QUANTITY='WALL_TEMPERATURE', IOR=-2, ID='TC N
U-2' /
&DEVC XYZ= 9.55, 7.04, 1.87, QUANTITY='WALL_TEMPERATURE', IOR=-2, ID='TC N
U-3' /
&DEVC XYZ=12.15, 7.04, 1.87, QUANTITY='WALL_TEMPERATURE', IOR=-2, ID='TC N
U-4' /
&DEVC XYZ=17.79, 7.04, 1.50, QUANTITY='WALL_TEMPERATURE', IOR=-2, ID='TC N
U-5' /
&DEVC XYZ=17.79, 7.04, 3.73, QUANTITY='WALL_TEMPERATURE', IOR=-2, ID='TC N
U-6' /

&DEVC XYZ= 3.91, 0.00, 1.49, QUANTITY='WALL_TEMPERATURE', IOR= 2, ID='TC S
U-1' /
&DEVC XYZ= 3.91, 0.00, 3.72, QUANTITY='WALL_TEMPERATURE', IOR= 2, ID='TC S
U-2' /
&DEVC XYZ= 9.55, 0.00, 1.87, QUANTITY='WALL_TEMPERATURE', IOR= 2, ID='TC S
U-3' /
&DEVC XYZ=12.15, 0.00, 1.87, QUANTITY='WALL_TEMPERATURE', IOR= 2, ID='TC S
U-4' /
&DEVC XYZ=17.79, 0.00, 1.50, QUANTITY='WALL_TEMPERATURE', IOR= 2, ID='TC S
U-5' /
&DEVC XYZ=17.79, 0.00, 3.73, QUANTITY='WALL_TEMPERATURE', IOR= 2, ID='TC S
U-6' /

&DEVC XYZ=21.70, 1.59, 1.12, QUANTITY='WALL_TEMPERATURE', IOR=-1, ID='TC E
U-1' /
&DEVC XYZ=21.70, 1.59, 2.43, QUANTITY='WALL_TEMPERATURE', IOR=-1, ID='TC E
U-2' /
&DEVC XYZ=21.70, 5.76, 1.12, QUANTITY='WALL_TEMPERATURE', IOR=-1, ID='TC E
U-3' /
&DEVC XYZ=21.70, 5.76, 2.43, QUANTITY='WALL_TEMPERATURE', IOR=-1, ID='TC E
U-4' /

&DEVC XYZ= 0.00, 1.59, 1.12, QUANTITY='WALL_TEMPERATURE', IOR= 1, ID='TC W
U-1' /
&DEVC XYZ= 0.00, 1.59, 2.43, QUANTITY='WALL_TEMPERATURE', IOR= 1, ID='TC W
U-2' /
&DEVC XYZ= 0.00, 5.76, 1.12, QUANTITY='WALL_TEMPERATURE', IOR= 1, ID='TC W
U-3' /
&DEVC XYZ= 0.00, 5.76, 2.43, QUANTITY='WALL_TEMPERATURE', IOR= 1, ID='TC W
U-4' /

&DEVC XYZ= 3.04, 3.59, 0.00, QUANTITY='WALL_TEMPERATURE', IOR= 3, ID='TC F
U-1' /

```

```

&DEVC XYZ= 9.11, 2.00, 0.00, QUANTITY='WALL_TEMPERATURE', IOR= 3, ID='TC F
U-2'/
&DEVC XYZ= 9.11, 5.97, 0.00, QUANTITY='WALL_TEMPERATURE', IOR= 3, ID='TC F
U-3'/
&DEVC XYZ=10.85, 2.39, 0.00, QUANTITY='WALL_TEMPERATURE', IOR= 3, ID='TC F
U-4'/
&DEVC XYZ=10.85, 5.17, 0.00, QUANTITY='WALL_TEMPERATURE', IOR= 3, ID='TC F
C-5'/
&DEVC XYZ=13.02, 2.00, 0.00, QUANTITY='WALL_TEMPERATURE', IOR= 3, ID='TC F
U-6'/
&DEVC XYZ=13.02, 5.97, 0.00, QUANTITY='WALL_TEMPERATURE', IOR= 3, ID='TC F
U-7'/
&DEVC XYZ=18.66, 3.59, 0.00, QUANTITY='WALL_TEMPERATURE', IOR= 3, ID='TC F
U-8'/

&DEVC XYZ= 3.04, 3.59, 3.82, QUANTITY='WALL_TEMPERATURE', IOR=-3, ID='TC C
U-1'/
&DEVC XYZ= 9.11, 2.00, 3.82, QUANTITY='WALL_TEMPERATURE', IOR=-3, ID='TC C
C-2'/
&DEVC XYZ= 9.11, 5.97, 3.82, QUANTITY='WALL_TEMPERATURE', IOR=-3, ID='TC C
C-3'/
&DEVC XYZ=10.85, 2.39, 3.82, QUANTITY='WALL_TEMPERATURE', IOR=-3, ID='TC C
C-4'/
&DEVC XYZ=10.85, 5.17, 3.82, QUANTITY='WALL_TEMPERATURE', IOR=-3, ID='TC C
C-5'/
&DEVC XYZ=13.02, 2.00, 3.82, QUANTITY='WALL_TEMPERATURE', IOR=-3, ID='TC C
C-6'/
&DEVC XYZ=13.02, 5.97, 3.82, QUANTITY='WALL_TEMPERATURE', IOR=-3, ID='TC C
C-7'/
&DEVC XYZ=18.66, 3.59, 3.82, QUANTITY='WALL_TEMPERATURE', IOR=-3, ID='TC C
U-8'/

```

Bidirectional Probe TCs

```

&DEVC XYZ= 0.10, 2.81, 0.20, QUANTITY='THERMOCOUPLE', ID='TC Door 1'/
&DEVC XYZ= 0.10, 2.81, 0.60, QUANTITY='THERMOCOUPLE', ID='TC Door 2'/
&DEVC XYZ= 0.10, 2.81, 1.00, QUANTITY='THERMOCOUPLE', ID='TC Door 3'/
&DEVC XYZ= 0.10, 2.81, 1.20, QUANTITY='THERMOCOUPLE', ID='TC Door 4'/
&DEVC XYZ= 0.10, 2.81, 1.40, QUANTITY='THERMOCOUPLE', ID='TC Door 5'/
&DEVC XYZ= 0.10, 2.81, 1.60, QUANTITY='THERMOCOUPLE', ID='TC Door 6'/
&DEVC XYZ= 0.10, 2.81, 1.80, QUANTITY='THERMOCOUPLE', ID='TC Door 7'/
&DEVC XYZ= 0.10, 2.81, 1.90, QUANTITY='THERMOCOUPLE', ID='TC Door 8'/
&DEVC XYZ= 0.10, 3.61, 0.20, QUANTITY='THERMOCOUPLE', ID='TC Door 9'/
&DEVC XYZ= 0.10, 3.61, 0.60, QUANTITY='THERMOCOUPLE', ID='TC Door 10'/
&DEVC XYZ= 0.10, 3.61, 1.00, QUANTITY='THERMOCOUPLE', ID='TC Door 11'/
&DEVC XYZ= 0.10, 3.61, 1.20, QUANTITY='THERMOCOUPLE', ID='TC Door 12'/
&DEVC XYZ= 0.10, 3.61, 1.40, QUANTITY='THERMOCOUPLE', ID='TC Door 13'/
&DEVC XYZ= 0.10, 3.61, 1.60, QUANTITY='THERMOCOUPLE', ID='TC Door 14'/
&DEVC XYZ= 0.10, 3.61, 1.80, QUANTITY='THERMOCOUPLE', ID='TC Door 15'/
&DEVC XYZ= 0.10, 3.61, 1.90, QUANTITY='THERMOCOUPLE', ID='TC Door 16'/
&DEVC XYZ= 0.10, 4.21, 0.20, QUANTITY='THERMOCOUPLE', ID='TC Door 17'/
&DEVC XYZ= 0.10, 4.21, 0.60, QUANTITY='THERMOCOUPLE', ID='TC Door 18'/
&DEVC XYZ= 0.10, 4.21, 1.00, QUANTITY='THERMOCOUPLE', ID='TC Door 19'/
&DEVC XYZ= 0.10, 4.21, 1.20, QUANTITY='THERMOCOUPLE', ID='TC Door 20'/
&DEVC XYZ= 0.10, 4.21, 1.40, QUANTITY='THERMOCOUPLE', ID='TC Door 21'/

```

&DEVC XYZ= 0.10, 4.21, 1.60, QUANTITY='THERMOCOUPLE', ID='TC Door 22' /
 &DEVC XYZ= 0.10, 4.21, 1.80, QUANTITY='THERMOCOUPLE', ID='TC Door 23' /
 &DEVC XYZ= 0.10, 4.21, 1.90, QUANTITY='THERMOCOUPLE', ID='TC Door 24' /
 &DEVC XYZ=11.35, 0.00, 2.40, QUANTITY='THERMOCOUPLE', ID='TC Supply 25' /
 &DEVC XYZ=11.35, 7.04, 2.40, QUANTITY='THERMOCOUPLE', ID='TC Exhaust 26' /
 &DEVC XYZ= 0.00, 0.30, 0.08, QUANTITY='THERMOCOUPLE', ID='TC Leak 27' /

Cable TCs

&DEVC XYZ=10.85, 1.30, 2.80, QUANTITY='WALL_TEMPERATURE', IOR=-3, ID='B
 Ts-14' /
 &DEVC XYZ=10.85, 1.30, 2.80, QUANTITY='INSIDE_WALL_TEMPERATURE', IOR=-
 3, ID='B Tc-15', DEPTH=0.0012 /
 &DEVC XYZ=10.85, 2.00, 3.20, QUANTITY='WALL_TEMPERATURE', IOR=-3, ID='D
 Ts-12' /
 &DEVC XYZ=10.85, 1.25, 2.70, QUANTITY='WALL_TEMPERATURE', IOR=-3, ID='E
 Ts-16' /
 &DEVC XYZ=10.85, 1.25, 2.85, QUANTITY='WALL_TEMPERATURE', IOR= 3, ID='E
 Ts-16p' /
 &DEVC XYZ=10.85, 1.25, 2.70, QUANTITY='INSIDE_WALL_TEMPERATURE', IOR=-
 3, ID='E Tc-17', DEPTH=0.0025 /
 &DEVC XYZ=10.85, 0.50, 2.20, QUANTITY='WALL_TEMPERATURE', IOR=-3, ID='F
 Ts-20' /
 &DEVC XYZ=14.85, 2.00, 3.20, QUANTITY='WALL_TEMPERATURE', IOR=-3, ID='D
 Ts-26' /
 &DEVC XYZ=14.85, 0.50, 2.20, QUANTITY='WALL_TEMPERATURE', IOR=-3, ID='F
 Ts-30' /
 &DEVC XYZ=10.80, 6.80, 0.35, QUANTITY='WALL_TEMPERATURE', IOR=-2, ID='G
 Ts-31' /
 &DEVC XYZ=10.80, 6.80, 0.70, QUANTITY='WALL_TEMPERATURE', IOR=-2, ID='G
 Ts-32' /
 &DEVC XYZ=10.80, 6.80, 1.75, QUANTITY='WALL_TEMPERATURE', IOR=-2, ID='G
 Ts-33' /
 &DEVC XYZ=10.80, 6.80, 2.45, QUANTITY='WALL_TEMPERATURE', IOR=-2, ID='G
 Ts-35' /
 &DEVC XYZ=10.80, 6.80, 3.15, QUANTITY='WALL_TEMPERATURE', IOR=-2, ID='G
 Ts-36' /
 &DEVC XYZ=17.70, 3.58, 3.72, QUANTITY='BACK_WALL_TEMPERATURE', IOR=-
 3, ID='Junction Box TC-37' /
 &DEVC XYZ=17.70, 3.58, 3.72, QUANTITY='WALL_TEMPERATURE', IOR=-
 3, ID='Junction Box Ts-38' /
 &DEVC XYZ=17.55, 3.52, 3.77, QUANTITY='WALL_TEMPERATURE', IOR=-
 1, ID='Junction Box Ts-39' /

Aspirated TCs

&DEVC XYZ= 0.10, 3.61, 0.20, QUANTITY='TEMPERATURE', ID='ATC Door 1' /
 &DEVC XYZ= 0.10, 3.61, 1.00, QUANTITY='TEMPERATURE', ID='ATC Door 2' /
 &DEVC XYZ= 0.10, 3.61, 1.80, QUANTITY='TEMPERATURE', ID='ATC Door 3' /
 &DEVC XYZ=11.35, 7.04, 2.40, QUANTITY='TEMPERATURE', ID='ATC Exhaust 4' /
 &DEVC XYZ=10.85, 0.55, 1.05, QUANTITY='TEMPERATURE', ID='ATC 5' /
 &DEVC XYZ=10.85, 0.55, 2.80, QUANTITY='TEMPERATURE', ID='ATC 6' /

Wall Flux Gauges

```
&DEVC XYZ= 3.91, 7.04, 1.49, QUANTITY='HEAT_FLUX', IOR=-2, ID='N U-1' /
&DEVC XYZ= 3.91, 7.04, 3.72, QUANTITY='HEAT_FLUX', IOR=-2, ID='N U-2' /
&DEVC XYZ= 9.55, 7.04, 1.87, QUANTITY='HEAT_FLUX', IOR=-2, ID='N U-3' /
&DEVC XYZ=12.15, 7.04, 1.87, QUANTITY='HEAT_FLUX', IOR=-2, ID='N U-4' /
&DEVC XYZ=17.79, 7.04, 1.50, QUANTITY='HEAT_FLUX', IOR=-2, ID='N U-5' /
&DEVC XYZ=17.79, 7.04, 3.73, QUANTITY='HEAT_FLUX', IOR=-2, ID='N U-6' /

&DEVC XYZ= 3.91, 0.00, 1.49, QUANTITY='HEAT_FLUX', IOR= 2, ID='S U-1' /
&DEVC XYZ= 3.91, 0.00, 3.72, QUANTITY='HEAT_FLUX', IOR= 2, ID='S U-2' /
&DEVC XYZ= 9.55, 0.00, 1.87, QUANTITY='HEAT_FLUX', IOR= 2, ID='S U-3' /
&DEVC XYZ=12.15, 0.00, 1.87, QUANTITY='HEAT_FLUX', IOR= 2, ID='S U-4' /
&DEVC XYZ=17.79, 0.00, 1.50, QUANTITY='HEAT_FLUX', IOR= 2, ID='S U-5' /
&DEVC XYZ=17.79, 0.00, 3.73, QUANTITY='HEAT_FLUX', IOR= 2, ID='S U-6' /

&DEVC XYZ=21.70, 1.59, 1.12, QUANTITY='HEAT_FLUX', IOR=-1, ID='E U-1' /
&DEVC XYZ=21.70, 1.59, 2.43, QUANTITY='HEAT_FLUX', IOR=-1, ID='E U-2' /
&DEVC XYZ=21.70, 5.76, 1.12, QUANTITY='HEAT_FLUX', IOR=-1, ID='E U-3' /
&DEVC XYZ=21.70, 5.76, 2.43, QUANTITY='HEAT_FLUX', IOR=-1, ID='E U-4' /

&DEVC XYZ= 0.00, 1.59, 1.12, QUANTITY='HEAT_FLUX', IOR= 1, ID='W U-1' /
&DEVC XYZ= 0.00, 1.59, 2.43, QUANTITY='HEAT_FLUX', IOR= 1, ID='W U-2' /
&DEVC XYZ= 0.00, 5.76, 1.12, QUANTITY='HEAT_FLUX', IOR= 1, ID='W U-3' /
&DEVC XYZ= 0.00, 5.76, 2.43, QUANTITY='HEAT_FLUX', IOR= 1, ID='W U-4' /

&DEVC XYZ= 3.04, 3.59, 0.00, QUANTITY='HEAT_FLUX', IOR= 3, ID='F U-1' /
&DEVC XYZ= 9.11, 2.00, 0.00, QUANTITY='HEAT_FLUX', IOR= 3, ID='F U-2' /
&DEVC XYZ= 9.11, 5.97, 0.00, QUANTITY='HEAT_FLUX', IOR= 3, ID='F U-3' /
&DEVC XYZ=10.85, 2.39, 0.00, QUANTITY='HEAT_FLUX', IOR= 3, ID='F U-4' /
&DEVC XYZ=10.85, 5.17, 0.00, QUANTITY='HEAT_FLUX', IOR= 3, ID='F C-5' /
&DEVC XYZ=13.02, 2.00, 0.00, QUANTITY='HEAT_FLUX', IOR= 3, ID='F U-6' /
&DEVC XYZ=13.02, 5.97, 0.00, QUANTITY='HEAT_FLUX', IOR= 3, ID='F U-7' /
&DEVC XYZ=18.66, 3.59, 0.00, QUANTITY='HEAT_FLUX', IOR= 3, ID='F U-8' /

&DEVC XYZ= 3.04, 3.59, 3.82, QUANTITY='HEAT_FLUX', IOR=-3, ID='C U-1' /
&DEVC XYZ= 9.11, 2.00, 3.82, QUANTITY='HEAT_FLUX', IOR=-3, ID='C C-2' /
&DEVC XYZ= 9.11, 5.97, 3.82, QUANTITY='HEAT_FLUX', IOR=-3, ID='C C-3' /
&DEVC XYZ=10.85, 2.39, 3.82, QUANTITY='HEAT_FLUX', IOR=-3, ID='C C-4' /
&DEVC XYZ=10.85, 5.17, 3.82, QUANTITY='HEAT_FLUX', IOR=-3, ID='C C-5' /
&DEVC XYZ=13.02, 2.00, 3.82, QUANTITY='HEAT_FLUX', IOR=-3, ID='C C-6' /
&DEVC XYZ=13.02, 5.97, 3.82, QUANTITY='HEAT_FLUX', IOR=-3, ID='C C-7' /
&DEVC XYZ=18.66, 3.59, 3.82, QUANTITY='HEAT_FLUX', IOR=-3, ID='C U-8' /
```

Rad and Total Flux Gauges

```
&DEVC XYZ=10.87, 0.50, 2.20, QUANTITY='GAUGE_HEAT_FLUX', IOR=-3, ID='Total
Flux Gauge 2' /
&DEVC XYZ=10.87, 1.25, 2.70, QUANTITY='GAUGE_HEAT_FLUX', IOR=-3, ID='Total
Flux Gauge 4' /
&DEVC XYZ=10.87, 1.30, 2.80, QUANTITY='GAUGE_HEAT_FLUX', IOR= 2, ID='Total
Flux Gauge 6' /
&DEVC XYZ=10.87, 2.00, 3.20, QUANTITY='GAUGE_HEAT_FLUX', IOR=-3, ID='Total
Flux Gauge 8' /
```

&DEVC XYZ=10.81, 6.80, 1.75, QUANTITY='GAUGE_HEAT_FLUX', IOR=-2, ID='Total Flux Gauge 9'/'

&DEVC XYZ=10.87, 0.50, 2.20, QUANTITY='RADIOMETER', IOR=-3, ID='Rad Gauge 1'/'

&DEVC XYZ=10.87, 1.25, 2.70, QUANTITY='RADIOMETER', IOR=-3, ID='Rad Gauge 3'/'

&DEVC XYZ=10.87, 1.30, 2.80, QUANTITY='RADIOMETER', IOR= 2, ID='Rad Gauge 5'/'

&DEVC XYZ=10.87, 2.00, 3.20, QUANTITY='RADIOMETER', IOR=-3, ID='Rad Gauge 7'/'

&DEVC XYZ=10.81, 6.80, 1.75, QUANTITY='RADIOMETER', IOR=-2, ID='Rad Gauge 10'/'

Gaseous Sampling

&DEVC XYZ= 6.85, 3.48, 3.22, QUANTITY='oxygen', ID='O2 1'/'

&DEVC XYZ= 6.85, 3.48, 0.50, QUANTITY='oxygen', ID='O2 2'/'

&DEVC XYZ= 6.85, 3.48, 3.22, QUANTITY='carbon monoxide', ID='CO 3'/'

&DEVC XYZ= 6.85, 3.48, 3.22, QUANTITY='carbon dioxide', ID='CO2 4'/'

Bidirectional Probes

&DEVC XYZ= 0.10, 2.71, 0.20, QUANTITY='VELOCITY', ID='BP Door 1'/'

&DEVC XYZ= 0.10, 2.71, 0.60, QUANTITY='VELOCITY', ID='BP Door 2'/'

&DEVC XYZ= 0.10, 2.71, 1.00, QUANTITY='VELOCITY', ID='BP Door 3'/'

&DEVC XYZ= 0.10, 2.71, 1.40, QUANTITY='VELOCITY', ID='BP Door 4'/'

&DEVC XYZ= 0.10, 2.71, 1.80, QUANTITY='VELOCITY', ID='BP Door 5'/'

&DEVC XYZ= 0.10, 3.51, 0.20, QUANTITY='VELOCITY', ID='BP Door 6'/'

&DEVC XYZ= 0.10, 3.51, 0.60, QUANTITY='VELOCITY', ID='BP Door 7'/'

&DEVC XYZ= 0.10, 3.51, 1.00, QUANTITY='VELOCITY', ID='BP Door 8'/'

&DEVC XYZ= 0.10, 3.51, 1.40, QUANTITY='VELOCITY', ID='BP Door 9'/'

&DEVC XYZ= 0.10, 3.51, 1.80, QUANTITY='VELOCITY', ID='BP Door 10'/'

&DEVC XYZ= 0.10, 4.31, 0.20, QUANTITY='VELOCITY', ID='BP Door 11'/'

&DEVC XYZ= 0.10, 4.31, 0.60, QUANTITY='VELOCITY', ID='BP Door 12'/'

&DEVC XYZ= 0.10, 4.31, 1.00, QUANTITY='VELOCITY', ID='BP Door 13'/'

&DEVC XYZ= 0.10, 4.31, 1.40, QUANTITY='VELOCITY', ID='BP Door 14'/'

&DEVC XYZ= 0.10, 4.31, 1.80, QUANTITY='VELOCITY', ID='BP Door 15'/'

&DEVC XYZ=11.35, 0.00, 2.40, QUANTITY='VELOCITY', ID='BP Supply 16'/'

&DEVC XYZ=11.35, 7.04, 2.40, QUANTITY='VELOCITY', ID='BP Exhaust 17'/'

&DEVC XYZ= 0.00, 0.30, 0.08, QUANTITY='VELOCITY', ID='BP Leak 18'/'

Smoke Obscuration/Concentration

&DEVC XYZ=21.10, 0.50, 3.60, QUANTITY='DENSITY', SPEC_ID='soot', UNITS='mg/m3', CONVERSION_FACTOR=1.E6, ID='Smoke Concentration' /

Compartment Pressure

&DEVC XYZ=10.85, 0.10, 0.10, QUANTITY='PRESSURE', ID='Pressure'/'

Integrated Quantities

&DEVC XB= 0.00, 0.00, 2.51, 4.51, 0.00, 2.00, QUANTITY='MASS FLOW', ID='Door Mass FLOW' /

&DEVC XB= 0.00, 0.00,2.51,4.51,0.00,2.00,QUANTITY='HEAT FLOW',ID='E-
FLOW' /

&DEVC XB=16.70,16.70,3.58,3.58,0.00,3.82,QUANTITY='LAYER
HEIGHT',ID='Layer Height' /

&DEVC XB=16.70,16.70,3.58,3.58,0.00,3.82,QUANTITY='UPPER
TEMPERATURE',ID='HGL Temp' /

Spray Nozzles

&DEVC XYZ=10.8,3.6,0.6, PROP_ID='nozzle', QUANTITY='TIME', SETPOINT=0.,
ID='fuel_nozzle' /

&TAIL /

A.4 Sample Corridor FDS File

```
&HEAD CHID='Corridor_31_bo', TITLE='Walls_No_Beams_Bo_Depo' /

&TIME T_END=90 /

&MISC FDS6=.TRUE., SOOT_DEPOSITION=.TRUE., SURF_DEFAULT='WALL' /

&MESH XB=-6.7056, 6.7056,-0.7620, 0.7620, 1.5240, 2.7432,
      IJK=264, 30, 24 /
&MESH XB=-6.7056,-0.9144,-0.7620, 0.7620, 0.0000, 1.5240,
      IJK= 57, 15, 15 /
&MESH XB=-0.9144, 0.9144,-0.7620, 0.7620, 0.0000, 1.5240,
      IJK= 36, 30, 30 /
&MESH XB= 0.9144, 6.7056,-0.7620, 0.7620, 0.0000, 1.5240,
      IJK= 57, 15, 15 /

&REAC ID          = 'PROPYLENE'
      C           = 8
      H           = 14
      O           = 1
      SOOT_YIELD  = 0.0477
      CO_YIELD    = 0.017
      HEAT_OF_COMBUSTION = 45800/

&MATL ID          = 'GYPSUM_BOARD'
      DENSITY     = 771
      CONDUCTIVITY = 1.7
      SPECIFIC_HEAT = 1.09/

&MATL ID          = 'CONCRETE'
      DENSITY     = 1860
      CONDUCTIVITY = 0.72
      SPECIFIC_HEAT = 0.78/

&SURF ID          = 'WALL'
      COLOR       = 'KHAKI'
      MATL_ID     = GYPSUM_BOARD
      THICKNESS   = 0.0011
      BACKING     = 'EXPOSED' /

&SURF ID          = 'FLOOR'
      COLOR       = 'IVORY'
      MATL_ID     = CONCRETE
      THICKNESS   = 0.025/

&SURF ID          = 'BURNER'
      MLRPUA      = 0.0235
      COLOR       = 'RED' /
```

Beams

&OBST XB=-6.0198,-5.8674,-0.7620, 0.7620, 2.4384, 2.7432, /
&OBST XB=-5.1054,-4.9530,-0.7620, 0.7620, 2.4384, 2.7432, /
&OBST XB=-4.1910,-4.0386,-0.7620, 0.7620, 2.4384, 2.7432, /
&OBST XB=-3.2766,-3.1242,-0.7620, 0.7620, 2.4384, 2.7432, /
&OBST XB=-2.3622,-2.2098,-0.7620, 0.7620, 2.4384, 2.7432, /
&OBST XB=-1.4478,-1.2954,-0.7620, 0.7620, 2.4384, 2.7432, /
&OBST XB=-0.5334,-0.3810,-0.7620, 0.7620, 2.4384, 2.7432, /
&OBST XB= 0.3810, 0.5334,-0.7620, 0.7620, 2.4384, 2.7432, /
&OBST XB= 1.2954, 1.4478,-0.7620, 0.7620, 2.4384, 2.7432, /
&OBST XB= 2.2098, 2.3622,-0.7620, 0.7620, 2.4384, 2.7432, /
&OBST XB= 3.1242, 3.2766,-0.7620, 0.7620, 2.4384, 2.7432, /
&OBST XB= 4.0386, 4.1910,-0.7620, 0.7620, 2.4384, 2.7432, /
&OBST XB= 4.9530, 5.1054,-0.7620, 0.7620, 2.4384, 2.7432, /
&OBST XB= 5.8674, 6.0198,-0.7620, 0.7620, 2.4384, 2.7432, /

Burner

&OBST XB=-0.1524, 0.1524,-0.1524, 0.1524, 0.0000, 0.0508,
SURF_IDS='BURNER','INERT','INERT' /

Baffle

&OBST XB=-0.6096, 0.6096,-0.6096,-0.6096, 0.0508, 0.6604 /
&OBST XB=-0.6096, 0.6096, 0.6096, 0.6096, 0.0508, 0.6604 /
&OBST XB=-0.6096,-0.6096,-0.6096, 0.6096, 0.0508, 0.6604 /
&OBST XB= 0.6096, 0.6096,-0.6096, 0.6096, 0.0508, 0.6604 /

&VENT PBX=-6.7056, SURF_ID='OPEN' /
&VENT PBX= 6.7056, SURF_ID='OPEN' /
&VENT PBZ= 0.0000, SURF_ID='FLOOR' /

Thermocouples

&DEVC XYZ=-5.9436, 0.0000, 2.4193, ID='T-19.5-B',
QUANTITY='THERMOCOUPLE' /
&DEVC XYZ=-5.0292, 0.0000, 2.4193, ID='T-16.5-B',
QUANTITY='THERMOCOUPLE' /
&DEVC XYZ=-4.1148, 0.0000, 2.4193, ID='T-13.5-B',
QUANTITY='THERMOCOUPLE' /
&DEVC XYZ= 4.1148, 0.0000, 2.4193, ID='T+13.5-B',
QUANTITY='THERMOCOUPLE' /
&DEVC XYZ= 5.0292, 0.0000, 2.4193, ID='T+16.5-B',
QUANTITY='THERMOCOUPLE' /
&DEVC XYZ= 5.9436, 0.0000, 2.4193, ID='T+19.5-B',
QUANTITY='THERMOCOUPLE' /
&DEVC XYZ=-6.3398, 0.0000, 2.7241, ID='T-20.8-C',
QUANTITY='THERMOCOUPLE' /
&DEVC XYZ=-4.5110, 0.0000, 2.7241, ID='T-14.8-C',
QUANTITY='THERMOCOUPLE' /
&DEVC XYZ=-2.6822, 0.0000, 2.7241, ID='T-08.8-C',
QUANTITY='THERMOCOUPLE' /
&DEVC XYZ=-0.8534, 0.0000, 2.7241, ID='T-02.8-C',
QUANTITY='THERMOCOUPLE' /
&DEVC XYZ= 0.0000, 0.0000, 2.7241, ID='T0.00-C',
QUANTITY='THERMOCOUPLE' /
&DEVC XYZ= 0.9753, 0.0000, 2.7241, ID='T+03.2-C',
QUANTITY='THERMOCOUPLE' /

```

&DEVC XYZ= 2.7432, 0.0000, 2.7241, ID='T+09-C',
  QUANTITY='THERMOCOUPLE' /
&DEVC XYZ= 4.5720, 0.0000, 2.7241, ID='T+15-C',
  QUANTITY='THERMOCOUPLE' /
&DEVC XYZ= 6.4008, 0.0000, 2.7241, ID='T+21-C',
  QUANTITY='THERMOCOUPLE' /
&DEVC XYZ= 4.5720, 0.7429, 2.4384, ID='T+15-W-12',
  QUANTITY='THERMOCOUPLE' /
&DEVC XYZ= 4.5720, 0.7429, 2.6670, ID='T+15-W-3',
  QUANTITY='THERMOCOUPLE' /
&DEVC XYZ= 4.5720,-0.7429, 2.4384, ID='T+15-W-12-',
  QUANTITY='THERMOCOUPLE' /
&DEVC XYZ= 6.4008, 0.7429, 2.4384, ID='T+21-W-12',
  QUANTITY='THERMOCOUPLE' /
&DEVC XYZ= 6.4008, 0.7429, 2.6670, ID='T+21-W-3',
  QUANTITY='THERMOCOUPLE' /
&DEVC XYZ= 6.4008,-0.7429, 2.4384, ID='T+21-W-12-',
  QUANTITY='THERMOCOUPLE' /

```

Optical Density Devices

```

&DEVC XYZ=-4.4196, 0.0000, 2.7241, ID='O-14.5-C_EC',
  QUANTITY='EXTINCTION COEFFICIENT' /
&DEVC XYZ=-4.4196, 0.0000, 2.7241, ID='O-14.5-C_OD',
  QUANTITY='OPTICAL DENSITY' /
&DEVC XB= -4.4196,-4.4196,-0.7620, 0.7620, 2.7241, 2.7241,
  ID='O-14.5-C_PO', QUANTITY='PATH OBSCURATION' /

&DEVC XYZ= 0.7620, 0.0000, 2.7241, ID='O+2.5-C_EC',
  QUANTITY='EXTINCTION COEFFICIENT' /
&DEVC XYZ= 0.7620, 0.0000, 2.7241, ID='O+2.5-C_OD',
  QUANTITY='OPTICAL DENSITY' /
&DEVC XB= 0.7620, 0.7620,-0.7620, 0.7620, 2.7241, 2.7241,
  ID='O+2.5-C_PO', QUANTITY='PATH OBSCURATION' /

&DEVC XYZ= 2.6212, 0.0000, 2.7241, ID='O+8.6-C_EC',
  QUANTITY='EXTINCTION COEFFICIENT' /
&DEVC XYZ= 2.6212, 0.0000, 2.7241, ID='O+8.6-C_OD',
  QUANTITY='OPTICAL DENSITY' /
&DEVC XB= 2.6212, 2.6212,-0.7620, 0.7620, 2.7241, 2.7241,
  ID='O+8.6-C_PO', QUANTITY='PATH OBSCURATION' /

&DEVC XYZ= 4.7548, 0.0000, 2.7241, ID='O+15.6-C_EC',
  QUANTITY='EXTINCTION COEFFICIENT' /
&DEVC XYZ= 4.7548, 0.0000, 2.7241, ID='O+15.6-C_OD',
  QUANTITY='OPTICAL DENSITY' /
&DEVC XB= 4.7548, 4.7548,-0.7620, 0.7620, 2.7241, 2.7241,
  ID='O+15.6-C_PO', QUANTITY='PATH OBSCURATION' /

&DEVC XYZ= 4.7548,-0.7429, 2.4384, ID='O+15.6-W_EC',
  QUANTITY='EXTINCTION COEFFICIENT' /
&DEVC XYZ= 4.7548,-0.7429, 2.4384, ID='O+15.6-W_OD',
  QUANTITY='OPTICAL DENSITY' /
&DEVC XB= 3.9928, 5.5168,-0.7429,-0.7429, 2.4384, 2.4384,
  ID='O+15.6-W_PO', QUANTITY='PATH OBSCURATION' /

```

```
&DEVC XYZ= 6.4617, 0.0000, 2.7241, ID='O+21.2-C_EC',
  QUANTITY='EXTINCTION COEFFICIENT' /
&DEVC XYZ= 6.4617, 0.0000, 2.7241, ID='O+21.2-C_OD',
  QUANTITY='OPTICAL DENSITY' /
&DEVC XB= 6.4617, 6.4617,-0.7620, 0.7620, 2.7241, 2.7241,
  ID='O+21.2-C_PO', QUANTITY='PATH OBSCURATION' /
```

Anemometer Devices

```
&DEVC XYZ= 4.5720, 0.4572, 2.7241, ID='V+15-C_T',
  QUANTITY='THERMOCOUPLE' /
&DEVC XYZ= 4.5720, 0.4572, 2.7241, ID='V+15-C_U',
  QUANTITY='U-VELOCITY' /
&DEVC XYZ= 4.5720, 0.4572, 2.7241, ID='V+15-C_V',
  QUANTITY='V-VELOCITY' /
&DEVC XYZ= 4.5720, 0.4572, 2.7241, ID='V+15-C_W',
  QUANTITY='W-VELOCITY' /
```

```
&DEVC XYZ= 6.4008, 0.4572, 2.7241, ID='V+21-C_T',
  QUANTITY='THERMOCOUPLE' /
&DEVC XYZ= 6.4008, 0.4572, 2.7241, ID='V+21-C_U',
  QUANTITY='U-VELOCITY' /
&DEVC XYZ= 6.4008, 0.4572, 2.7241, ID='V+21-C_V',
  QUANTITY='V-VELOCITY' /
&DEVC XYZ= 6.4008, 0.4572, 2.7241, ID='V+21-C_W',
  QUANTITY='W-VELOCITY' /
```

```
&BNDF QUANTITY='BURNING RATE' /
&BNDF QUANTITY='CONVECTIVE HEAT FLUX' /
&BNDF QUANTITY='GAUGE HEAT FLUX' /
&BNDF QUANTITY='HEAT TRANSFER COEFFICIENT' /
&BNDF QUANTITY='NET HEAT FLUX' /
&BNDF QUANTITY='NORMAL VELOCITY' /
&BNDF QUANTITY='RADIATIVE HEAT FLUX' /
&BNDF QUANTITY='WALL TEMPERATURE' /
```

```
&SLCF PBX=0, QUANTITY='OPTICAL DENSITY' /
&SLCF PBX=0, QUANTITY='SOOT VOLUME FRACTION' /
&SLCF PBX=0, QUANTITY='U-VELOCITY' /
&SLCF PBX=0, QUANTITY='VELOCITY' /
&SLCF PBX=0, QUANTITY='V-VELOCITY' /
&SLCF PBX=0, QUANTITY='W-VELOCITY' /
&SLCF PBX=0, QUANTITY='TEMPERATURE' /
```

```
&SLCF PBY=0, QUANTITY='OPTICAL DENSITY' /
&SLCF PBY=0, QUANTITY='SOOT VOLUME FRACTION' /
&SLCF PBY=0, QUANTITY='U-VELOCITY' /
&SLCF PBY=0, QUANTITY='VELOCITY' /
&SLCF PBY=0, QUANTITY='V-VELOCITY' /
&SLCF PBY=0, QUANTITY='W-VELOCITY' /
&SLCF PBY=0, QUANTITY='TEMPERATURE' /
```

```
&DUMP DT_RESTART=60 /
&TAIL/
```

A.5 Sample Thermophoretic Deposition Chamber FDS File

```
&HEAD CHID='Octane_th_2cm_mpi', TITLE='09-Octane_th_mpi' /

&TIME T_END=1200 /

&MISC FDS6=.TRUE., SOOT_DEPOSITION=.TRUE.,
      TURBULENT_DEPOSITION=.FALSE., SURF_DEFAULT='WALL' /

&MESH XB=-0.30, 0.30,-0.30, 0.30, 0.00, 0.90, IJK= 30, 30, 45,
      ID='MAIN' /
&MESH XB=-0.30, 0.30,-0.30, 0.30,-0.30, 0.00, IJK= 30, 30, 15,
      ID='MAIN' /
&MESH XB= 0.30, 0.76,-0.16, 0.14,-0.30, 0.30, IJK= 23, 15, 30,
      ID='EXHAUST' /

&REAC ID          = 'OCTANE'
      C            = 8
      H            = 18
      SOOT_YIELD   = 0.08
      CO_YIELD     = 0.011
      HEAT_OF_COMBUSTION = 43540/

&RAMP ID='DURABOARD_K', T=20, F=0.063 /
&RAMP ID='DURABOARD_K', T=204, F=0.080 /
&RAMP ID='DURABOARD_K', T=316, F=0.091 /
&RAMP ID='DURABOARD_K', T=427, F=0.105 /
&RAMP ID='DURABOARD_K', T=538, F=0.122 /
&RAMP ID='DURABOARD_K', T=649, F=0.143 /

&RAMP ID='DURABOARD_C', T=20, F=0.835 /
&RAMP ID='DURABOARD_C', T=125, F=0.870 /
&RAMP ID='DURABOARD_C', T=225, F=0.903 /
&RAMP ID='DURABOARD_C', T=325, F=0.936 /
&RAMP ID='DURABOARD_C', T=425, F=0.969 /
&RAMP ID='DURABOARD_C', T=525, F=1.002 /
&RAMP ID='DURABOARD_C', T=625, F=1.135 /

&RAMP ID='OCTANE_RAMP', T=0, F=0.00, FYI='0.000' /
&RAMP ID='OCTANE_RAMP', T=20, F=0.52, FYI='0.015' /
&RAMP ID='OCTANE_RAMP', T=75, F=0.97, FYI='0.028' /
&RAMP ID='OCTANE_RAMP', T=100, F=0.97, FYI='0.028' /
&RAMP ID='OCTANE_RAMP', T=150, F=1.00, FYI='0.029' /
&RAMP ID='OCTANE_RAMP', T=200, F=1.00, FYI='0.029' /
&RAMP ID='OCTANE_RAMP', T=450, F=1.00, FYI='0.029' /
&RAMP ID='OCTANE_RAMP', T=525, F=1.00, FYI='0.029' /
&RAMP ID='OCTANE_RAMP', T=600, F=1.00, FYI='0.029' /
&RAMP ID='OCTANE_RAMP', T=675, F=1.00, FYI='0.029' /
&RAMP ID='OCTANE_RAMP', T=750, F=1.00, FYI='0.029' /
&RAMP ID='OCTANE_RAMP', T=825, F=1.00, FYI='0.029' /
&RAMP ID='OCTANE_RAMP', T=900, F=1.00, FYI='0.029' /
&RAMP ID='OCTANE_RAMP', T=1050, F=1.00, FYI='0.029' /
&RAMP ID='OCTANE_RAMP', T=1125, F=0.59, FYI='0.017' /
```

```

&RAMP ID='OCTANE_RAMP', T=1150, F=0.41, FYI='0.012' /
&RAMP ID='OCTANE_RAMP', T=1170, F=0.34, FYI='0.010' /
&RAMP ID='OCTANE_RAMP', T=1180, F=00.0, FYI='0.000' /

&MATL ID                = 'DURABOARD'
  DENSITY                = 272
  EMISSIVITY             = 1
  CONDUCTIVITY_RAMP     = 'DURABOARD_K'
  SPECIFIC_HEAT_RAMP    = 'DURABOARD_C' /

&SURF ID                = 'WALL'
  COLOR                  = 'BURLY WOOD'
  MATL_ID                = 'DURABOARD'
  THICKNESS              = 0.01
  BACKING                = 'EXPOSED' /

&SURF ID                = 'EXHAUST'
  COLOR                  = 'GRAY'
  MASS_FLUX_TOTAL       = 2.0233 /

&SURF ID                = 'FILTER'
  COLOR                  = 'CRIMSON'
  MATL_ID                = 'DURABOARD'
  THICKNESS              = 0.01
  BACKING                = 'EXPOSED' /

&SURF ID                = 'FUEL'
  MLRPUA                 = 0.0104
  COLOR                  = 'RED'
  RAMP_Q                 = 'OCTANE_RAMP' /

&OBST XB= 0.64, 0.72, -0.06, 0.04, 0.30, 0.30,
  SURF_ID='EXHAUST' /
&OBST XB=-0.04, 0.04, -0.30, -0.30, 0.72, 0.80,
  SURF_ID='FILTER', FYI='Upper' /
&OBST XB=-0.04, 0.04, -0.30, -0.30, 0.50, 0.58,
  SURF_ID='FILTER', FYI='Lower' /
&OBST XB=-0.02, 0.02, -0.04, 0.04, -0.02, 0.00,
  SURF_IDS='FUEL','INERT','INERT' /

Main Open
&VENT XB=-0.30, 0.30, -0.30, -0.30, -0.30, 0.00,
  SURF_ID='OPEN' / Front
&VENT XB=-0.30, 0.30, 0.30, 0.30, -0.30, 0.00,
  SURF_ID='OPEN' / Back
&VENT XB=-0.30, -0.30, -0.30, 0.30, -0.30, 0.00,
  SURF_ID='OPEN' / Left
&VENT XB= 0.30, 0.30, -0.30, -0.16, -0.30, 0.00,
  SURF_ID='OPEN' / Right Front
&VENT XB= 0.30, 0.30, 0.14, 0.30, -0.30, 0.00,
  SURF_ID='OPEN' / Right Back

```

```

Exhaust Open
&VENT XB= 0.30, 0.76, -0.16, -0.16, -0.30, 0.00,
  SURF_ID='OPEN' / Front
&VENT XB= 0.30, 0.76, 0.14, 0.14, -0.30, 0.00,
  SURF_ID='OPEN' / Back
&VENT XB= 0.76, 0.76, -0.16, 0.14, -0.30, 0.00,
  SURF_ID='OPEN' / Right
&VENT PBZ=-0.3, SURF_ID='OPEN' /

&DEVC XYZ=-0.24, 0.24, 0.82, ID='TC_T01', QUANTITY='THERMOCOUPLE' /
&DEVC XYZ=-0.24, 0.24, 0.74, ID='TC_T02', QUANTITY='THERMOCOUPLE' /
&DEVC XYZ=-0.24, 0.24, 0.66, ID='TC_T03', QUANTITY='THERMOCOUPLE' /
&DEVC XYZ=-0.24, 0.24, 0.58, ID='TC_T04', QUANTITY='THERMOCOUPLE' /
&DEVC XYZ=-0.24, 0.24, 0.50, ID='TC_T05', QUANTITY='THERMOCOUPLE' /
&DEVC XYZ=-0.24, 0.24, 0.42, ID='TC_T06', QUANTITY='THERMOCOUPLE' /
&DEVC XYZ=-0.24, 0.24, 0.34, ID='TC_T07', QUANTITY='THERMOCOUPLE' /
&DEVC XYZ=-0.24, 0.24, 0.26, ID='TC_T08', QUANTITY='THERMOCOUPLE' /
&DEVC XYZ=-0.24, 0.24, 0.18, ID='TC_T09', QUANTITY='THERMOCOUPLE' /
&DEVC XYZ=-0.24, 0.24, 0.10, ID='TC_T10', QUANTITY='THERMOCOUPLE' /
&DEVC XYZ=-0.24, 0.24, 0.02, ID='TC_T11', QUANTITY='THERMOCOUPLE' /

&DEVC XYZ= 0.00,-0.28, 0.76, ID='Gas TC',
  QUANTITY='THERMOCOUPLE' /
&DEVC XYZ= 0.00,-0.28, 0.76, ID='Gas Temp',
  QUANTITY='TEMPERATURE' /
&DEVC XYZ= 0.00,-0.30, 0.76, ID='Wall Temp',
  QUANTITY='WALL TEMPERATURE', IOR=2 /
&DEVC XYZ= 0.00,-0.30, 0.76, ID='CHF',
  QUANTITY='CONVECTIVE HEAT FLUX', IOR=2 /
&DEVC XYZ= 0.00,-0.30, 0.76, ID='RHF',
  QUANTITY='RADIATIVE HEAT FLUX', IOR=2 /
&DEVC XYZ= 0.00,-0.30, 0.76, ID='NHF',
  QUANTITY='NET HEAT FLUX', IOR=2 /
&DEVC XYZ= 0.00,-0.30, 0.76, ID='EXTW',
  QUANTITY='EXTINCTION COEFFICIENT' /
&DEVC XYZ= 0.00,-0.30, 0.76, ID='ODW',
  QUANTITY='OPTICAL DENSITY' /
&DEVC XYZ= 0.00,-0.29, 0.76, ID='EXT',
  QUANTITY='EXTINCTION COEFFICIENT' /
&DEVC XYZ= 0.00,-0.29, 0.76, ID='OD',
  QUANTITY='OPTICAL DENSITY' /
&DEVC XB=-0.04, 0.04, -0.30, -0.30, 0.72, 0.80, ID='Soot Depo',
  QUANTITY='SOOT SURFACE DENSITY', STATISTICS='SURFACE INTEGRAL' /

```

```

&DEVC XYZ= 0.00,-0.28, 0.54, ID='Gas TC',
    QUANTITY='THERMOCOUPLE' /
&DEVC XYZ= 0.00,-0.28, 0.54, ID='Gas Temp',
    QUANTITY='TEMPERATURE' /
&DEVC XYZ= 0.00,-0.30, 0.54, ID='Wall Temp',
    QUANTITY='WALL TEMPERATURE' , IOR=2/
&DEVC XYZ= 0.00,-0.30, 0.54, ID='CHF',
    QUANTITY='CONVECTIVE HEAT FLUX' , IOR=2/
&DEVC XYZ= 0.00,-0.30, 0.54, ID='RHF',
    QUANTITY='RADIATIVE HEAT FLUX' , IOR=2/
&DEVC XYZ= 0.00,-0.30, 0.54, ID='NHF',
    QUANTITY='NET HEAT FLUX' , IOR=2/
&DEVC XYZ= 0.00,-0.30, 0.54, ID='EXTW',
    QUANTITY='EXTINCTION COEFFICIENT' /
&DEVC XYZ= 0.00,-0.30, 0.54, ID='ODW',
    QUANTITY='OPTICAL DENSITY' /
&DEVC XYZ= 0.00,-0.29, 0.54, ID='EXT',
    QUANTITY='EXTINCTION COEFFICIENT' /
&DEVC XYZ= 0.00,-0.29, 0.54, ID='OD',
    QUANTITY='OPTICAL DENSITY' /
&DEVC XB= -0.04, 0.04, -0.30, -0.30, 0.50, 0.58, ID='Soot Depo',
    QUANTITY='SOOT SURFACE DENSITY', STATISTICS='SURFACE INTEGRAL' /

&DEVC XB= 0.00, 0.00, 0.00, 0.00, 0.00, 0.90, FYI='21',
    ID='Layer Height', QUANTITY='LAYER HEIGHT' /

&BNDF QUANTITY='RADIATIVE HEAT FLUX' /
&BNDF QUANTITY='CONVECTIVE HEAT FLUX' /
&BNDF QUANTITY='NET HEAT FLUX' /
&BNDF QUANTITY='WALL TEMPERATURE' /
&BNDF QUANTITY='BURNING RATE' /

&SLCF PBX=0, QUANTITY='OPTICAL DENSITY' /
&SLCF PBX=0, QUANTITY='SOOT VOLUME FRACTION' /
&SLCF PBX=0, QUANTITY='VELOCITY' /
&SLCF PBX=0, QUANTITY='U-VELOCITY' /
&SLCF PBX=0, QUANTITY='V-VELOCITY' /
&SLCF PBX=0, QUANTITY='W-VELOCITY' /
&SLCF PBX=0, QUANTITY='TEMPERATURE' /

&SLCF PBY=0, QUANTITY='OPTICAL DENSITY' /
&SLCF PBY=0, QUANTITY='SOOT VOLUME FRACTION' /
&SLCF PBY=0, QUANTITY='VELOCITY' /
&SLCF PBY=0, QUANTITY='U-VELOCITY' /
&SLCF PBY=0, QUANTITY='V-VELOCITY' /
&SLCF PBY=0, QUANTITY='W-VELOCITY' /
&SLCF PBY=0, QUANTITY='TEMPERATURE' /
&DUMP DT_RESTART=60 /
&TAIL/

```

Appendix B – FDS Soot Deposition Function

```
SUBROUTINE CALC_SOOT_DEPOSITION(NM)
USE PHYSICAL_FUNCTIONS, ONLY: GET_VISCOSITY,GET_CONDUCTIVITY
USE GLOBAL_CONSTANTS, ONLY: EVACUATION_ONLY,SOLID_PHASE_ONLY,
    SOLID_BOUNDARY,I_PROG_SOOT,N_SPECIES,TUSED
INTEGER, INTENT(IN) :: NM
!REAL(EB), PARAMETER ::
    CS=1.147_EB,CT=2.18_EB,CM=1.146_EB,KPKG=1._EB,PARTD=2.E-8_EB
REAL(EB) :: U_THERM,U_TURB,TGAS,TWALL,MUGAS,Y_SOOT,RHOG,
    YIN(1:N_SPECIES),YDEP,K_AIR
INTEGER :: IIG,JJG,KKG,IW,IOR,ITMP
!REAL(EB), PARAMETER :: A=8.3_EB,B=1._EB/7._EB,Z_PLUS_TURBULENT =
    11.81_EB,ALPHA=7.202125273562269_EB
!REAL(EB), PARAMETER ::
    BETA=1._EB+B,ETA=(1._EB+B)/A,GAMMA=2._EB/(1._EB+B)
IF (EVACUATION_ONLY(NM)) RETURN
IF (SOLID_PHASE_ONLY) RETURN
CALL POINT_TO_MESH(NM)
U_THERM=0._EB
U_TURB=0._EB
WALL_CELL_LOOP: DO IW=1,NWC+NVWC
    IF (BOUNDARY_TYPE(IW)/=SOLID_BOUNDARY .OR. UW(IW) < 0._EB) CYCLE
        WALL_CELL_LOOP
        IOR = IJKW(4,IW)
        IIG = IJKW(6,IW)
        JJG = IJKW(7,IW)
        KKG = IJKW(8,IW)
        YIN = MAX(0._EB,YY(IIG,JJG,KKG,:))
        IF (YIN(I_PROG_SOOT) < 1.E-14_EB) CYCLE WALL_CELL_LOOP
        TGAS = TMP(IIG,JJG,KKG)
        TWALL = TMP_F(IW)
        ITMP = MIN(NINT(0.5_EB*(TGAS+TWALL)),5000)
        RHOG=RHO(IIG,JJG,KKG)
        CALL GET_VISCOSITY(YIN,MUGAS,ITMP)
        CALL GET_CONDUCTIVITY(YIN,K_AIR,ITMP)
        IF (THERMOPHORETIC_DEPOSITION) U_THERM =
            0.55_EB*HEAT_TRANS_COEF(IW)*(TGAS-TWALL)*MUGAS/(TGAS*RHOG*K_AIR)
        IF (TURBULENT_DEPOSITION) U_TURB = 0.037_EB*U_TAU(IW)
        IF (U_THERM+U_TURB < 0._EB) CYCLE WALL_CELL_LOOP
        YIN = YIN * RHOG
        Y_SOOT = YIN(I_PROG_SOOT)
        YDEP =Y_SOOT*MIN(1._EB,(U_THERM+U_TURB)*DT*RDN(IW))
        YIN(I_PROG_SOOT) = Y_SOOT - YDEP
        AWMSOOT(IW)=AWMSOOT(IW)+YDEP/RDN(IW)
        RHO(IIG,JJG,KKG) = RHOG - YDEP
        YY(IIG,JJG,KKG,:) = YIN / RHO(IIG,JJG,KKG)
    ENDDO WALL_CELL_LOOP
END SUBROUTINE CALC_SOOT_DEPOSITION
```

References

- 1 Dreisbach, J., & McGrattan, K. (2006). Verification and Validation of Selected Fire Models for Nuclear Power Plant Applications.
- 2 Mealy, C., Floyd, J., & Gottuk, D. (2008). Smoke Detector Spacing Requirements Complex Beamed and Sloped Ceilings - Volume 1: Experimental Validation of Smoke Detector Spacing Requirements. Baltimore: Hughes Associates, Inc.
- 3 Rowekamp, M., Dreisbach, J., Klein-Hebling, W., McGrattan, K., Miles, S., Plys, M., (2008). International Collaborative Fire Modeling Project. GRS.
- 4 McGrattan, K., Peacock, R., & Hamins, A. (2006). Verification and Validation of Selected Fire Models for Nuclear Power Plant Applications. Washington: NRC.
- 5 O'Connor, D. J., Cui, E., Klaus, M. J., Lee, C. H., Su, C., Sun, Z. (2006). Smoke Detector Performance for Level Ceilings With Deep Beams and Deep Beam Pocket Configurations Research Project. Quincy: The Fire Protection Research Foundation.
- 6 Riahi, S., Beyler, C. L., Hartman, J. A., & Roddis, W. M. (2010). Development of Tools for Smoke Residue and Deposition Analysis. 2009 Fall Technical Meeting Organized by the Eastern States Section of the Combustion Institute.
- 7 Riahi, S., Beyler, C. L., & Hartman, J. A. (2010). Measurement and Prediction of Smoke Deposition in Fires. 12th International Conference of Fire Science and Engineering, Interflam.
- 8 McGrattan, K., McDermott, R., Hostikka, S., & Floyd, J. (2010). Fire Dynamics Simulator Version 5 Users Guide. Gaithersburg, MD: NIST.
- 9 McDermott, R. (2009). FDS Wall Flows Part 1: Straight Channels. Gaithersburg: NIST.
- 10 Klote, J. H., & Milke, J. A. (2002). Principles of Smoke Management. ASHRAE.
- 11 Tewarson, A. (2002). Generation of Heat and Chemical Compounds in Fires. In SFPE Handbook of Fire Protection Engineering. Quincy: National Fire Protection Association.
- 12 Karlsson, B., & Quintiere, J. G. (1999). Enclosure Fire Dynamics. CRC.
- 13 Quintiere, J. G. (2006). Fundamentals of Fire Phenomena. Wiley.

- 14 Ciro, W. D., Eddings, E. G., & Sarofim, A. F. (2006). Experimental and Numerical Investigation of Transient Soot Buildup on a Cylindrical Container Immersed in a Jet Fuel Pool Fire. *Combustion Science and Technology*.
- 15 Sippola, M. R. (2002). Particle Deposition in Ventilation Ducts. University of California, Berkeley.
- 16 Tanaka, T. J. (1997). Effects of Smoke on Functional Circuits.
- 17 Tewarson, A. (2004). Smoke Contamination of Surfaces. Fourth International Seminar of Fire and Explosions Hazard.
- 18 Butler, K. M., & Mulholland, G. W. (2004). Generation and Transport of Smoke Components. Kluwer Academic Publishers.
- 19 Beyler, C. (2007). Development of Forensic Tools for Smoke Residue and Deposition Analysis.
- 20 Turns, S. R. (2006). An Introduction to Combustion. Singapore: McGraw Hill.
- 21 Mulholland, G. W., & Croarkin, C. (2000). Specific Extinction Coefficient of Flame Generated Smoke. John Wiley & Sons, Ltd.
- 22 Mulholland, G. W. (2002). Smoke Production and Properties. In SFPE Handbook of Fire Protection Engineering. Quincy: National Fire Protection Association.
- 23 ASTM E 1355 (2004). Standard Guide for Evaluating the Predictive Capability of Deterministic Fire Models.
- 24 Incropera, F. P., Dewitt, D. P., Bergman, T. L., & Lavine, A. S. (2007). Fundamentals of Heat and Mass Transfer 6th ed. Wiley.
- 25 Hamins, A., Maranghides, A., Johnsson, R., Donnelly, M., Yang, J., Mulholland, G., (2003). Report of Experimental Results for the International Fire Model Benchmarking and Validation Exercise #3. Gaithersburg, MD: NIST.
- 26 Mulholland, G. W., Henzel, V., & Babrauskas, V. (1989). The Effect of Scale on Smoke Emission. Fire Safety Science, Second International Symposium.
- 27 Floyd, J., Riahi, S., Mealy, C., & Gottuk, D. (2008). Smoke Detector Spacing Requirements Complex Beamed and Sloped Ceilings - Volume 2: Modeling of and Requirements for Parallel Beamed, Flat Ceiling Corridors and Beamed, Sloped Ceilings. Baltimore: Hughes Associates, Inc.
- 28 McDermott, R., McGrattan, K., Hostikka, S., & Floyd, J. (2010). Fire Dynamics Simulator (Version 5) Technical Reference Guide Volume 2: Verification. Gaithersburg, MD: NIST.

- 29 Friedlander, S. (2000). *Smoke, Dust, and Haze: Fundamentals of Aerosol Dynamics*, 2nd ed. New York: Oxford University.
- 30 Floyd, J., & McDermott, R. (2010). *Modeling Soot Deposition Using Large Eddy Simulation with a Mixture Fraction Based Framework*.
- 31 Floyd, J. E., Baum, H. R., & McGrattan, K. B. (2001). *A Mixture Fraction Combustion Model for Fire Simulation Using CFD*. San Francisco: International Conference on Engineered Fire Protection Design.
- 32 Gottuk, D., Mealy, C., & Floyd, J. (2008). *Smoke Transport and FDS Validation*. Baltimore.
- 33 Holman, J. P. (1990). *Heat Transfer*. McGraw-Hill.
- 34 McGrattan, K. B., Baum, H. R., & Rehm, R. G. (1998). *Large Eddy Simulations of Smoke Movement*. 30.
- 35 Sippola, M. R., & Nazaroff, W. W. (2003). *Modeling Particle Loss in Ventilation Ducts*. *Atmospheric Environment*.
- 36 Talbot, L., Cheng, R. K., Schefer, R. W., & Willis, D. R. (1980). *Thermophoresis of Particles in a Heated Boundary Layer*. 101.
- 37 Waldmann, L., & Schmitt, K. H. (1966). *Thermophoresis and Diffusiophoresis of Aerosols*. *Aerosol Science*.
- 38 Munson, B. R., Young, D. F., & Okiishi, T. H. (2006). *Fundamentals of Fluid Mechanics* 5th ed. Wiley.